

EUR 3651 e

EUROPEAN ATOMIC ENERGY COMMUNITY - EURATOM

TWISTED TAPE BOILING WATER REACTOR

(Final Report July 1965 - September 1966)

1967



LIBRARY

Report prepared by
AEG - Allgemeine Elektrizitätsgesellschaft, Frankfurt (Main) - Germany
and
SNECMA - Société Nationale d'Etude et de Construction de Moteurs d'Aviation,
Suresnes - France

Euratom Contract No. 070-65-7 TEEC

LEGAL NOTICE

This document was prepared under the sponsorship of the Commission of the European Communities.

Neither the Commission of the European Communities, its contractors nor any person acting on their behalf :

Make any warranty or representation, express or implied, with respect to the accuracy, completeness, or usefulness of the information contained in this document, or that the use of any information, apparatus, method, or process disclosed in this document may not infringe privately owned rights ; or

Assume any liability with respect to the use of, or for damages resulting from the use of any information, apparatus, method or process disclosed in this document.

This report is on sale at the addresses listed on

at the price of FF 15.— FB 150 DM 12.—

When ordering, please refer to the addresses which are indicated on the cover of this document.

This document

CHF correlations and experimental results on TT clusters proved the safety of such an experiment. The bundle has been manufactured with few difficulties and an important technological knowledge about twisted tape clusters manufacturing has been gained.

As a first step to solve the technological problems about TT behaviour in a BWR, an out of pile experiment has been conducted on a 9 rod TT bundle with the aim to test its behaviour under corrosion. Satisfactory results, especially about fretting corrosion, allow to expect a good behaviour of the twisted tape clusters under actual reactor conditions.

Thermal tests which were not initially foreseen in this contract have also been performed at the SET of the EURATOM CCR ISPRA. Critical Heat Flux were measured on a 4 rod bundle with twisted tapes, at inlet conditions (high subcooling) which had never been tested previously. The results are in good agreement with those obtained by SNECMA during former tests. However, since no suitable explanation of them could be given, a new test program has been defined which involves in a closer way the SET of CCR ISPRA.

EUR 3651 e

EUROPEAN ATOMIC ENERGY COMMUNITY - EURATOM

TWISTED TAPE BOILING WATER REACTOR

(Final Report July 1965 - September 1966)

1967



Report prepared by
AEG - Allgemeine Elektrizitätsgesellschaft, Frankfurt (Main) - Germany
and
SNECMA - Société Nationale d'Etude et de Construction de Moteurs d'Aviation,
Suresnes - France

Euratom Contract No. 070-65-7 TEEC

SUMMARY

Theoretical work about the feasibility and economical interest of a 600 MWe Twisted Tape BWR led to the first conclusion that an appreciable gain on the kWh cost can be expected for a core power density of about 60-70 kW/l. However, before giving a final answer, some technological problems would have to be solved and also more information about basic thermal-hydraulics phenomena should be obtained from further tests.

An in-pile experiment of Twisted Tape prototype fuel element in the Kahl VAK BWR has been prepared. Calculations using both usual CHF correlations and experimental results on TT clusters proved the safety of such an experiment. The bundle has been manufactured with few difficulties and an important technological knowledge about twisted tape clusters manufacturing has been gained.

As a first step to solve the technological problems about TT behaviour in a BWR, an out of pile experiment has been conducted on a 9 rod TT bundle with the aim to test its behaviour under corrosion. Satisfactory results, especially about fretting corrosion, allow to expect a good behaviour of the twisted tape clusters under actual reactor conditions.

Thermal tests which were not initially foreseen in this contract have also been performed at the SET of the EURATOM CCR ISPRA. Critical Heat Flux were measured on a 4 rod bundle with twisted tapes, at inlet conditions (high subcooling) which had never been tested previously. The results are in good agreement with those obtained by SNECMA during former tests. However, since no suitable explanation of them could be given, a new test program has been defined which involves in a closer way the SET of CCR ISPRA.

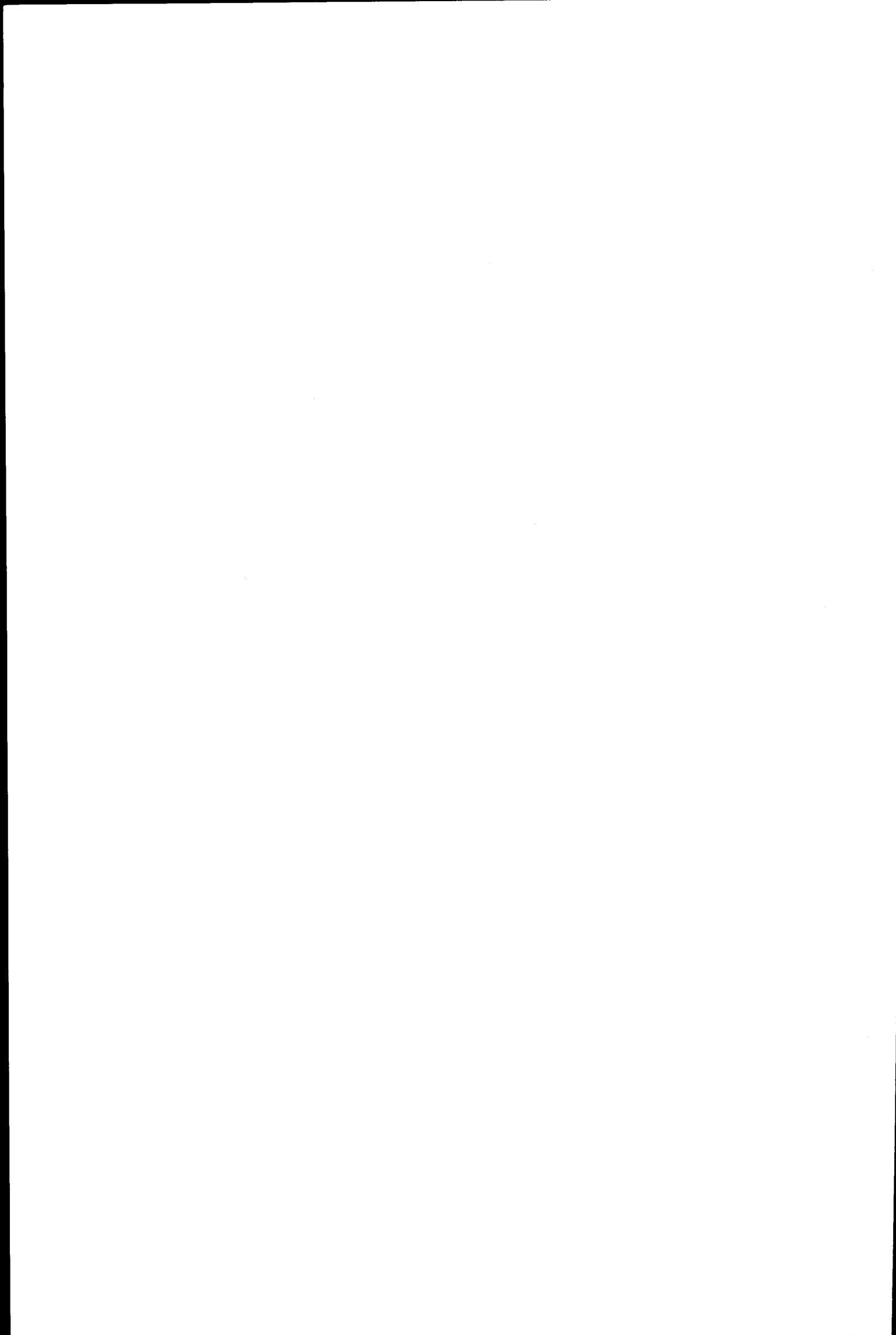
KEYWORDS

DESIGN
BOILING
WATER MODERATOR
WATER COOLANT
POWER
ECONOMICS
FUEL ELEMENTS

FUEL ELEMENT CLUSTERS
CONFIGURATION
TESTING
REACTOR SAFETY
CORROSION
CRITICAL HEAT FLUX
EURATOM
PERFORMANCE

TABLE OF CONTENTS

	Page
0 - INTRODUCTION	5
1 - TASK A - 600 MWe TWISTED TAPE B.W.R. PARAMETRIC AND ECONOMICAL STUDIES.	6
1.1 - Preliminary choice of lattices	6
1.2 - Detailed core calculations	18
1.3 - Definition of Reactor components	32
1.4 - Economic calculations	34
2 - TASK B - PREPARATION OF A PROTOTYPE FUEL ASSEMBLY FOR AN IN-PILE EXPERIMENT.	39
2.1 - Design of the prototype T.T. fuel assembly	39
2.2 - Safety calculations	45
2.3 - Fabrication of the twisted tape prototype fuel bundle	53
3 - TASK C - EXPERIMENTAL PROGRAM.	63
3.1 - Corrosion test	63
3.2 - Definition of further experimental work	91
3.3 - Critical Heat Flux experiments	95
Références	108



TWISTED TAPE BOILING WATER REACTOR⁽⁺⁾

0 - INTRODUCTION

It is well known that limitations to an increase of BWR power densities (kW/l or kW/kg U) are critical heat flux and fuel centerline temperature.

Since several years the Division Atomique of SNECMA had been conducting a research and development program on twisted tape clusters, a device allowing rather high increases (from 60% to 100%) of critical heat flux. Twisted tapes are inserted between the fuel rods of an usual BWR square lattice forcing larger water layers on the rod surface. Their cruciform shape allows a perfect fitting between rods and twisted tape cluster manufactured in the usual fuel rod cladding materials (Zircaloy or stainless steel).

In parallel to this technological development work, tests have been carried out with the aim to study the phenomena involved in the swirling flow induced by Twisted Tapes and to inquire into what extend Critical Heat Flux can be so increased. This work has been carried out by SNECMA with EURATOM support under the EURATOM-US AEC/SNECMA contracts N° 017.60.4 R.D F , 058.61.7 R.D F and 061.64.7 TEE F - Ref, (1) to (27).

Though some work has also been done by SNECMA with the purpose of designing a high power density BWR core, it was preferable to involve in these researches a Company more experimented in Boiling Water Reactor building. So, EURATOM invited AEG-KERNENERGIEANLAGEN and SNECMA-Division Atomique to combine their efforts on that goal of designing a Twisted Tape Boiling Water Reactor (TTBWR).

⁽⁺⁾ Manuscript received on September 15, 1967.

The first contract of this Twisted Tape Boiling Water Reactor Research and Development Program (EURATOM/AEG-SNECMA Contract N°070-65-7 TEE C), at first, continues the experimental work about the CHF phenomenon in swirling flow and, besides, starts on a work more directly aimed to industrial development of a TTBWR. It includes exploratory studies for the economical evaluation of the energy produced by a TTBWR the High Power Density of which is reached because of the T.T., and also experiments to test the TT fuel elements behaviour with regard to corrosion in boiling water at 70 bars, first on a mockup in a simulation loop and then in full scale in a reactor.

This contract, the general report of which is constituted by the present paper, will be followed, again in the AEG-SNECMA collaboration setting, with EURATOM financial support and also with the collaboration of the CCR ISPRA " Service des Etudes Thermiques ", by new thermal and hydraulic experiments (CHF measurements, slip ratio and friction pressure drop coefficients measurements and transfer function measurements) and by studies which will result in the design of a TTBWR.

1. TASK A - 600 MWe TWISTED TAPE B.W.R. parametric and economical studies.
- 1.1. Subtask A.1 - Preliminary choice of lattices. (by G. du BOUCHERON, SNECMA).

When we started on the work of preliminary studies of a 600 MWe Twisted Tape Boiling Water Reactor economical optimisation, some parameters had to be chosen and also some guesses had to be put down. Without these assumptions, the number of parameters would have been too big to be handled.

- 1.1.1. General Remarks.
- 1.1.1.1. Critical Heat Flux.

The first problem was about Critical Heat Flux laws in swirling flow induced by twisted tapes.

From experimental data available at the beginning of this task (October 1965), it was possible to make only assumptions on the very phenomenon. Thus there was no possibility to give any Critical Heat Flux limit curve or correlation which could be used to determine a safety margin.

To get a first idea of this margin, a Critical Heat Flux correlation has been established, coming from several assumptions.

It was first supposed that the critical phenomenon was depending on inlet conditions only. This assumption comes out from the following remarks. On the one hand the CHF results plotted versus outlet quality give two values of the CHF for the same value of the quality, and this has no possible explanation but this one that the CHF is not a function of outlet quality. On the other hand the CHF results plotted versus inlet quality give an always defined curve, each value of the inlet quality corresponding to one value of the CHF. Another fact that could confirm this assumption is the fact that several actual burnout spots have been detected at the lower part of the test section.

Since the experiments had led to decreasing Critical Heat Flux curves versus inlet quality, it could be considered that using zero inlet quality critical heat flux as constant reference heat flux for margin calculation was a rather conservative condition. A limit curve could therefore be plotted representing zero inlet quality critical heat flux versus specific flow rate (Fig; A.1).

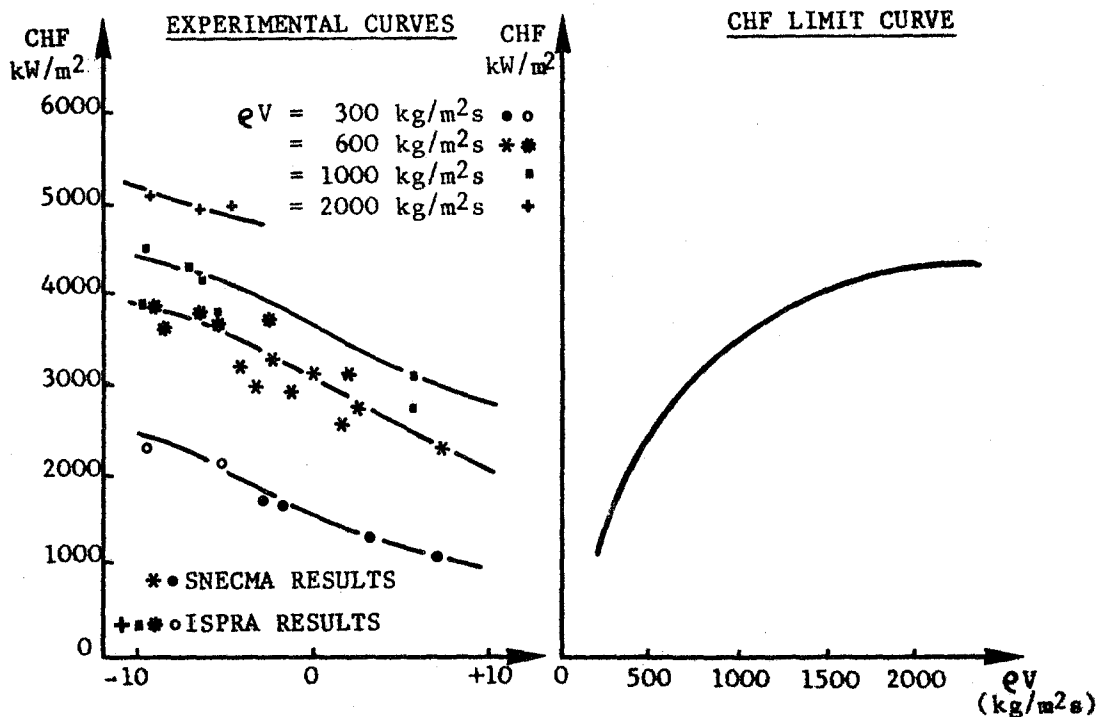


Fig. A.1 - EXPLANATION OF THE CHF LIMIT CURVE

But it must be emphasized that such a curve is too much dependent on a basic assumption which has not been experimentally checked to be considered as the actual limitation. So it has been used as an indicative curve giving only an idea of the allowed increase of Critical Heat Flux.

An exploratory study (28) showed that this critical heat flux limit curve leads to a large margin even for rather high core exit steam qualities. Figures A2, A3 and A4 show, in the case of a 2,4 water to fuel ratio lattice, a representation of this margin.

On a rod diameter versus core power density diagram, critical heat flux limit curves are drawn at constant average exit steam quality and at constant Minimum Critical Heat Flux ratio (MCHFR).

The MCHFR is the minimum value of the Critical Heat Flux Ratio (CHFR) in the reactor operated at 120 % of its nominal power. The CHFR is the ratio of the Critical Heat Flux at local conditions to the heat flux at the same point.

Curves are drawn for three values of this MCHFR : 1,5 - 2,0 and 2,5. Since the CHF correlation used here is independent of the local quality, the MCHFR is then calculated at the maximum power point of the reactor.

Limit curves are also drawn at constant fuel thermal conductivity integral (5 kW/m and 8 kW/m) which can roughly be considered as a present and a future limitations on fuel temperature.

If it is put down that the lowest admissible MCHFR is 1,5, the curves on figure A2 prove that even for exit steam qualities larger than 24 %, CHF limit curve is still above the present fuel temperature limit curve. It can then be stated that CHF is no longer a limit.

All the following calculations have been made with this assumption.

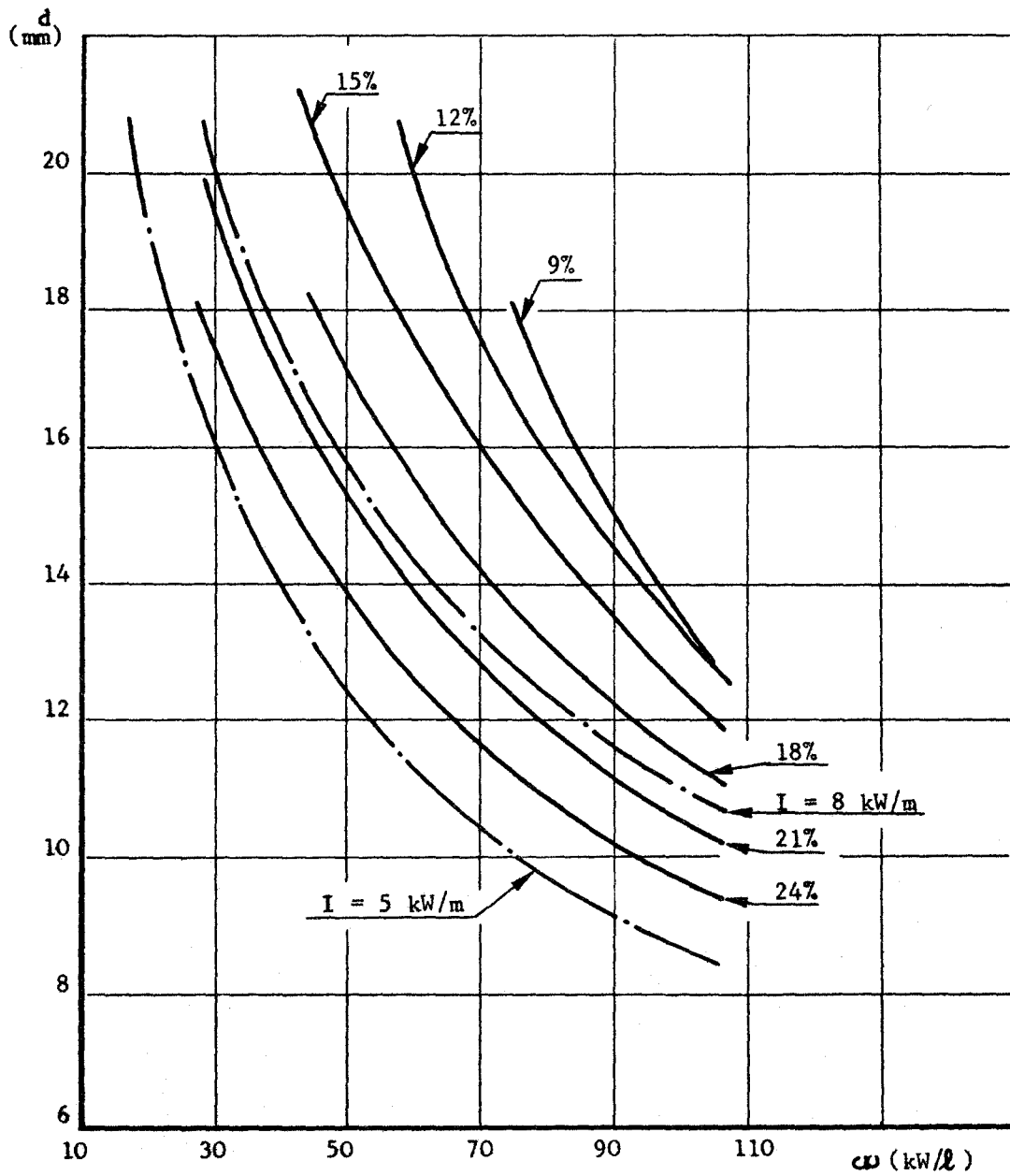


Fig. A2

600 MWe TTBWR EXPLORATORY STUDY - LIMIT CURVES FOR MCHFR = 1,5

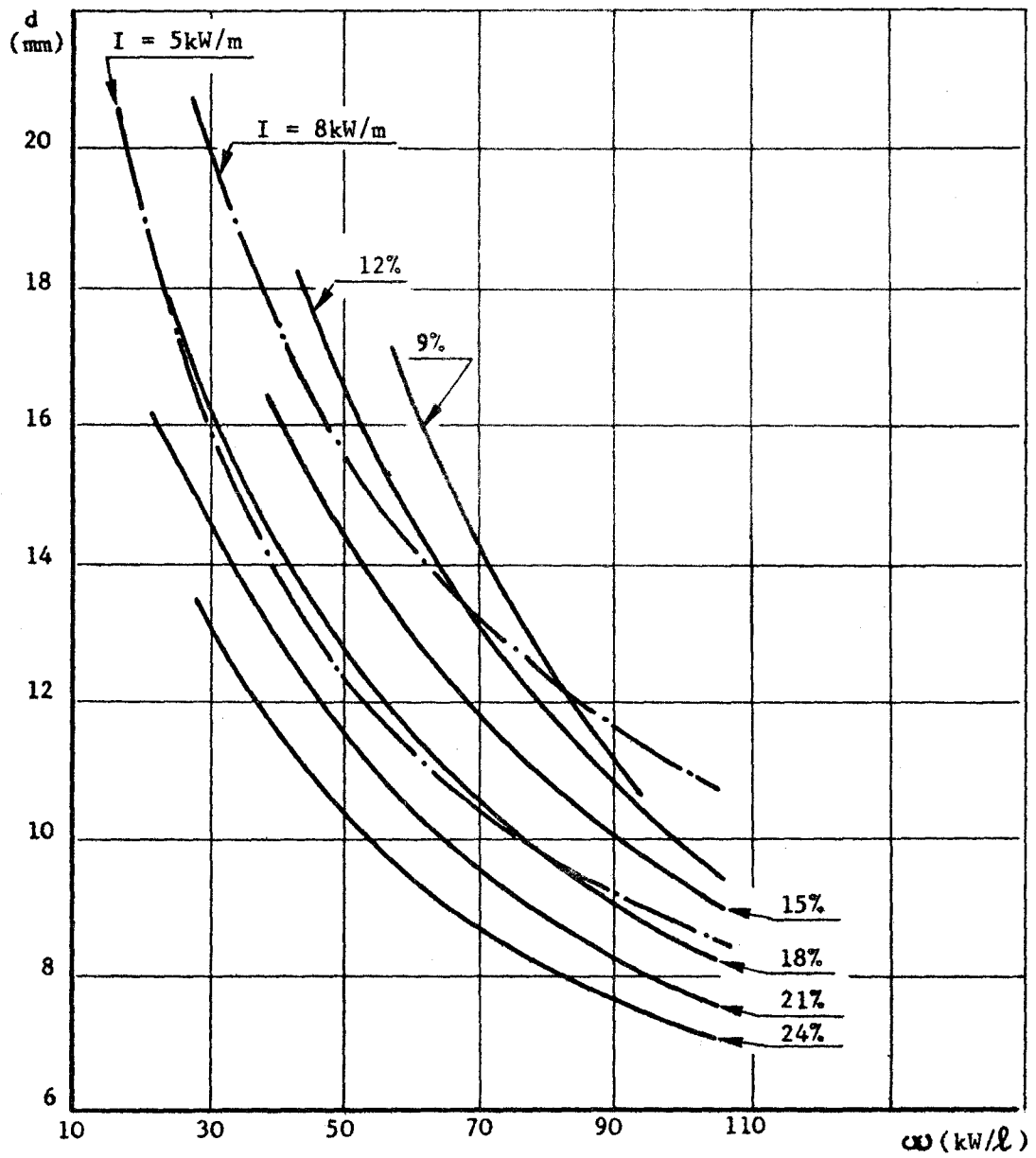
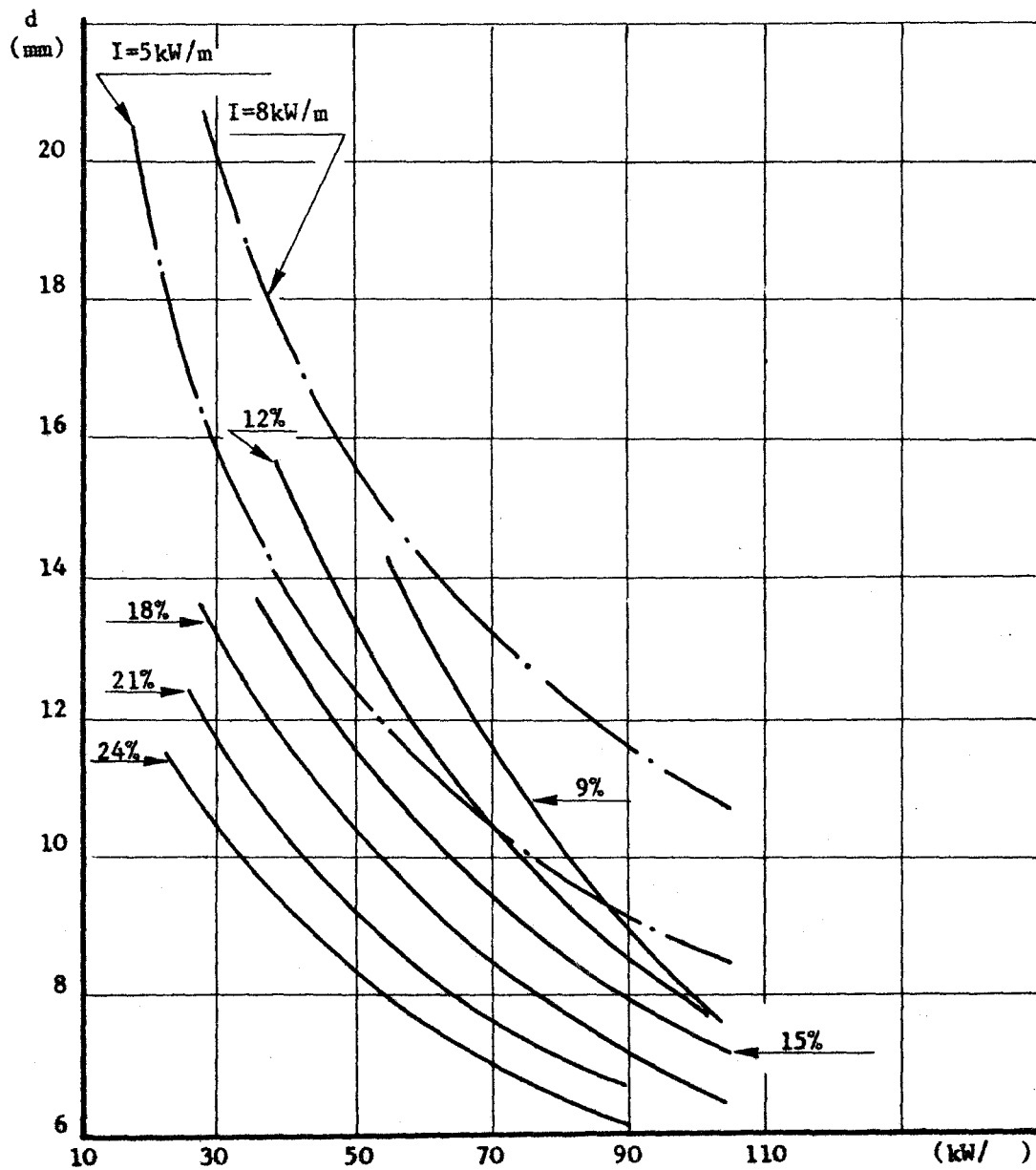


Fig. A3

600 MWe TTBWR EXPLORATORY STUDY - LIMIT CURVES FOR MCHFR = 2,0

Fig. A4 - 600 MWe TTBWR EXPLORATORY STUDY - LIMIT CURVES FOR MCHFR = 2,5



1.1.1.2. Maximum fuel temperature.

It is known that in a Boiling Water Reactor of the usual type, the Critical Heat Flux limits the power density more than the Fuel temperature. Thus, conservative conditions can be kept with regard to fuel central melting. This can be seen on a diagram representing fuel rod diameter versus core power density (fig. A5). For constant conditions about water to fuel ratio, power peaking factors and average exit steam quality, curves can be plotted for critical heat flux at constant CHF ratio and for fuel temperature at constant temperature or at constant power margin to central melting.

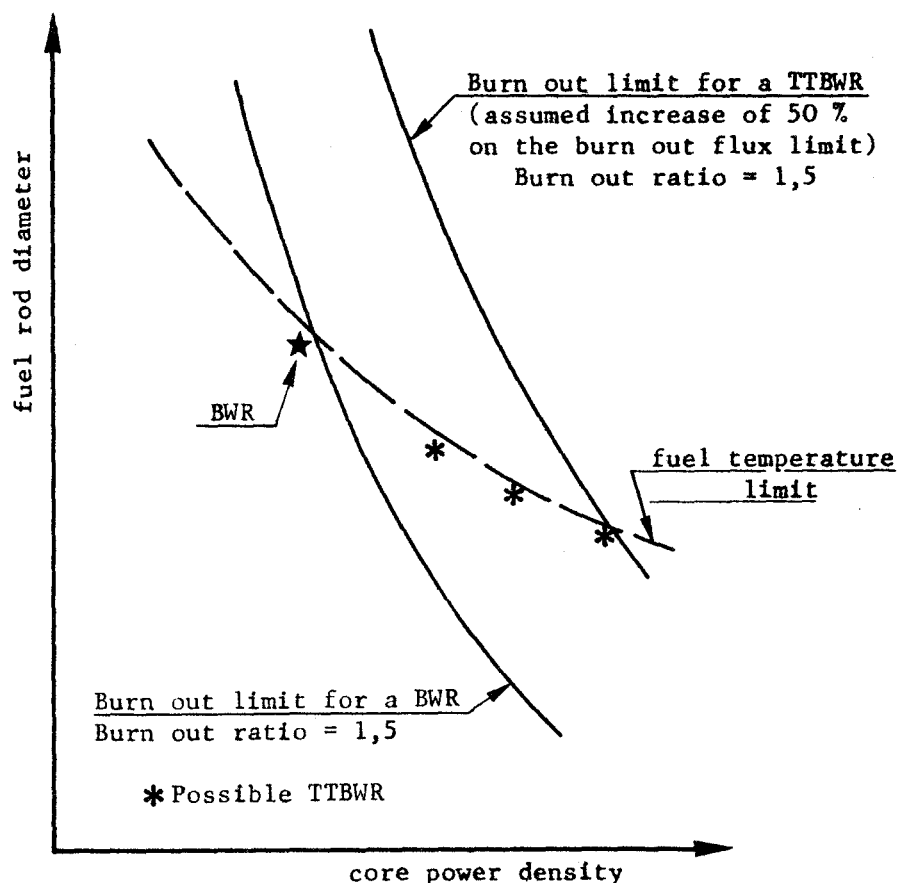


Fig. A5 - TEMPERATURE AND CRITICAL HEAT FLUX LIMIT CURVES FOR BWR AND TTBR

As long as the Critical Heat Flux curve is lower than the Temperature limit curve, there is no strong advantage of increasing allowed fuel temperature. But since the twisted tapes lead to higher Critical Heat Flux curves, there is a major interest to go to more severe fuel temperature conditions. It is obvious that, for a given core power density, the best reactor corresponds to such conditions on fuel temperature that will give the reactor operation point at the crossing of the two limit curves. This reactor would be operated with the smallest allowed margins with respect to both critical heat flux

and fuel melting.

Though it was known that a large research program was in progress concerning the feasibility of fuels operating with central melting, it has been decided to limit the present study to more conservative conditions. Because the economical evaluation was performed by comparison with a reference reactor design, it has been preferred to keep the fuel temperature conditions of this design, namely a margin of about 15 % in power, before central melting. The increasing of the allowable fuel temperature would give an additional economical potential which was not considered during the study. The economical evaluation of this should be investigated during the continued Twisted Tape Boiling Water Reactor Research and Development Program.

For fuel temperature calculations, Lyons and coll. correlation was used (★) for UO_2 thermal conductivity :

$$k_{UO_2} = \frac{38,24}{T + 129,4} + 4,79 \cdot 10^{-13} T^3$$

(T in °K and k in W/cm°C)

1.1.2 - The Reference Reactor.

The reactor which has been taken as a comparison reference for economical evaluations was a 600 MWe Boiling Water Reactor Design by AEG, dated February 1966.

The main characteristics of this design are given in table AI.

(★) GEAP 4624 - UO_2 Pellet Thermal Conductivity From irradiations with central Melting - by M. F. LYONS, O. H. COPLIN, T. J. PASHOS and B. WEIDENBAUM.

TABLE AI

The Reference Reactor

Electrical net power	603,2 MW
Electrical gross power	632 MW
Thermal power	1800 MW
Core power density	35,8 kW/l
Total mass of Uranium	117 250 kg
Water to fuel ratio	2,4
Core average pressure	72,25 bars
Core average void fraction	25%
Fuel average power density	15,8 kW/kg U
Average Burn-up	22 500 Mwd/tU
Number of bundles	592
Number of fuel rods per bundle	7 x 7
Active length	3,66 m
Fuel pellet diameter	~ 12,5 mm
Fuel rod diameter	14,4 mm
Cladding thickness	0,9 mm
Cladding material	Zircaloy 2
UO ₂ density	10,4 kg/dm ³
Control rod pitch	12 in = 304,8 mm
Number of control rods	148
Type of control rod lattice	D
Channel box internal side length	135,9 mm
Channel wall thickness	2 mm
Channel material	Zircaloy 2
Total mass flow rate	34 000 t/hr
Percentage of the flow inside the channel	90%
Feed water temperature	171,5°C
Active length over Equivalent Diameter	0,9
Power peaking factors :	
Radial + tolerance + intercontrol rod	1,47
Axial	1,57
Hot spot	1,33
Overpower	1,20
Total	3,68
Minimum Critical Heat Flux Ratio	1,5
Fuel cycle length	5 years
Refueled batch size	20%

1.1.3 Geometrical characteristics of the twisted tape reactors.

As far as it was needed for economical comparison, the characteristics of the twisted tape reactors were kept as they were in the reference reactor. However, several changes have been done for different reasons.

1.1.3.1 Control Rod Pitch.

Increased power density with constant cycle length leads to increased reload batch fuel enrichment and therefore to higher reactivity which has to be controlled. This increased control can be partially obtained by decreasing the control rod pitch and the channel pitch and side length.

If it is wanted to keep presently developed control rod drives, a minimum value of the control rod pitch is 254 mm (10 in.). This value has been chosen for the twisted tape reactors.

The control rod shape, thickness and technology is supposed unchanged. The water gap thickness is also unchanged.

1.1.3.2 Bundles.

Channel side length is defined from the control rod pitch. With a 17 mm gap between the channels for the control rod and a 8 mm gap for the poisoned sheets, the outside dimension of the channel box is 114,5 mm.

In a first approach, it was decided to keep the channel wall thickness of 2 mm. This is not obviously feasible because of the expected increased difference of pressure between inside and outside of the channel which can lead to a nonadmissible bowing. This has to be avoided to provide a plane surface for the control rod rollings.

The channel cross section is then a square of 110,5 mm side with round corners of 5,5 mm radius. The corner radius is chosen as small as it can be expected from technological knowledge about Zircaloy plate folding. A radius smaller than in the reference reactor is needed to give room enough for corner twisted tape. This tape is cut to fit with the channel wall but of course it is necessary to keep the tape centerline undamaged. For this, a minimum distance of 1 mm has to be kept between the tape centerline and the edge of the channel round corner.

Because of fabrication cost, the active fuel length has to be as long as possible with a constructive maximum of 3,66 m which is the same than in the reference case. This length could be decreased for two reasons :

- too high pressure drop,
- too high active length to equivalent diameter ratio.

1.1.3.3 Fuel rods.

Fuel rod diameter and pitch and fuel pellet diameter are carried out from considerations on water to fuel ratio and cladding thickness.

A water to fuel ratio of 2,4 is kept because it gives the more safe reactivity void coefficient : nearly zero at cold conditions and negative but with a not too large absolute value at hot conditions.

The cladding thickness has been roughly defined to insure undamaged fuel even with regard to surface corrosion and hydrogen corrosion. The cladding material is Zircaloy 2.

The twisted Tape material is Zircaloy 2. The tapes are 0,2 mm thick and of the usual cruciform SNECMA type. General design of the clusters is supposed to be the same as for the experimental assembly already manufactured for an irradiation test in the V.A.K. Kahl Boiling Water Reactor (See § 2.1 of the present report).

1.1.4 Choice of typical power densities and corresponding Fuel rod lattices.

As it was our purpose to investigate a large range of core power densities (from reference reactor power density to about 100 kW/l) four lattices have been chosen.

The fuel length depends on the rod and pellet diameters and on the cladding thickness. The criterion was a constant margin with respect to central melting or a maximum fuel temperature of 2 650°C at overpower conditions.

The fuel rod lattices (pitch and rod diameter) were determined for a fixed water to fuel ratio of 2,4 and for different numbers of fuel rods per bundle. Four configurations only can fit with this conditions : 49 , 64 , 81 and 100 rods per bundle.

The main characteristics of these lattices are given in Table A.II.

Temperature calculations have been carried out using the following data :

Zircaloy 2 thermal conductivity of 0,014 kW/m°C

UO₂-cladding contact equivalent heat transfer coefficient of
5,8 kW/m²°C

TABLE A II

Characteristics of the reference Reactor and of the 4 lattices

	Reference Reactor	lattice I	lattice II	lattice III	lattice IV
Number of rods per bundle	49	49	64	81	100
Rod outer diametermm	14,4	11,9	10,4	9,3	8,4
Pellet diameter mm	12,5	10,2	8,9	7,9	7,1
Cladding thickness mm	0,9	0,75	0,65	0,60	0,55
Fuel rod pitch mm		15,11	13,22	11,75	10,57
Twisted tapes thickness mm		0,2	0,2	0,2	0,2
Water to fuel ratio		2,408	2,420	2,402	2,400
Channel inside length mm	135,9	110,5	110,5	110,5	110,5
Channel wall thickness mm	2	2	2	2	2
Flow area inside the channelmm ²	10 489	6 617	6 616	6 528	6 465
Total fuel length m.	106 169	109 039	112 435	115 026	117 920
Total heating surface m ²	4 647,7	4 076,4	3 673,5	3 360,7	3 111,8
Core power density kW/l.	35,8	51,7	63,7	78,8	95
Fuel power density kW/kgU	15,8	22,1	23,2	24,95	42,2
Maximum fuel temperature at over- power °C	2 666	2 634	2 614	2 615	2 606
Hydraulic diameter with twisted tapes mm		7,12	6,29	5,47	5,08
Hydraulic diameter without twisted tapes mm	15,71	11,63	10,45	9,29	8,38

1.2 Subtask A.2 - Detailed core calculations.

1.2.1 Thermal-hydraulic analysis. - by G. du BOUCHERON - SNECMA.

Calculations have been performed in view to define feasible reactors with the four lattices previously mentioned.

1.2.1.1 Data and correlations.

1.2.1.1.1 - Subcooled voids.

No measurements have been done of subcooled voids in swirling-flow induced by twisted tapes. Lacking specific informations we used Bowring correlation (*).

1.2.1.1.2 - Void fraction.

Void fraction measurements have been performed in air-water and steam-water mixtures at atmospheric pressure for twisted tape non heated channels (27) . Obtained results fit quite well with known correlations for straight flow channels.

For high pressure steam-water mixture, experiments still have to be done.

Therefore, because of the agreement of the results of void fraction measurements at atmospheric pressure in straight flow and in swirling flow, it was assumed that, at high pressure, the known correlations for straight flow could also be applicable to swirling flow.

...

(*) HPR. 29 . OECD HALDEN REACTOR PROJECT - Physical Model, Based on bubble detachment, and calculation of steam voidage in the sub-cooled region of a heated channel - by R. W. BOWRING.

The MARCHATERRE correlation (★) was used for local slip ratio with hydraulic diameters computed as if there were no twisted tapes (Fig. A6).

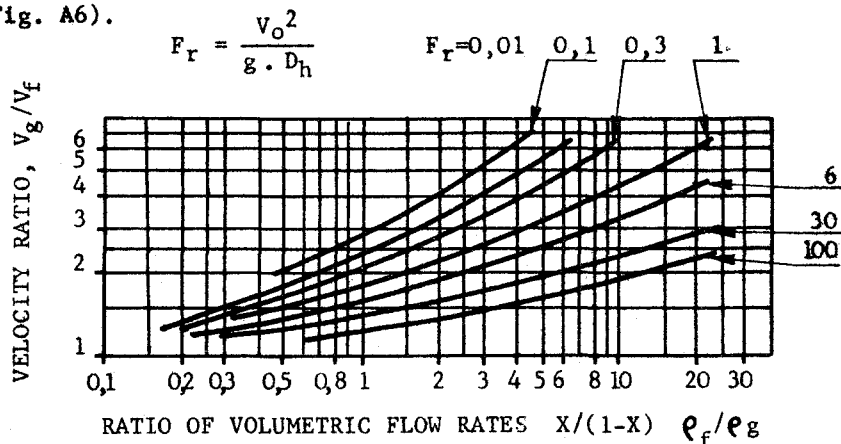


Fig. A6 - MARCHATERRE correlation for slip ratio (reproduced from ★)

Void fraction is then calculated by

$$\alpha = \frac{X}{X + (1 - X) \frac{\rho_g}{\rho_f} \frac{V_g}{V_f}}$$

where X is the local steam quality

ρ_g and ρ_f are steam and water densities

$\frac{V_g}{V_f}$ is the local slip ratio

1.2.1.1.3 Friction pressure drop.

Friction factor and two-phase friction pressure drop multiplier have been carried out from experiments on a 9 rod twisted tape fitted channel (★★).

Friction factor can be represented by the following correlations.

$$C_f = 0,4 e^{-0,367} \quad \text{for } Re \leq 80\,000$$

$$\text{and } C_f = 0,0063 \quad \text{for } Re > 80\,000$$

Re is the Reynolds number considering an hydraulic diameter computed with twisted tapes taken into account

$$d_h = \frac{4 S}{p}$$

★ Correlation for two-phase flow - by J. F. MARCHATERRE and B. M. HOGLUND - Nucleonics, August 1962.

★★ Essais hydromécaniques sur une maquette d'assemblage combustible équipée de vrilles - par J. DOLLE, G. SOURIOUX et J. FREUND (SNECMA internal report).

S being the channel flow area
and p the total wetted perimeter.

Two-phase pressure drop multiplier r is shown in Fig. A7 as a function of local quality. Measurements have been made for steam qualities up to 12%. For higher qualities, the experimental curve has been extrapolated by a tangent straight line. For purpose of numerical calculations, the following correlations have been established :

$$\text{For } x \leq 0,14 \quad r = 1 + \frac{1000 x^3 - 318 x^2 + 77,36 x}{1,92}$$

$$\text{For } x > 0,14 \quad r = 1,7 + 22,5 x$$

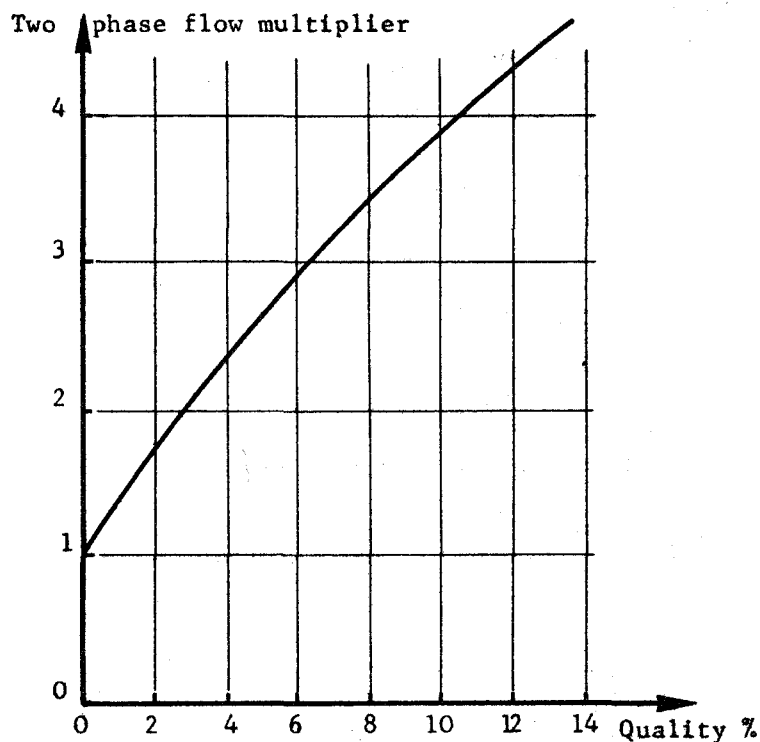


Fig. A7 - TWO PHASE PRESSURE DROP MULTIPLIER IN A TWISTED TAPE CHANNEL

Friction pressure drop through the channel is then :

$$\Delta P_f = \int_0^L 2 C_f r \left(\frac{q}{S} \right)^2 \frac{dl}{\rho_f}$$

where $\frac{q}{S}$ is the specific mass flow rate.

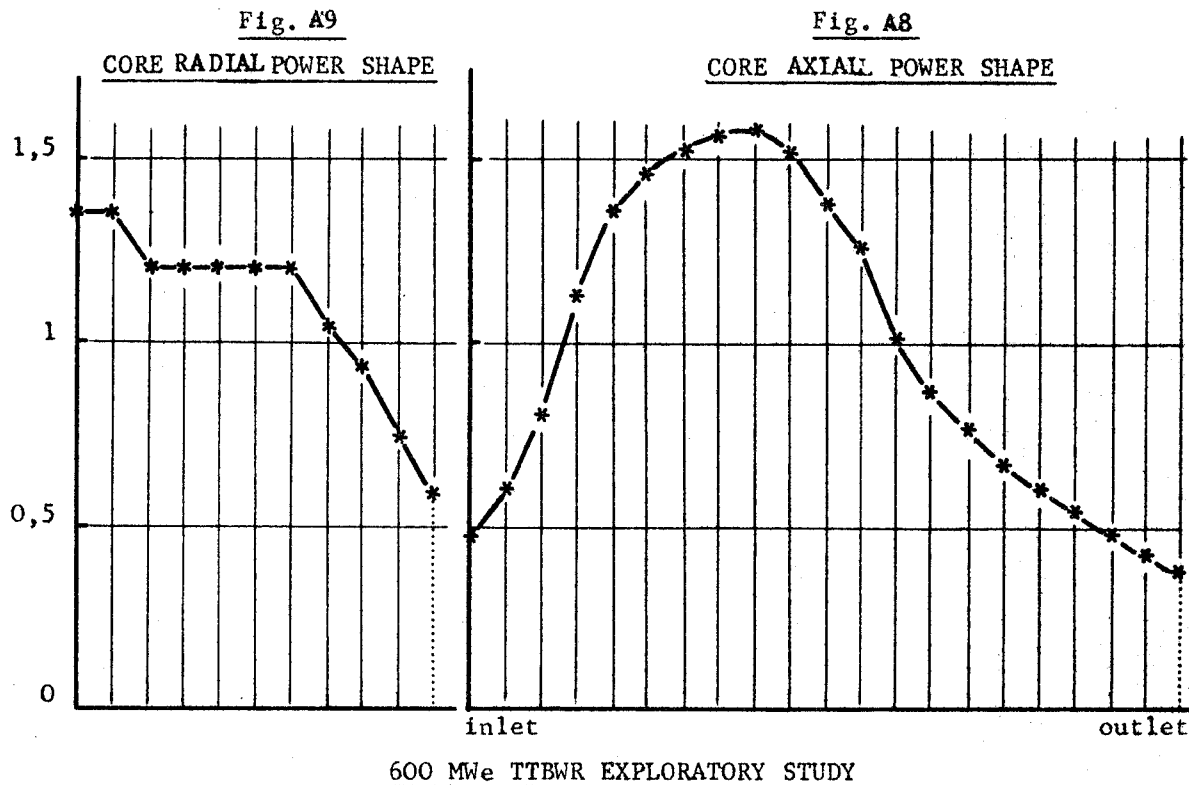
1.2.1.2 Thermal hydraulic characteristics.

Thermal hydraulic calculations have been made using AEG computation program UMLAUFRECHNUNG 43 on IBM 7040 computer.

This program determines the total coolant flow and the coolant flow distribution in the channels for a given power distribution and a constant pumping head. Slip ratio and friction pressure drop coefficient are input data tables. This particular feature of the code

allows to input any special friction correlation and makes it very convenient for twisted tape reactor calculations.

Axial power distribution used for calculations is such that it gives a maximum void fraction which is the worse condition for reactivity and stability behaviour. It is a bottom peaked shaped power distribution which is given on Fig. A8 for a 21 axial mesh point distribution. Radial power shape is given on plate A9 for the 11 radial mesh point distribution.



As a first phase of the study it has been tried to define the flow rate and the recirculation factor for maximum active length reactors in which average void fraction would be equal to reference reactor void fraction.

Results of these calculations are presented on table A III. Though the active length of the two highest power density cores has been decreased, the calculated pressure drops are still very high. This will have the following consequences :

- High pumping heads associated with maximum flow rates would lead to prohibitive pumping power which acts directly both on the plant cost and efficiency.
- High difference of pressure between inlet and outlet plenums would produce a strong lifting force on the bundle. This would ask for a new technology to keep the bundles in place.
- High pressure drops means also high difference of pressure between

inside and outside of the channels. It is then necessary to increase the channel wall thickness to provide a plane rolling surface for control rod blades. This increase would lead of course to increased material cost and also to increased manufacturing costs because of more technological problems, especially in folding thick Zircaloy plates.

For these reasons, it has been decided to allow higher void fractions coming from smaller flows. A standard pumping head of 1,1 at. was defined as a maximum core contribution (plenum to plenum minus corresponding part of the downcomer) to the total pumping head with regard to internal pumps capacity. This value has however been increased up to 1,5 at. for core power density highest value. Results of these calculations on 12 different reactors are given on table A IV.

TABLE A III- THERMO HYDRAULICS CHARACTERISTICS

	Ref	R I	R 2	R 5	R 6
Thermal power	1 800 MW	1 805 MW	1 817 MW	1 818 MW	1 824 MW
Number of bundles	592	608	480	480	448
Type of lattice		I	II	III	IV
Active length	3,66 m	3,66 m	3,66 m	2,958 m	2,635 m
Total flow rate	$31,15 \times 10^3$ t/h	$28,40 \times 10^3$ t/h	$32,55 \times 10^3$ t/h	$34,40 \times 10^3$ t/h	$35,35 \times 10^3$ t/h
Core void fraction	27,15 %	27,15 %	27,15 %	27,15 %	27,15 %
Average inlet velocity.	1,70 m/s	2,38 m/s	3,46 m/s	3,72 m/s	4,12 m/s
Specific flow rate	$1\ 255\ \text{kg/m}^2\text{s}$	$1\ 765\ \text{kg/m}^2\text{s}$	$2\ 560\ \text{kg/m}^2\text{s}$	$2\ 745\ \text{kg/m}^2\text{s}$	$3\ 045\ \text{kg/m}^2\text{s}$
Recirculation factor ..	9,50	8,95	10,15	10,72	10,95
Pumping Δp	0,80 at	1,85 at	4,50 at	4,70 at	5,90 at
Core equivalent diameter	4,178 m	3,540 m	3,140 m	3,140 m	3,035 m
H/D	0,876	1,032	1,166	0,942	0,868
Average power density	35,8 kW/1	51,7 kW/1	63,7 kW/1	78,8 kW/1	95,0 kW/1
Shroud I.D.		3,875 m	3,685 m	3,685 m	3,430 m
Vessel I.D.		4,805 m	4,615 m	4,615 m	4,360 m

TABLE A IV

	R1	R2	R3	R4	R5	R6	R7	R8	R9	R10	R11	R12
Type of lattice	I	II	III	IV	III	IV	II	II	III	I	III	IV
Power density kW/1	51,7	63,7	78,8	95	78,8	95	63,7	63,7	78,8	51,7	78,8	95
Number of bundles	608	480	388	352	480	448	548	608	516	708	480	448
Active length m.	3,660	3,660	3,660	3,350	2,958	2,634	3,205	2,890	2,752	3,14	2,958	2,634
Core contribution to pumping head at.	1,1	1,1	1,5	1,5	1,1	1,1	1,1	1,1	1,1	1,1	1,5	1,5
Recirculation factor	6,90	5,09	3,96	3,57	4,75	4,36	6,16	7,10	5,25	8,41	5,69	5,31
Total flow rate 10^6 kg/hs	21,83	16,17	12,60	11,35	15,10	13,96	19,59	22,57	16,92	26,75	18,08	16,88
Average void fraction %	29,28	32,14	34,63	35,78	33,51	34,30	30,53	29,31	32,08	27,47	31,66	32,54
Average exit steam quality %	14,56	19,66	25,23	28,01	21,05	22,77	16,23	14,08	18,79	11,89	17,58	18,83
Maximum local steam quality %	24,90	34,31	49,34	53,20	41,30	42,07	27,85	23,91	35,51	19,92	31,93	33,27
Plenum to plenum pressure drop at.	1,45	1,53	1,90	1,88	1,42	1,43	1,48	1,43	1,40	1,38	1,85	1,82
Expected critical heat flux ratio	2,85	2,44	2,07	1,95	2,04	1,95	2,56	2,64	2,11	2,98	2,37	2,25
Active length to equivalent diameter ratio	1,03	1,17	1,30	1,245	0,942	0,868	0,955	0,817	0,846	0,824	0,942	0,868

1.2.2 Physics calculations. - by P. HOCHSTEIN - AEG.

In this contribution the considerations, the assumptions, and the results of the physics calculations for the 600 MW high power density TTBWR design study are described.

The main task of the physics calculations had been to obtain the data which were needed for the economical evaluations of this reactor concept.

These data are :

- the initial enrichment and the discharge exposure for the first core and for the equilibrium core,
- the unloaded fuel enrichment and Plutonium content,
- the time between two refuelings,
- the time between the start-up and the first refueling.

Four different cores have been considered, which characteristics are given in Table A II. The main differences of the four cores are the various power densities.

In the calculations, two different modifications have been considered :

- a) The time between two refuelings is one year (6500 h. full operations), the quantity of changed fuel per refueling is 25%.
- b) No additional reactivity controls by burnable poisons are available in the equilibrium cores. As a result of this assumption the fuel cycles become shorter than one year. The amount of the changed fuel per refueling has been kept 25%.

An essential change of the refueled charge would be paid with some disadvantages, so the worse fuel utilization, and the very high amount of the excess reactivity, which would be no more controllable.

First, for the four reactor modifications, the cross sections of the unexposed bundles, the k_{∞} and k_{eff} with and without control rods have been calculated. In these calculations it has been assumed that the average void contents of the cores are 25% and that the enrichment would be 2,5% U-235. The objective of these calculations has been to determine the control rod worth and the influence of changing the geometry of the fuel rods, fuel bundles and cores, which result from the various power densities. In these calculations the AEG programs TG-EA and ESG-EA, and the PDQ-program were used.

The TG-EA program calculates the thermal cross sections of fuel rod cells, the ESG-EA program calculates the epithermal and fast cross sections of fuel bundle cells. These cross sections are homogenized with the flux ratios, which were gained from the PDQ calculations.

In the following short descriptions of the programs TG-EA and ESG-EA are given. In TG-EA the asymptotic thermal flux spectrum is calculated as at Wilkins and the thermal flux ratios are calculated with the integral transport theory (*). The thermal cross sections are yielded by homogeneization over the fuel rod cell with these flux ratios and flux spectrum.

The microscopic fast cross sections are calculated over an average spectrum, assuming that the fuel flux is constant within the bundle. The macroscopic fast cross sections are just the products of atomic number densities and the microscopic cross-sections. The epithermal range is divided in three subgroups. In each subgroup and fuel rod zone the resonance integrals of the resonance absorbers are calculated. For U 238 an empirical correlation is used, which is combined out of a volume term and a surface term. This relation bases on measurements from Hellstrand et al. (**), (***) and Nordheim (****). The Doppler effect is considered and the Dancoff correction in the surface term. σ_{+r} and σ_{se} are calculated taking into consideration spectrum effects. With the resonance integrals and the σ_{se} the resonance absorption is ascertained. A smooth $1/V$ term is added to get the epithermal absorption cross sections.

The resulting values for k_{∞} and k_{eff} are given in Table A V.

-
- * A. SAUER. Reactor Science and Technology - 18, 1964 page 425.
 - ** E. HELLSTRAND - Journal of Applied Physics, Vol. 28, Nr. 12, Dec. 57.
 - *** E. HELLSTRAND et al. - Nuclear Science and Engineering. 8, 1960, p.497.
 - **** L. W. NORDHEIM - Nuclear Science and Engineering. 12, 1962, page 457.

T A B L E A.V
 k_{∞} and k_{eff} of the four reactor types

	k_{∞} without control rod	k_{eff} without control rod	k_{∞} with control rod
variant I	1,2544	1,2335	0,8884
variant II	1,2483	1,2239	0,8829
variant III	1,2412	1,2129	0,8769
variant IV	1,2355	1,2041	0,8737

With the results of the described calculations extensive hand calculations were performed. Based on reactivity balances they should give the requested data. The dependences of the reactivity on the exposure and on the void content have been taken from a series of existing corresponding parameter studies.

One result of the modification a) (one year refueling cycle length) is that in equilibrium cores additional reactivity controls by burnable poisons are needed and, in the first cores, poison curtains and burnable poisons are needed. It should be mentioned that especially for modifications III and IV further investigations of the technical feasibility of these assumptions are necessary.

The U 235 enrichment and the isotopic concentration of the discharged fuel have been taken from a series of existing exposure calculations for BWR's.

The results are given in tables A.VII and A.VIII. The results differ from those given in (31) because there is another correction considered, which is based on various void contents in the various modifications (Table A.VI).

T A B L E A.VI
Average void content in the core

	R1	R2	R7	R8	R9	R12
Average void content in the core %	29,3	32,1	30,5	29,3	32,0	32,5

T A B L E A V I I

PHYSICS CORE CHARACTERISTICS

a) One year refueling cycle length - Reactivity control by burnable poisons

	R_1		R_2		R_7		R_8		R_9		R_{12}	
	First core	Equilibrium core										
Burnup during one cycle (MWd/t)	-	5980	-	7630	-	7630	-	7630	-	9450	-	11440
Burnup of the discharged fuel (MWd/t)	18260	23920	23300	30520	23300	30520	23300	30520	28850	37800	34930	45760
Initial enrichment (%)	2,03	2,38	2,54	3,03	2,52	2,99	2,51	2,98	3,07	3,66	3,63	4,37
Additionally controlled reactivity (% Δk)	17,3	0,7	24,7	3,5	24,4	3,2	24,2	3,0	31,6	5,9	40,3	8,7

Content of Pu and Isotopes of the discharged fuel.(%) :

U-235	0,72	0,83	0,81	0,80	0,93	1,04
Pu-239	0,373	0,368	0,368	0,368	0,359	0,350
Pu-240	0,234	0,298	0,298	0,298	0,308	0,303
Pu-241	0,033	0,133	0,133	0,133	0,137	0,134
Pu-242	0,042	0,094	0,094	0,094	0,115	0,115

T A B L E A V I I I

PHYSICS CORE CHARACTERISTICS

b) Refueling cycle length shorter than one year.

	R ₁ First equilibrium core core		R ₂ R ₇ R ₈ First equilibrium core core		R ₉ First equilibrium core core		R ₁₂ First equilibrium core core	
Burnup during one cycle (MWd/t)	-	5450	-	5450	-	5450	-	5450
Burnup of the discharged fuel (MWd/t)	16640	21800	16640	21800	16640	21800	16640	21800
Initial enrichment (%)	1,98	2,34	2,03	2,39	2,09	2,45	2,15	2,51
Additional controlled reactivity (% Δk)	16,3	-	16,3	-	16,3	-	16,3	-
Refueling cycle length	2,77	0,91	2,18	0,71	1,76	0,57	1,46	0,48

Content of Pu and Isotopes of the discharged fuel.

U-235	0,73	0,78	0,85	0,91
Pu-239	0,369	0,369	0,369	0,369
Pu-240	0,213	0,218	0,223	0,228
Pu-241	0,088	0,091	0,095	0,096
Pu-242	0,034	0,037	0,039	0,041

1.2.3 Stability consideration. - by H. ERNST - AEG.

Up to now there are no basic experimental informations on the dynamics of a TTBWR bundle available. Therefore, it was not possible to determine accurately enough the absolute stability of a given TTBWR.

Also, extrapolations from current BWR-design criteria and BWR-stability models seem to be not suitable without experimental results, because most of the parameters influencing the stability are different in a TTBWR. Both, the higher friction losses along the cooling channel and the higher power density of twisted tape fuel should lead to more stringent stability problems. The work which has been done is a comparison of the 12 reactor types given on table AIV regarding their relative stability.

The comparison should help to select some reactor types worthwhile for further detailed technical and economical evaluations. The basis for the comparison was the following criterion :

$$\frac{\text{void transit time}}{\text{fuel time constant}} \leq a$$

The value of a was determined to 0,074 according to AEG-design-standards for BWR's.

The reason for the choice of this criterion is, that the gain and phase lag of the transfer function "nuclear power - void reactivity" show always an improving relation with respect to total stability, if the ratio of void transport time to fuel time constant increases.

The fuel time constants for the rods of the 4 chosen lattices have been evaluated by the code "ANCO". This leads to a 4th order approximation from which the first order time constant has been employed for the above criteria.

The void transit time follows from thermohydraulic core calculations performed with the code "UMLAUF".

The following results have been obtained :

Fuel diameter (mm)	Max. Void- transit time (s)
10,2	0,73
8,9	0,57
7,9	0,47
7,1	0,39

The comparison of these values with the calculated travelling times gives a first approach of the stability behaviour. Table A VIIIa summarizes these results.

TABLE A VIIIa

	R1	R2	R7	R8	R9	R12
Calculated travelling time (s)	0,620	0,569	0,5236	0,4965	0,449	0,3435
Calculated limit (s)	0,73	0,57	0,57	0,57	0,45	0,36
Stability expectation	stable	just stable	stable	stable	just stable	stable

Theoretical and experimental studies will be performed during the continued TTBWR Research and Development Program in order to get the necessary informations for more detailed stability calculations.

1.3 Subtask A.3 - Definition of Reactor components - by K. H. THEISSL.

Under this subtask, the 6 reactors, the characteristics of which are listed in Table A IV, were analyzed in order to get a survey referring to economical investigations.

The components of the projected reactors are described below.

1.3.1 Description of the Reactor Vessel.

The main characteristics of the six variations are given in Table A IX.

TABLE A IX

Estimated data of the Reactor Vessels

	Ref	R 1	R 2	R 3	R 8	R 9	R 12
Power density kW/1	35,80	51,7	63,7	63,7	63,7	78,8	95
Vessel length m	19,2	19	19	18,5	18,4	18,3	18,15
Vessel diameter m	5,55	5,16	4,75	4,92	5,16	5,0	4,75

The inside diameter had been determined considering the water shielding and the area required by the internal pumps. The vessel length is mainly caused by length of core, length of control rods, steam-separators and dryers.

1.3.2 Steam separators and dryers.

The steam separators are of the AEG downcomer separator type, as they will be used in the Lingen KWL Reactor. 188 separators are necessary in each case of this study. They are located in the upper part of the downcomer and let the core free for refueling.

In order to keep the pressure vessel diameter as small as possible (i.e. the diameter required by the water shielding and the space needed by the internal recirculation pumps), it was necessary to find a very compact downcomer separator arrangement. Therefore it was required to change the separator inlet direction from tangential to axial in view to avoid the voluminous entrance boxes of the tangential separators.

Fig. A.10 shows a schematic design of the downcomer separator arrangement with both entrance directions. The number of cyclones of the axial entrance flow direction type that can be installed in the downcomer is about 1,5 times as much as in the case of tangential inlet direction.

Fig. A.11 shows a separator with axial entrance flow directions.

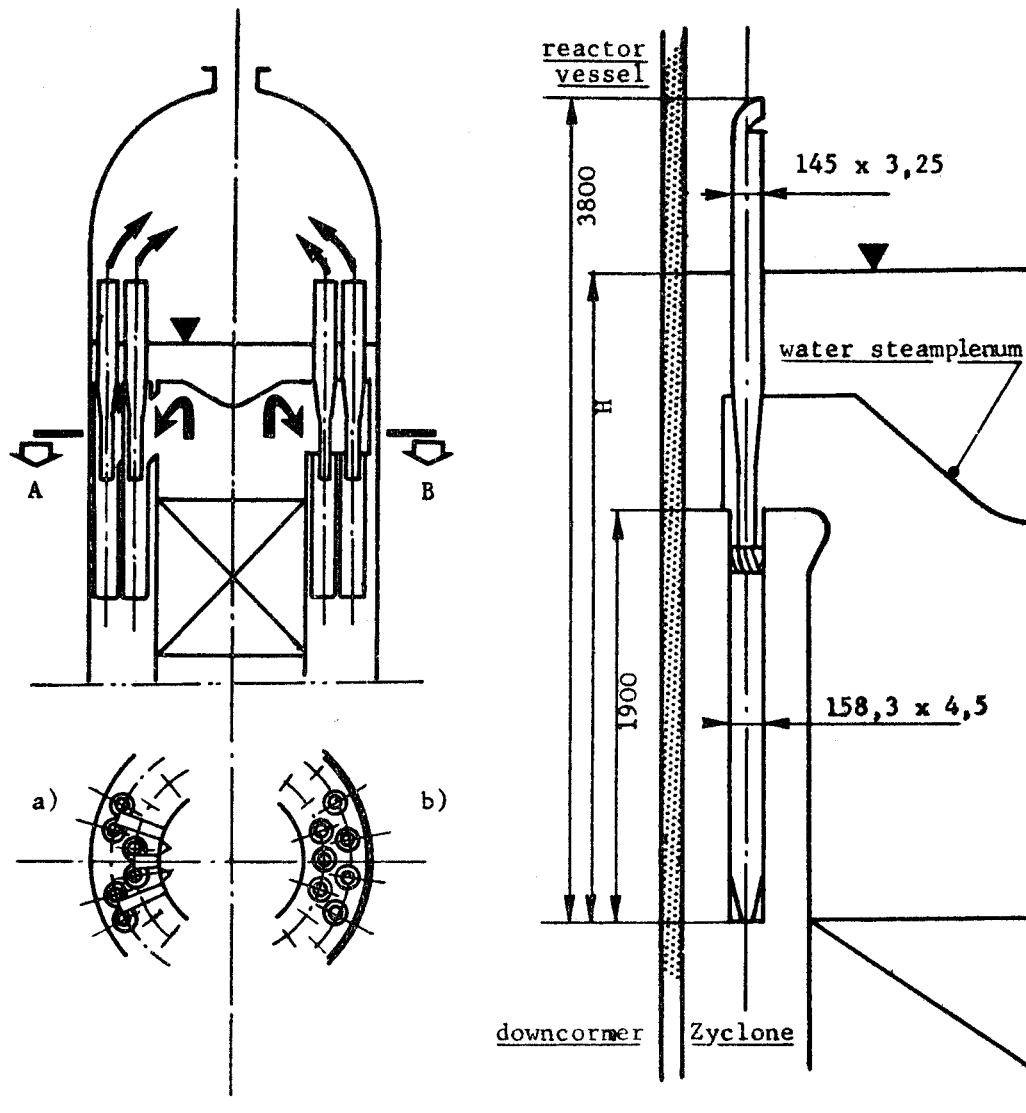


Fig. A10 - AEG-type Downcomer Cyclones for Internal Steam Separation.

Efficiency of Downcomer in Case of

- a. tangential inlet into the Separator
- b. axial inlet into the Separator

1.3.3

Recirculation pumps.

For all the Reactors of this study, recirculation pumps of the AEG internal type are proposed. The pumps are arranged in the recirculation chamber around the control rod guide tubes area. The pump driving shafts penetrate the bottom of the reactor vessel through a forged steel reinforcing ring.

The recirculation flow can be controlled in a range from 1 to 5.

The pumps are designed for an overpower of about 15%. Table A X shows the different pump requirements.

Fig. A11 - AEG-Steam Separator for Reactor Power up to 600 MWe.

TABLE A X

Pressure drop, Number of pumps and Power requirements

	R 1	R 2	R 7	R 8	R 9	R 12
Pressure drop at.	2,0	2,15	2,04	2,0	2,16	2,7
Estimated number of pumps	5	4	5	5	4	4
Power requirements of the pumps MW.	2,2	1,74	1,84	2,32	1,8	2,33

1.3.4 Reactor general arrangement.

Fig. A.12 shows the general arrangement of the reactor.

Because of the reactor size, a pressure suppression system will be needed as a suitable containment. The pressure suppression system size is mostly dependent on the size of the reactor steam outlet pipes. Only rough estimations of this was made in order to get the economical influence.

1.4 Subtask A.4 - Economic calculations - by H. MATTERN - AEG.

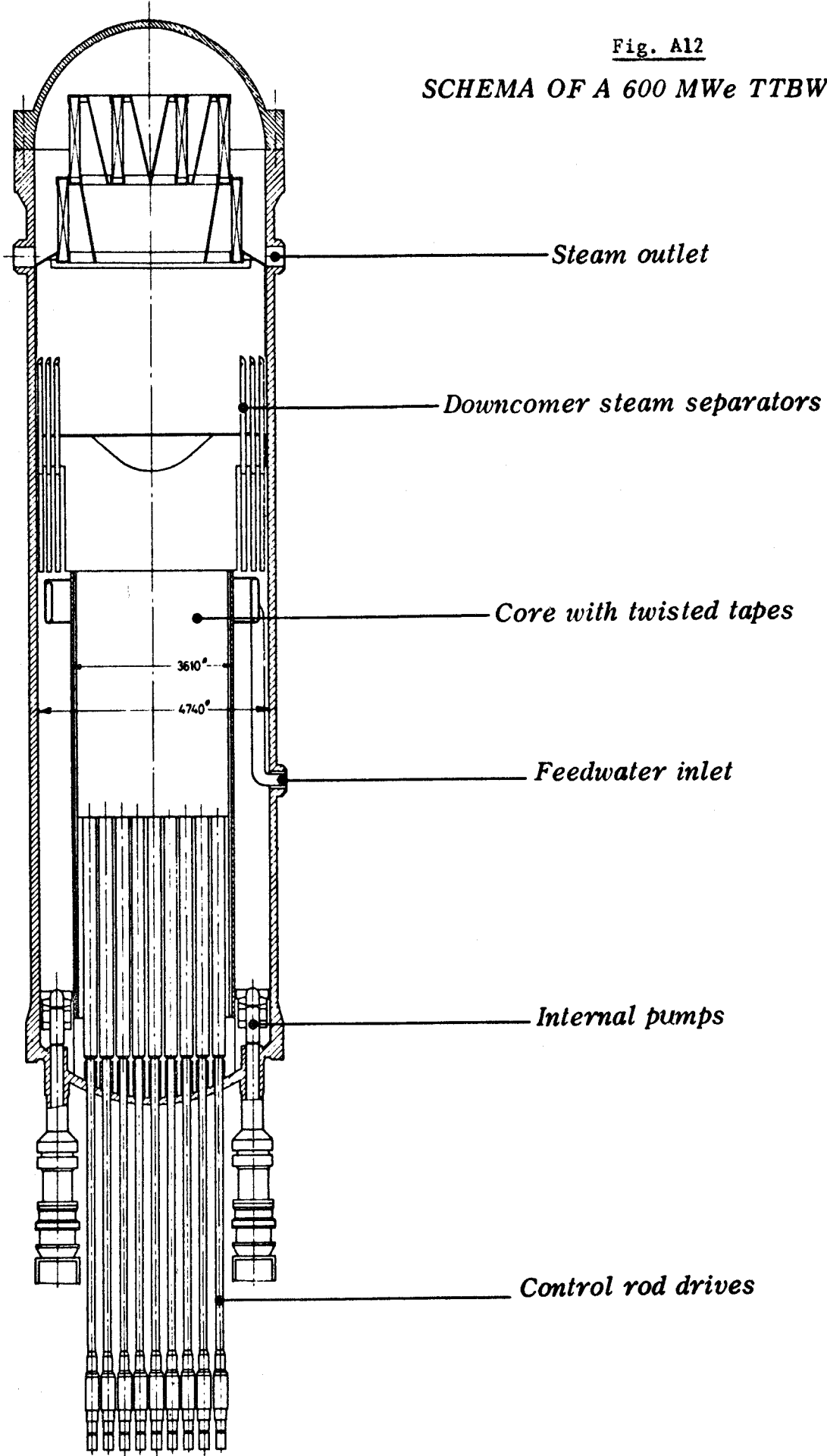
In the early 66 a first comparison was made (31) between a normal BWR and a TTBWR. Although this study was not optimized the results showed considerable cost reductions. Further a parametric study was performed in order to find the reactor with the lowest costs. In the preceding chapters the physics and the thermal hydraulic design calculations of the various TTBWR's were described.

As shown (Tables A VII and A VIII) two cases have been considered dealing with the cycle length. Because of maintaining a favorable power distribution and fuel handling procedure, a maximum of 25% of the elements have been considered to be replaced by unexposed fuel at the end of one cycle.

This is identical with the range of one fuel element within a control rod cell (scatter reloading). In order to keep a one year cycle, the burnup has to be increased consequently (Case No. 1). Up to now there are some uncertainties involved in this procedure e. g. the application of a large amount of burnable poison in order to handle the necessary excess reactivity and the mechanical integrity of the fuel elements for high burnups. The other possibility (Case No. 2) would be to keep the burnup as presently warranted in Boiling Water Reactors and to decrease

Fig. A12

SCHEMA OF A 600 MWe TTBWR



the cycle length below the one year's margin. Both cases has been calculated with respect to the fuel cycle costs.

The present worth method has been used for these calculations. This method is described in several publications (★) (★★) (★★★), the calculations were made using the following assumptions :

Hours of operation per year	6 500 h
Plant life time	17 a
Interest	7 %
Taxes	3 %
Operation efficiency	0,9664
Transportation for spent fuel	40 DM/kg U
Reprocessing	120 DM/kg U
Re-conversion costs for Uranium	22,4 DM/kg U
Re-conversion costs for Plutonium	6 DM/g Pu
Price for fissionable plutonium	40 DM/g Pu

The costs of the enriched uranium were taken from the AEC price list 1962.

Calculations showed equal fuel fafrication costs for twisted tapes and normal fuel spacers. Therefore the difference in the fabrication costs is given by the difference of the fuel rod size only.

Table A XI gives the differences in the fabrication costs.

TABLE A XI

	R 1	R 2	R 9	R 12
Fabrication costs Increase relative to normal BWRs.	43 DM/kgU	78 DM/kgU	142 DM/kgU	238 DM/kgU

It is believed that possible improvements in fabrication methods will lead to lower costs. It has been shown (★★★★) by a similar study that a decreasing pellet diameter will result in increased fabrication costs. So a 9,5 mm diameter pellet will cost 41,-- DM/kgU more than a normal BWR pellet. This is somewhat below our calculations.

-
- ★ M. SCHMALE et al. - Verfahren zur Berechnung der Brennstoffkreislaufkosten von Kernkraftwerken in Form eines festen und eines variablen Kostenanteils. - Wolkonferenz II C, Bericht 128, p. 1-23
Brennstoff-Wärme-Kraft 16 (Sept. 64) - Nr. 9, p. 448-453.
 - ★★ N. GRÜMM - Vereinfachtes Verfahren zur Berechnung des Brennstoffkostenanteils. - Atomwirtschaft 11 (Febr.1966) - Nr. 2, p;76-81.
 - ★★★ Euratom Economic Handbook, Vol. 1 - 1966.
 - ★★★★ Final Report 600 MWe High Power Density BWR. Core-conceptual design, GEAP 4974.

The results of the fuel cycle costs calculations are shown in Table A XII. The numbers are given in differences between normal BWR and TTBWR.

TABLE A XII

	R 1		R 2		R 9		R 12	
	Case 1	Case 2						
Savings in the costs for electricity DPf/kWh	0,047	0,030	0,049	0,029	0,047		0,047	-0,068

Case 1 : one year cycle

Case 2 : constant burnup

Reactor R 9 Case 2 has not been calculated because of the foreseen tendency as indicated in table A XII.

One result of an earlier optimisation study should be also mentioned. The reactor types R 2, R 7 and R 8 had the same power density but different core shapes. The reason was to study the influence of reduced pumping power and slightly decreased fuel enrichment changing the active fuel length. The results showed clearly an advantage of long fuel elements because of the fabrication costs which are dominant. Therefore the reactor types R 7 and R 8 were not longer considered.

It is obvious that the total cost savings will be mainly influenced by the capital costs, which will be reduced in the case of a TTBWR compared to a BWR, due to the smaller size of the nuclear system according to the higher power density. Having the same electrical output there are no changes to be made in the conventional parts of the plant. Among the components of the nuclear steam supply system, which will influence the costs by its decreased size are : pressure vessel, recirculation pumps, pressure suppression system, control rods, control rod drives, steam separators. Only the change of these parts has been taken into account. Special attention has to be paid to the number of control rods. Case 1 requires to a large extent burnable poisons. If this method should be applied to the reference case also, the same reduction in the number of the control rods should be possible. On the other hand the larger bundles offer some disadvantages, s. a. complex fuel handling, poor power distribution and severe fuel loading accident conditions. To be conservative there was no reducing of the amount of the control rods considered. Case 2 would allow a significant reduction

of control rods because the same amount of burnable poison will be used as in the reference case. Detailed calculations showed an approximate offset of the plant cost savings coming from fewer control rods by the lower annual operation time due to additional fuel loadings.

Steam separators will require more development works because of the unusual steam conditions. There are certainly cost reductions involved but no credit has been taken to that because of the so far involved uncertainties. Some changes in other plant components are also possible but they were not considered with respect to their effects. It should be noted however that they act in direction of further cost reductions.

In Table A XIII the differences in plant costs related to the reference case are listed.

TABLE A XIII - PLANT COST SAVING (DM)

	R 1	R 2	R 9	R 12
Pressure vessel	+ 1 680 000	+ 3 450 000	+ 2 870 000	+ 4 440 000
Pressure suppression system	+ 250 000	+ 400 000	+ 350 000	+ 500 000
Recirculation pumps	+ 1 200 000	+ 1 800 000	+ 1 800 000	+ 1 800 000
Miscellaneous	+ 280 000	+ 420 000	+ 420 000	+ 420 000
TOTAL	+ 3 410 000	+ 6 070 000	+ 5 440 000	+ 7 160 000
Specific plant cost savings DPf/kWh	+ 0,016	0,029	0,026	0,034

The prices are based on actual offers from suppliers for different plant sizes. If necessary, interpolation had been made.

The specific plant cost reductions were calculated according to the conditions used in the reference case. In addition to that, several taxes had to be taken into account. A detailed breakdown led to the following equivalence :

$$\pm 2.100.000,-- \text{ DM} = \pm 0,01 \text{ DPf/kWh}$$

Finally the following results could be obtained, showing total cost savings for the various TTBWR's, compared to a normal BWR.

TABLE A XIV

	R 1		R 2		R 9		R 12	
	Case 1	Case 2						
Total cost savings	+0,063	+0,046	+0,078	+0,058	+0,073	-	+0,081	- 0,034

2. TASK B - PREPARATION OF A PROTOTYPE FUEL ASSEMBLY FOR AN IN-PILE EXPERIMENT.

Under this task, it was planned to prepare an in-pile experiment on a prototype fuel assembly with twisted tapes. The purpose of this experiment was to test a T.T. fuel element in actual reactor conditions and to check the safety of its operation. As it was decided to perform this experiment in the Kahl VAK Boiling Water Reactor, it was not possible to reach High Power Density conditions because this reactor is of the natural circulation type. However the interest of this in-pile experiment is still very important as it should give information about corrosion, and specially fretting corrosion behaviour, of the T.T. fuel element under actual reactor conditions : irradiation and water chemical composition.

This task includes the following work :

- The design of the experimental bundle,
- Safety calculations which are an investigation of the thermal-hydraulic behaviour in order to guarantee sufficient burn-out margin during operation,
- Fabrication of the prototype fuel assembly.

2.1 Subtask B.1 - Design of the prototype T.T. fuel assembly. by A. ROSUEL,
(SNECMA)

2.1.1 General features of the design.

The purpose of this work was to design a twisted tape fuel element to be inserted in the VAK Kahl reactor to see the behaviour of such a fuel element under irradiation with the main purpose of an investigation of the fretting corrosion between the twisted tapes and the fuel rod claddings.

For the design of this fuel element it was tried to avoid major modifications of the geometrical characteristics of the standard Kahl element.

After thermal hydraulics and physics calculations the following dimensions were fixed :

- | | |
|--------------------------------|----------|
| - number of rods | 36 |
| - box internal dimension | 119 mm |
| - fuel rod O.D. | 14,4 mm |
| - lattice pitch | 19,03 mm |

During the design it was necessary to take into account particular assembling requirements. The following assembling operation sequence was foreseen :

- Fastening of the twisted tapes package to the lower casting,
- Insertion of the fuel rods into the twisted tape package,
- Fastening of the upper casting,
- Mounting of the channel.

2.1.2 Modifications of the conventional parts.

The first problem was to reduce the folding radius at the channel corner (See § 1.1.4.2). With respect to the geometrical requirements for the control rods a minimum radius of 5,5 mm was chosen.

The fastening of the Twisted Tapes package to the lower casting is achieved by the following way : two tapes, each of them in the middle of two opposite sides of the package, are ended by an about 45 mm long, non twisted part which is screwed to the casting. Fig. B1 and B2 show a schematic drawing and a photograph of this feature.

To avoid scratching of the rod surface by the twisted tapes during the assemblage, the rods should not be screwed into the lower casting as they are in the standard assemblies. For this reason, two rods at each corner of the fuel element are fastened by pins (see fig. B3).

The lower and the upper castings are standard Kahl fuel element parts but, because of the lattice pitch modification, the holes for the endplugs are bored with a pitch equal to 19,03 mm.

2.1.3 Characteristics of the twisted tapes.

The twisted tapes are of the usual cruciform type. The material is Zircaloy 2. The tape thickness is 0,2 mm.

The reduced half pitch of the twisted tapes is defined by

$$y = \frac{\text{helicoïd pitch}}{2 \times \text{lattice pitch}} = 3$$

The total length of the rod (1595 mm) corresponds to 14 helicoïd pitches.

A general drawing of the prototype fuel assembly is shown on Fig. B4.

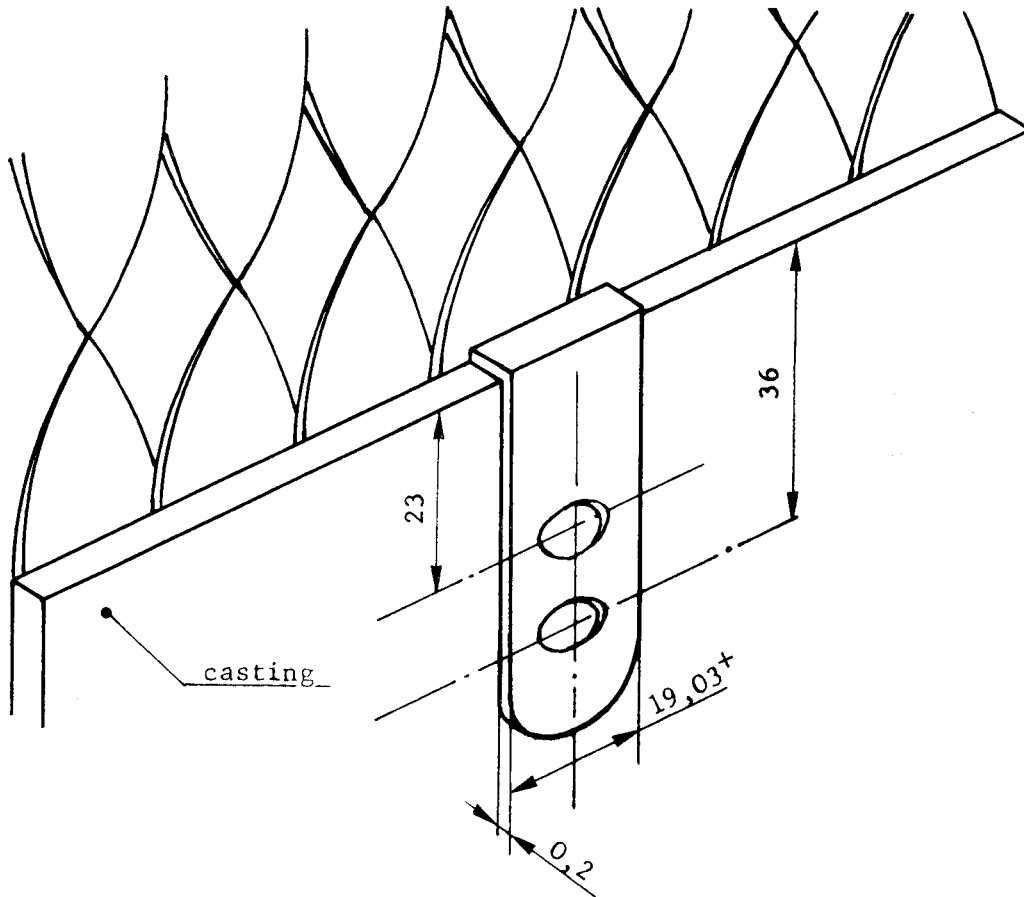


Fig. B1 - TWISTED TAPES PACKAGE FASTENING TO THE LOWER CASTING

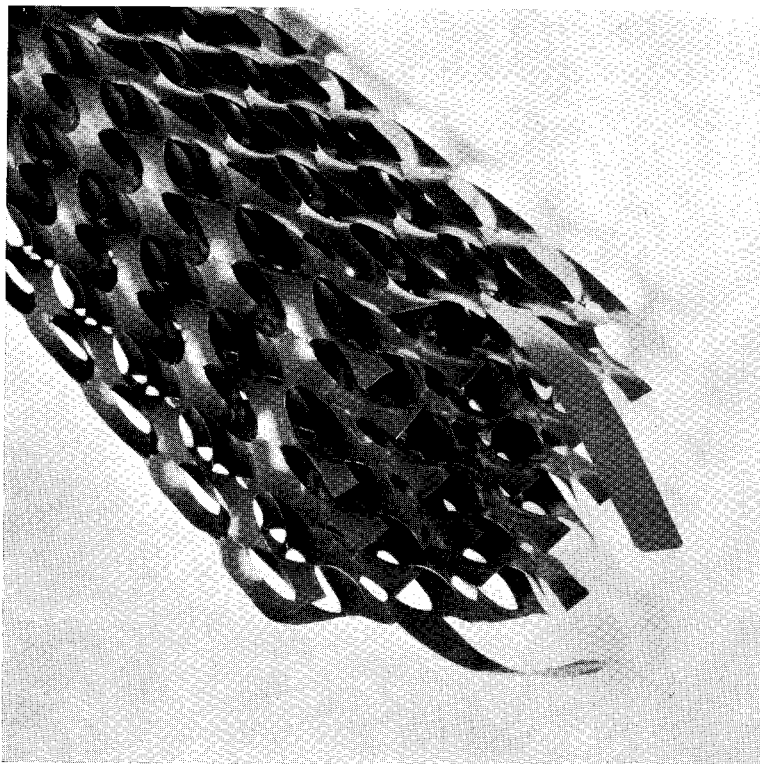
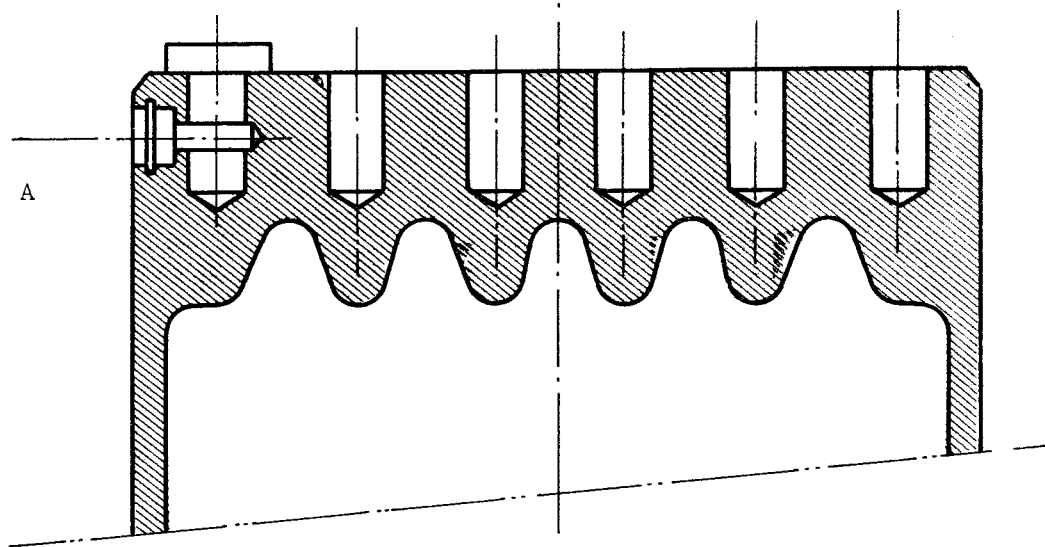
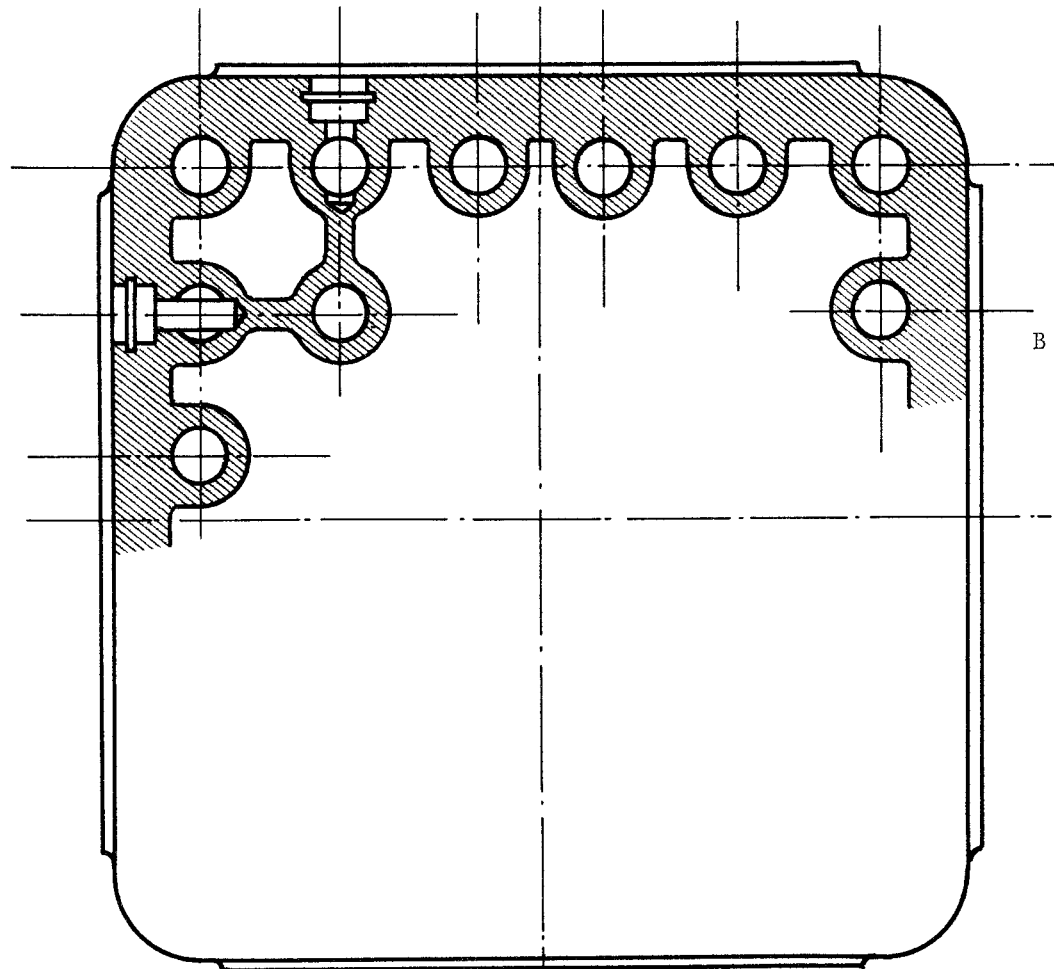
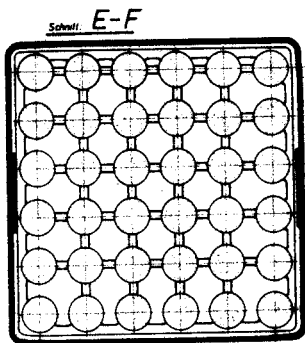
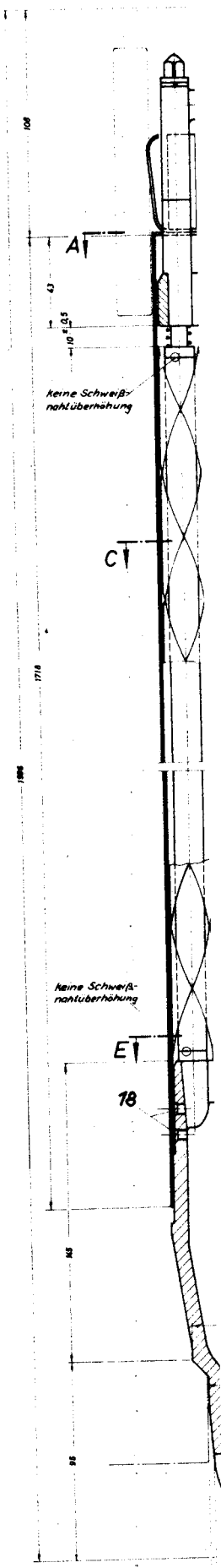


Fig. B2 - LOWER END OF THE TWISTED TAPES PACKAGE

Fig. B3 - PIN FASTENING OF THE FUEL RODS





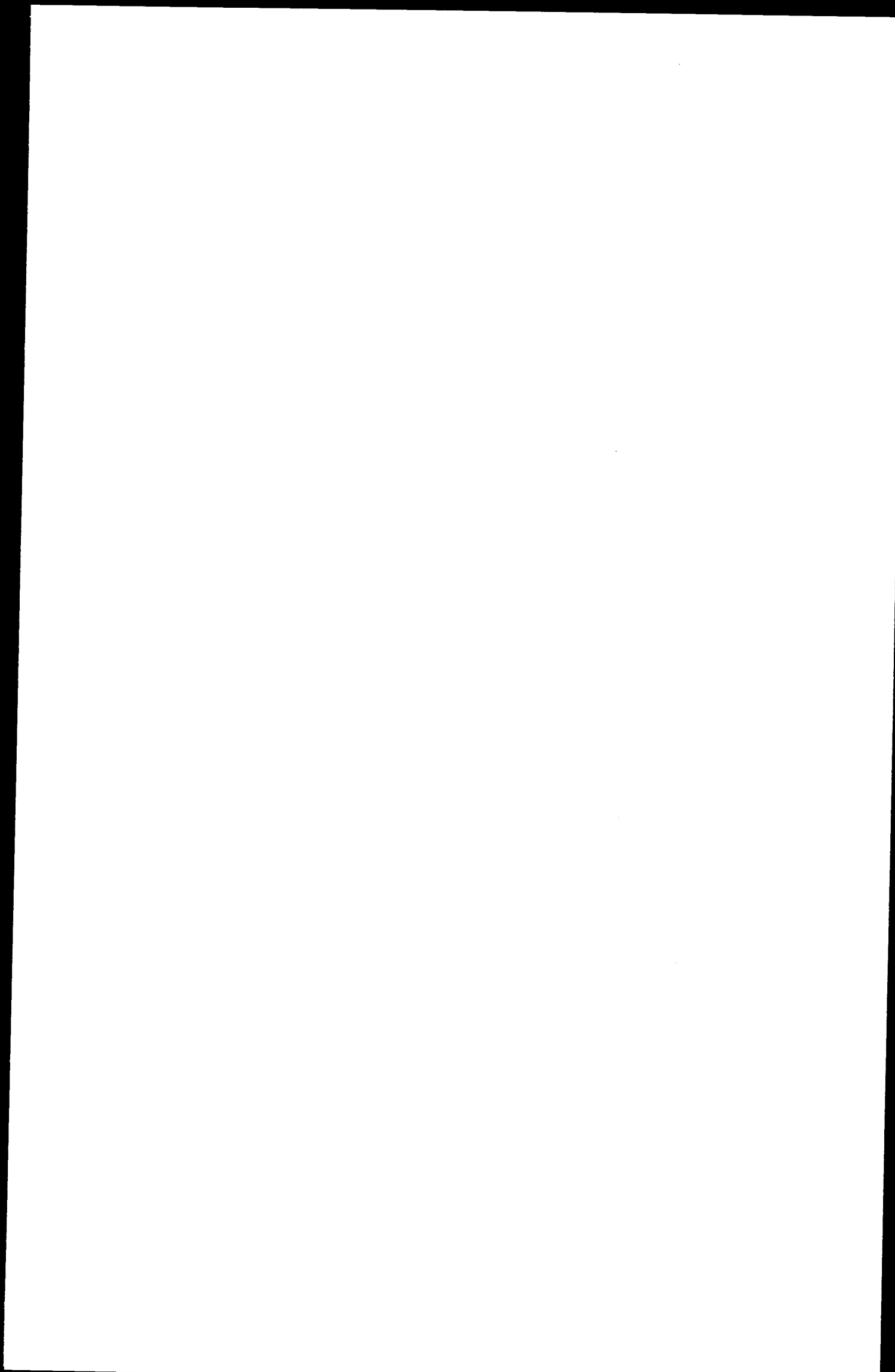
Die Abmessungen sind in mm angegeben. Die Toleranzen sind in der Zeichnung angegeben. Die Maße sind in der Zeichnung angegeben.

Nr.	Bezeichnung	Menge	Abmessung	Zeichn.-Nr.	Werkstoff	Bem.
16	Senkschrauben	16	A 4-6 DIN 913	Nr. 4550		
17	Spindelbolzen	17	BE 10000-2-2	Zirkonleg.		
18	Unter-Schraube	18	BE 10000-1-6	Nr. 4308		
19	Elementstift	19	BE 10000-1-7	Zirkonleg.		
20	Kylinderring (E)	20	4 x 8 x 20 DIN 7	Nr. 4550		
21	Elementstift (E)	21	BE 10000-2-6	Zirkonleg.		
22	Elementstift (E)	22	BE 10000-2-6	Zirkonleg.		
23	Druckfeder	10	10 x 10 x 19-8	Inconel		
24	Schraubenschlüssel	3	M 16 x 120	Nr. 4571		
25	Druckfeder	8	8 x 8 x 43-18	Nr. 4550		
26	Druckfeder	7	BE 10 000-1-5	Nr. 4308		
27	Druckfeder	6	BE DIN 127	Nr. 4310		
28	Druckfeder	5	60 1002-11-8	Nr. 4571		
29	Druckfeder	4	60 1002-11-7	Inconel		
30	Druckfeder	3	100 x 1002-11-3	Nr. 4308		
31	Druckfeder	2	BE DIN 127	Nr. 4310		
32	Druckfeder	2	60 1002-11-8	Nr. 4571		

Brennstoffstabbündel mit Turbulenzförderern
 Testeinheit VAK-KANL
 BE 10004-0-3

Maßstab: 1:1
 Zeichnung: 1:1

AGS
 ESE



2.2 Subtask B.2 - Preparation of the in-pile experiment Safety calculations,
by K. H. THEISSL (AEG)

2.2.1 Introduction.

Under this subtask all the necessary thermal-hydraulic calculations have been done in order to prove the safety of the T.T. fuel bundle which was intended to irradiate in the reactor Kahl (VAK). The reactor Kahl is designed for natural circulation. An increase of the Critical Heat Flux by means of twisted tapes becomes effective at higher mass flow rates than they are possible in the Kahl reactor. It was therefore intended to run the bundle not to prove its reliability at a high power level but to look for expected corrosion effects. For this reason the bundle power was limited to the same power as a standard Kahl type element would have at the same position.

For this reason, the fuel enrichment has been kept as it is in standard reload batch, that is 2,5%.

Because of this conditions the T.T. fuel bundle can be handled for thermal-hydraulic calculations like any other normal fuel bundle used in this reactor.

2.2.2 Geometric data of the fuel assembly.

As Table BI shows it, geometrical data of both fuel rod assemblies, Kahl standard and Twisted Tape prototype are not essentially different.

TABLE BI
comparison of geometric data

	<u>VAK</u> <u>standard</u>	<u>T.T.</u> <u>prototype</u>
Channel box internal side length	119 mm	119 mm
Channel wall thickness	1,53 mm	1,5 mm
Rod outer-diameter	14,45 mm	14,4 mm
Number of fuel rods	36	36
Active length	1532 mm	1532 mm
Twisted tape thickness		0,2 mm
Material of channel box and T.T.	Zircaloy 2	Zircaloy 2
Twisted tape pitch		114 mm

2.2.3 Calculation of coolant flow.

The calculations of the coolant flow were accomplished by usual methods to ascertain the necessary circulation in the reactor. (*)

* GEAP 3317 - Reactor thermal and hydraulic analysis for 60 MW_t RWE (Kahl) Nuclear Power plant.

Pressure drop calculations have been done using experimental results from tests which had formerly been run by SNECMA on a Twisted Tape bundle.(*)

For reasons explained above (§1.2.1.1.2) the slip ratio was found using the MARCHATERRE and HOGLUND correlation (**). Subcooled boiling was taken into account by the methods of BOWRING (***).

As the power production of the T.T. fuel element is the same as of a normal VAK bundle it can be assumed that the influence of the test bundle upon the driving head in the chimney and - as a consequence - upon circulation flow through the other VAK bundles is negligible.

For calculations, the same equations were used as applied for other Kahl fuel element calculations (****).

Fig. B5 shows the normalized axial power distribution used for these calculations. It is the same as for other Kahl standard bundles.

On this basis the mass flow through the T.T. bundle was calculated as a function of the bundle power. Results are shown in Fig. B6.

Steam quality and void fraction distribution were also determined for different values of the bundle power. Fig. B7 shows channel exit steam quality and hot spot local steam quality as a function of the power. Fig. B8 shows channel average void fraction as a function of the power.

2.2.4 Calculations of the Critical Heat Flux Ratio.

The calculations of the CHFR were accomplished by two methods :
- by the comparison with limit curves widely used to investigate usual Boiling Water Reactor performances (*****)
- and by the comparison with the measured Critical Heat Flux on test bundles with twisted tapes.

-
- * Essais hydromécaniques sur une maquette d'assemblage combustible équipée de vrilles - par J. DOLLE, G. SOURIOUX et J. FREUND (SNECMA internal report).
 - ** Correlation for two-phase flow - by J. F. MARCHATERRE and B. M. HOGLUND - Nucleonics, August 1962.
 - *** HPR. 29 - OECD HALDEN REACTOR PROJECT - Physical Model, Based on bubble detachment, and calculation of steam voidage in the subcooled region of a heated channel - by R. W. BOWRING.
 - **** AEG-KEA Bericht Nr. 344 - Durchbrennsicherheit des VKL Bündel I.
 - ***** JANSEN and S. LEVY - Burn-out Limit Curves for Boiling Water Reactors APED 3892.

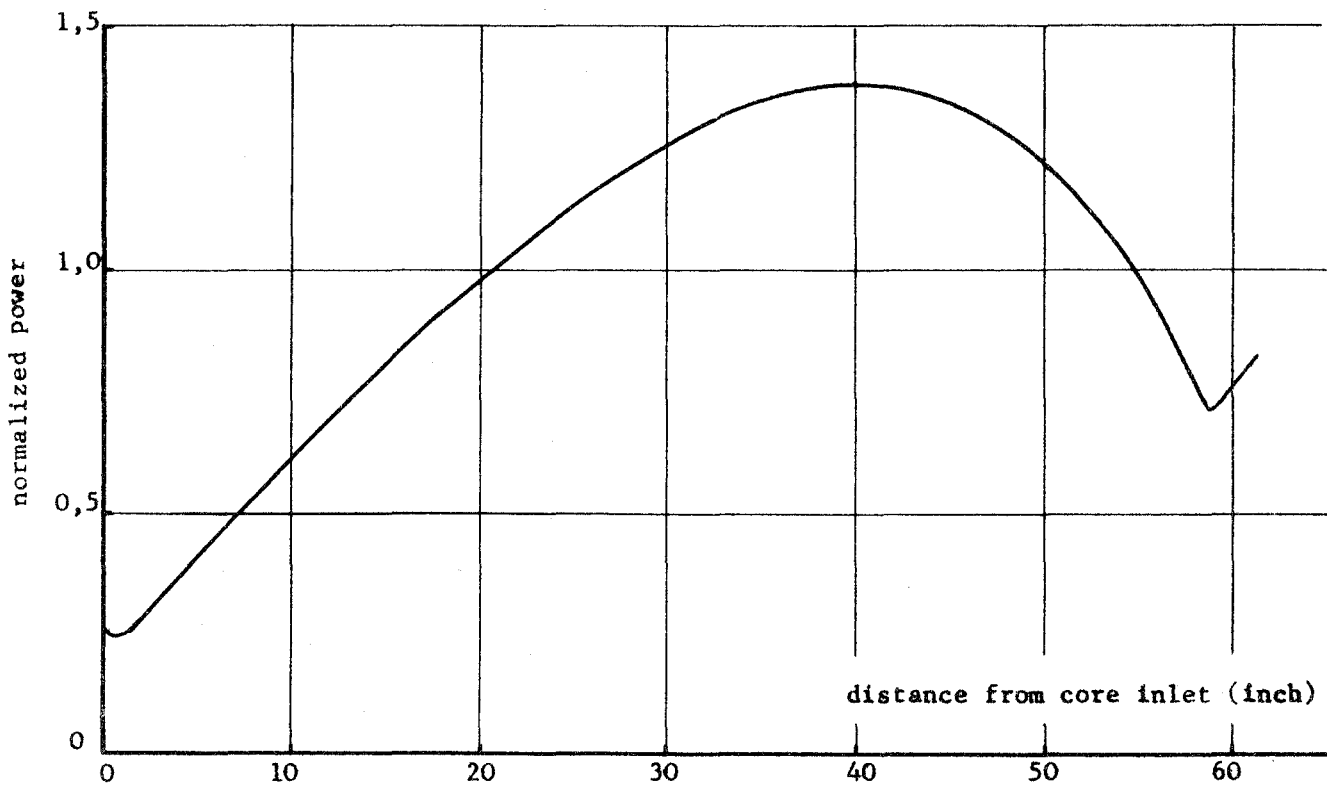


Fig. B5 - AXIAL POWER DISTRIBUTION

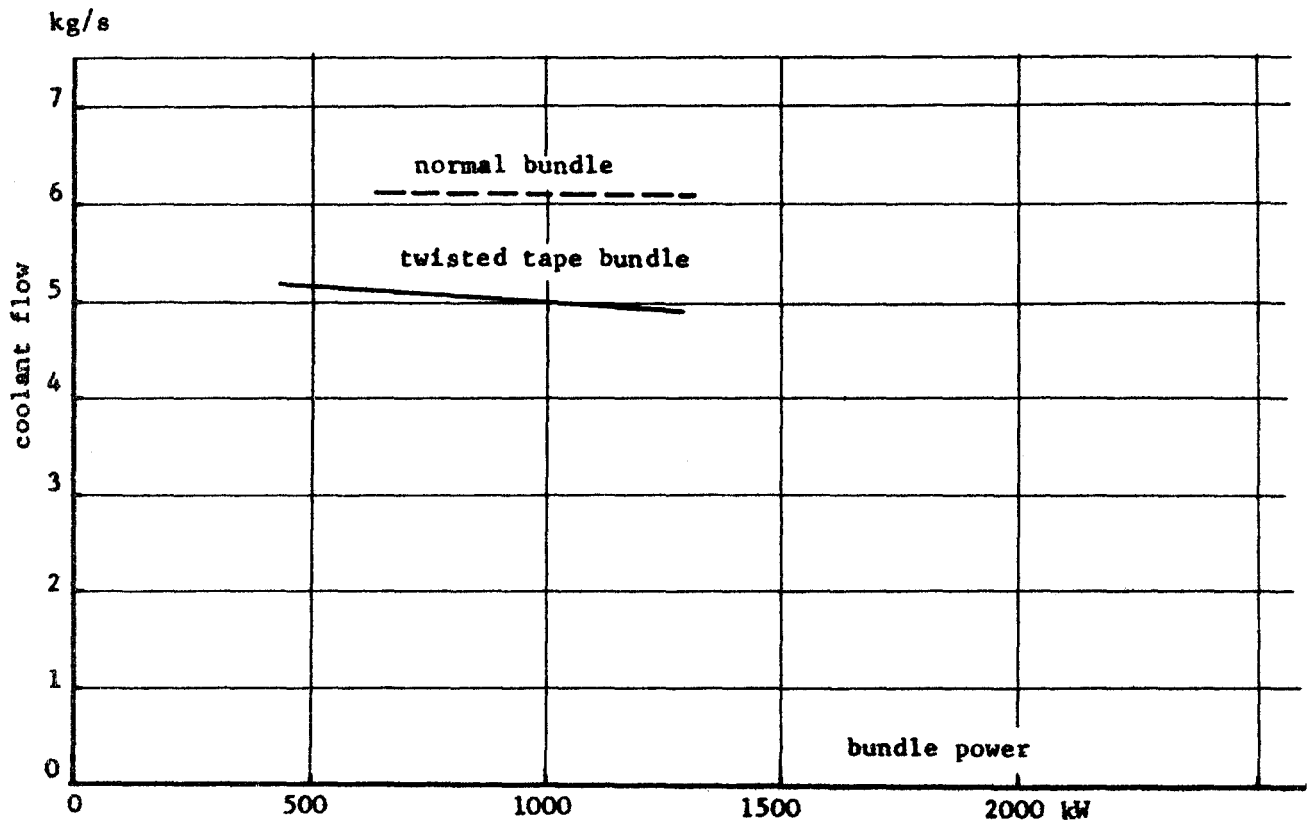


Fig. B6 - COOLANT FLOW AS A FUNCTION OF THE POWER

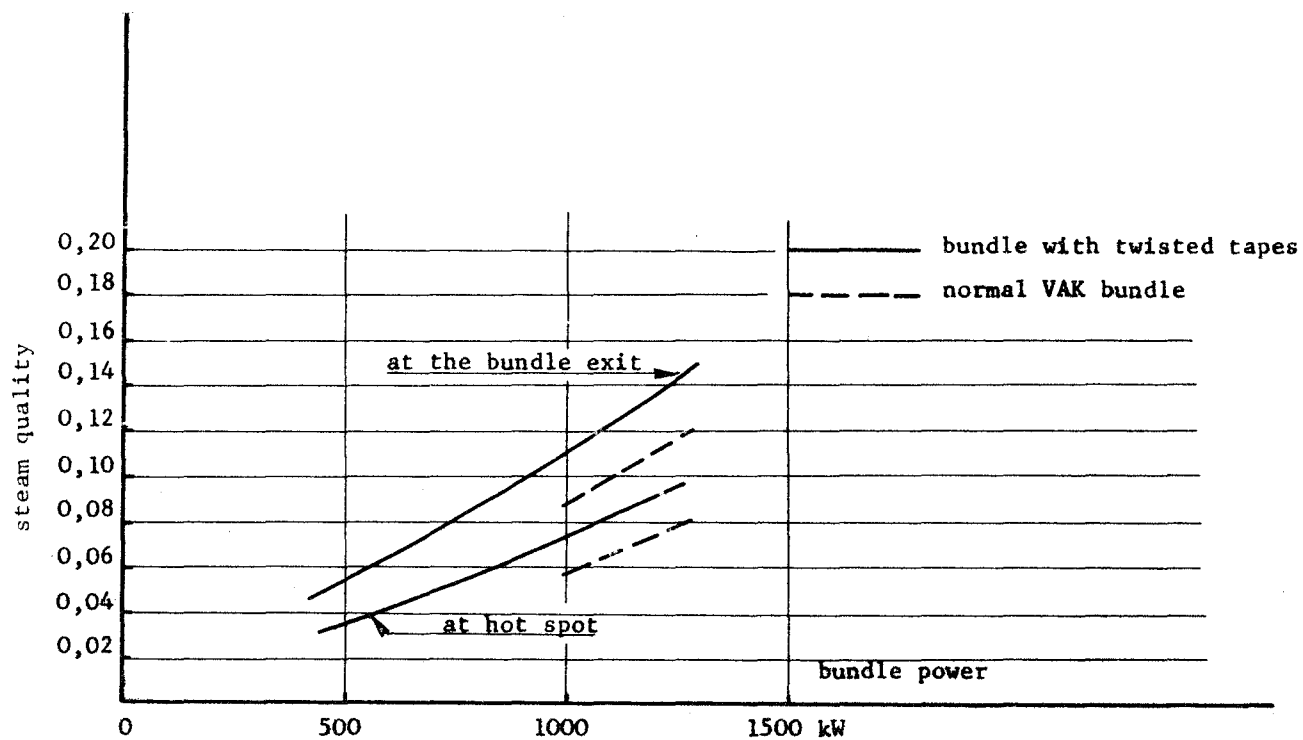


Fig. B7 - STEAM QUALITY AS A FUNCTION OF THE POWER

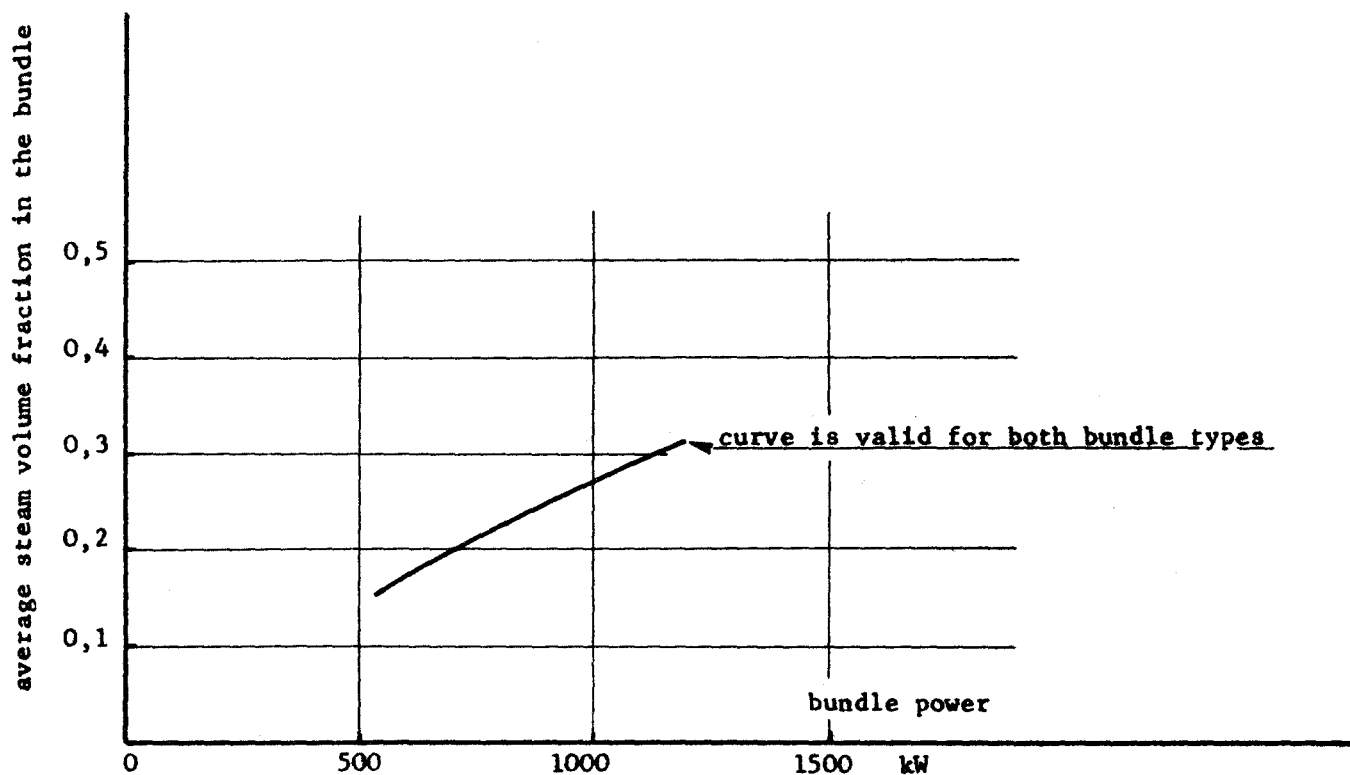


Fig. B8 - AVERAGE STEAM VOLUME FRACTION IN THE BUNDLE
AS A FUNCTION OF THE POWER.
(based on power distribution shown in Fig. B5)

While at mass flow rates corresponding to an inlet velocity of about 2 m/s the admissible CHF in T.T. bundles is about twice as high as in normal fuel bundles, there is no strong increase of the CHF at velocities like in natural circulation systems. The CHF of both bundles with or without twisted tapes will be consequently nearly the same.

For the calculation of the Minimum CHF the axial power distribution which is shown in Fig. B5 and which leads to an axial peaking factor of 1,4 was used. All the hot spot factors were taken from the Kahl thermal design report (page 26) and are listed below :

Corner Rod peaking factor	1,28
Microscopic Peaking factor	1,01
Overpower	1,14

The CHF is given by the equation :

$$S_{BO} = \frac{q_{crit}}{q_{aver} \cdot f_{over\ all}}$$

with :

S_{BO} = Critical Heat Flux Ratio

q_{crit} = Critical Heat Flux

q_{av} = average bundle heat flux

$f_{over\ all}$ = over all peaking factor

This results of the CHF calculations are shown in Fig. B9. It can be easily realised that both methods described lead to almost the same results : The CHF will be never smaller than 2 when bundle power is equal or smaller than 1280 kW corresponding to a hot channel factor of 1,87 which is the highest value that can be expected in the Kahl reactor.

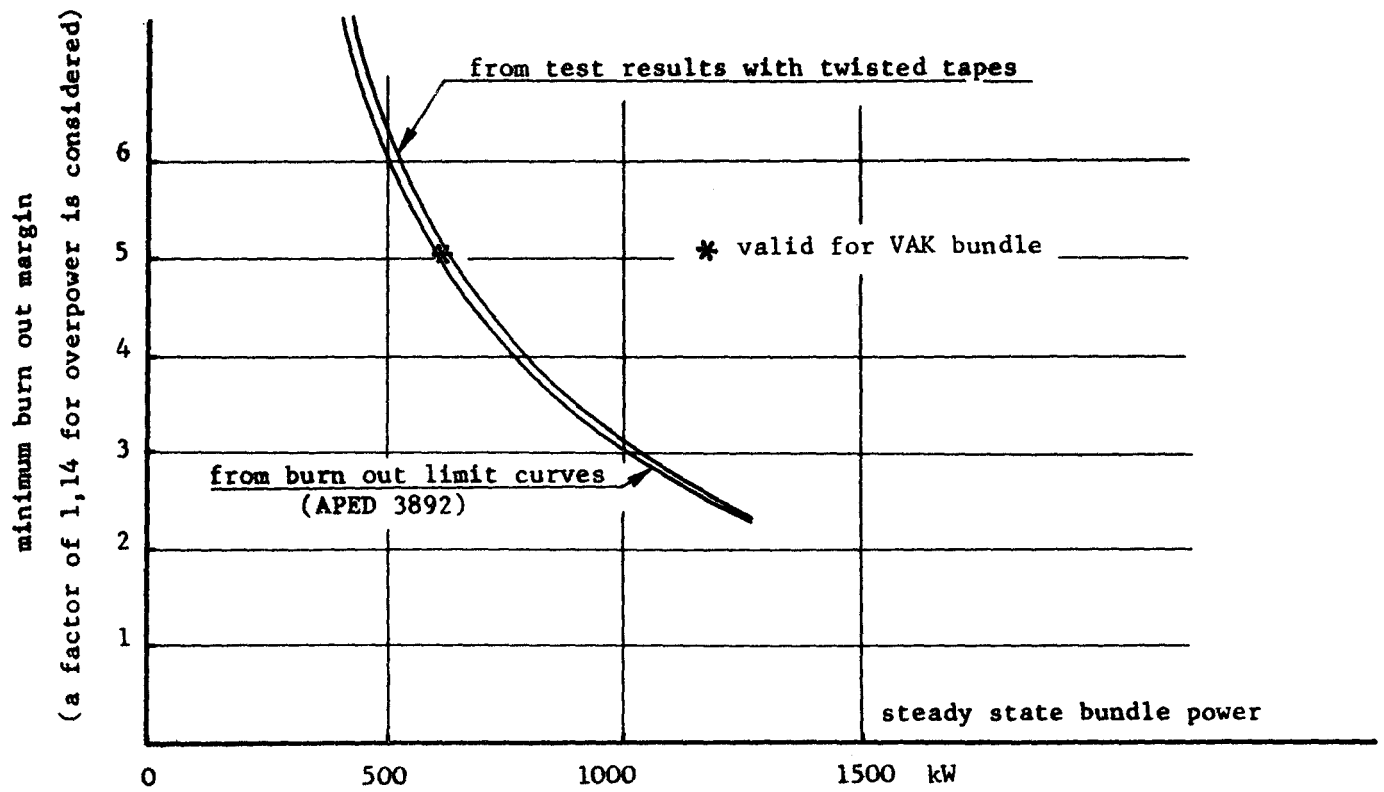


Fig. B9 - MINIMUM CHF AS A FUNCTION OF THE POWER
(curves are valid for bundles with twisted tapes)

2.3 Subtask B.3 - Fabrication of the twisted tape prototype fuel bundle.

2.3.1 The fabrication of the Twisted Tape package, by A. ROSUEL - SNECMA.

Zircaloy 2 material for the tapes was supplied by UGINE. The fabrication was done in different steps listed below :

- manufacturing of twisted tapes,
- cleaning in a bath defined by UGINE (1 vol. 2% $\text{FH-NO}_3\text{H}$ at 43°B for 2 vol. water)
- dimension control,
- electrical spot-welding with argon-shielding,
- grinding of the package sides with argon-shielding,
- quality control and cleaning,
- autoclavation,

These procedures have been defined after mockup tests especially to develop the welding process.

Molybdenum electrodes were used for the welding, Argon supply devices were fixed to both electrodes. During the assembly and the welding of the twisted tapes 14,5 mm diameter dummy rods and two grids were used to define the lattice pitch.

The purpose of the twisted tape package autoclavation was to check the quality of the weldings. It was achieved by a 24 hours exposure in vapor at 400°C. This autoclavation would make the oxygen and nitrogen pollution spots around the weldings come into sight.

Fig. B 10 shows the twisted tape cluster. This picture was taken after the autoclavation and no pollution appears around the welding spots.

After fabrication and control it was checked that :

- No pollution spot around the weldings were detected after the autoclavation process,
- Dummy rods with the same diameter as the Kahl actual fuel rods could be inserted into the twisted tape package without any difficulty,
- The bundle outer dimensions were consistent with the design tolerances.

It was also found that the twisted tape package was bowed for about 3 mm, which will not be considered as a matter of fabrication difficulties but has to be checked before a serial manufacturing process. It has also to be checked that the fuel rod pitch can be held within the design tolerances. Some differences of about $\pm 0,50$ mm were indicated.

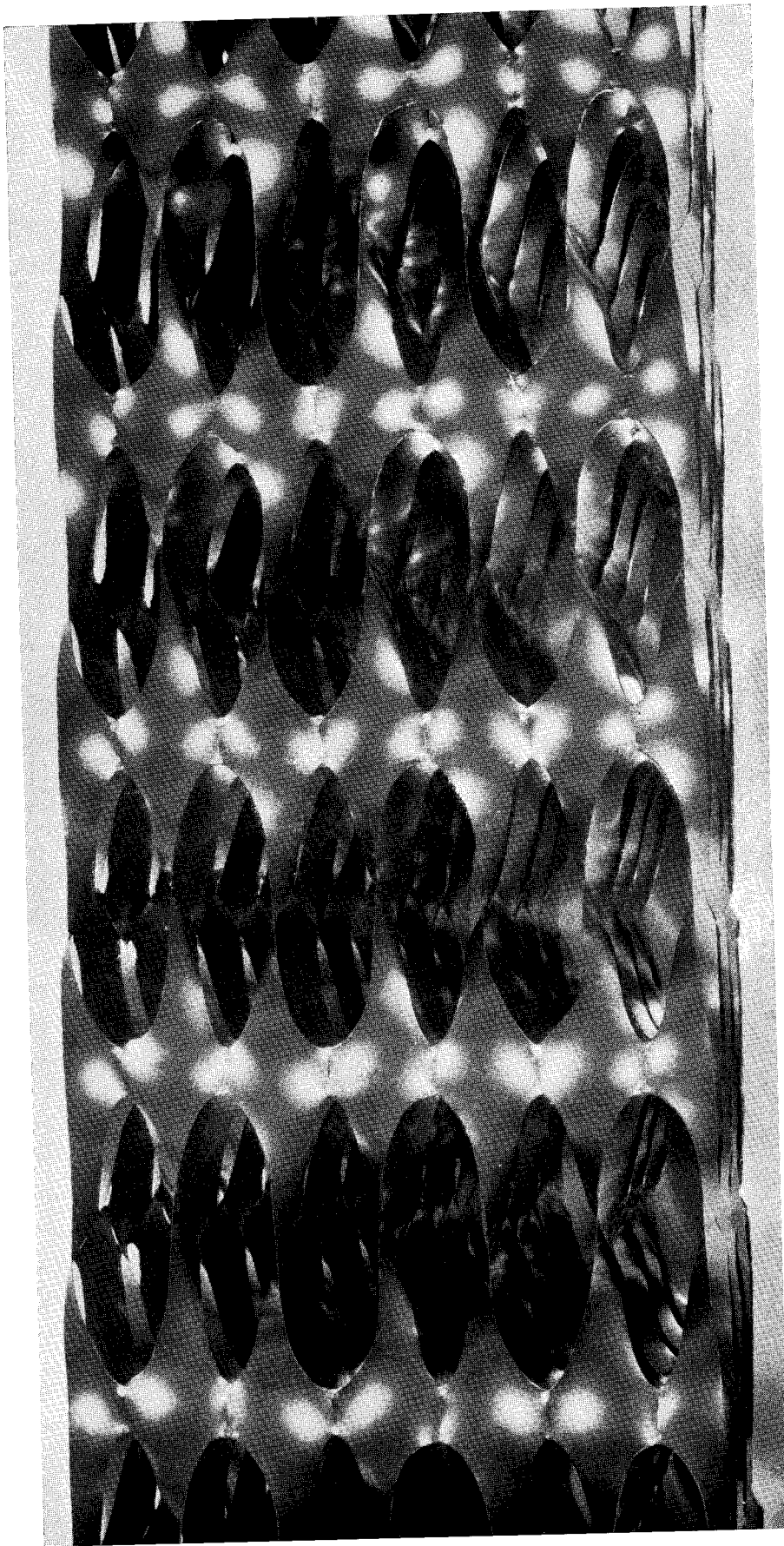


Fig. B. 10 - TWISTED TAPES PACKAGE AFTER AUTOCLAVATION

2.3.2 Manufacturing and Assembling of the Experimental Fuel Bundle.

by G. BECHTEL - AEG.

The construction of the twisted tape packages has been described in the previous sections, where the deviations in structure as compared with the standard Kahl elements were discussed. The following report therefore deals only with the fabrication and the assembling of conventional parts.

2.3.2.1 Fabrication of the fuel rods.

2.3.2.1.1 Fabrication program.

Treatment of the components

Tube	End plug material	Plenum springs	Al ₂ O ₃ disks	UO ₂ pellets
Arrival inspection	Arrival inspection	Arrival inspection	Arrival inspection	Laying out of the column sections
Autoclaving } De-oxidizing } outside work	Lower end plug	Hardening		Measuring the length
Dimension check	Upper end plug	Cleaning		Determining the weight
Supersonic check	Disks			
Visual inspection	Cleaning			
Cleaning				

Fabrication

- Lower end-plug welding
- Inspection of the welds (by X-ray or visually)
- Cutting off the tubes
- Loading the UO₂ column
- Inserting the Al₂O₃ disk

Inserting the Zircaloy disk

Inserting the plenum spring

Evacuation

Backfilling with helium

Putting in the Al_2O_3 ring and the upper end plug

Welding the upper end plug

Weld inspecting (X-ray, visual)

Helium leakage test

Rod inspection (dimensions, surface)

Cleaning

Welding into plastic bags

2.3.2.1.2 The testing of the tubings.

The outer and inner diameters of the tubings were mechanically tested. The wall thickness and excentricity were tested by the Vidigage process. Tests were made by means of a supersonic device for defects on the inner and outer surfaces. The results of these tests were very satisfactory. All the specified values were met. In the case of one tube only out of 48 the wall thickness was too high. The values were all noted and entered on the rod travel cards.

2.3.2.1.3 Welding tests.

The necessary welding parameters such as

Weld current

Weld voltage

Weld speed

Torch positioning

Argon supply

were determined in a test series. For this purpose, these parameters were varied for different samples. The optimal shapes of the end plugs and the optimal parameters were determined by roentgenological and metallographic tests on the specimen welds. The reproducibility of these optimal values was demonstrated in a second test series with constant weld parameters. Weld current and weld voltage were recorded at the same time.

For the proper insertion of the rods into the TT package, the maximum diameter of the tube was specified as the maximum diameter of the weld seam. It was found quite possible to adhere to these very

stringent conditions during the performance of the tests mentioned above.

2.3.2.1.4 Welding of the first end plug.

No difficulties arose during the welding of the lower end plugs (Fig. B11). The weld seams were visually inspected and also X-rayed. They were found to be entirely satisfactory. Current and voltage were recorded during the welding process. No irregularities could be ascertained on the recording instruments.

After every six welds, a test weld was carried out and examined by metallographic means. These tests showed completely satisfactory results.

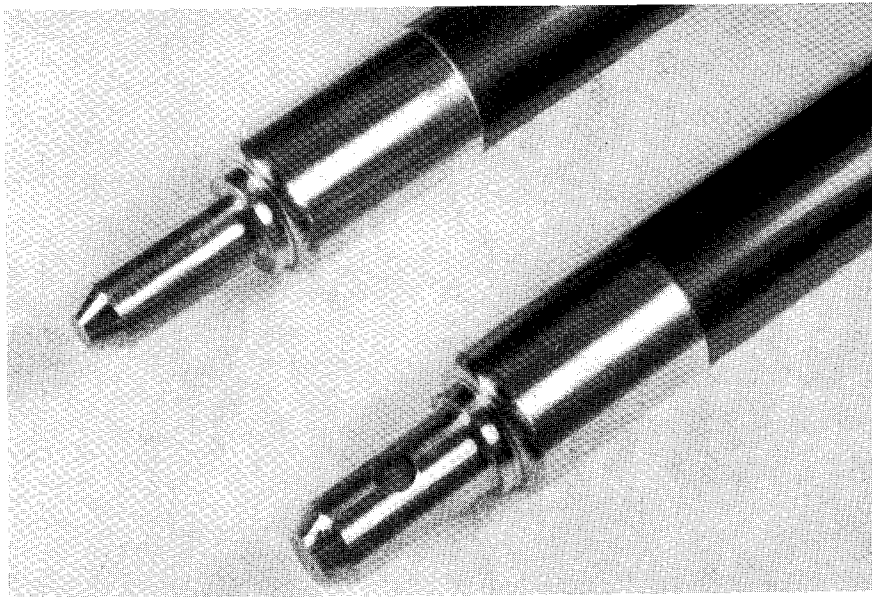


Fig. B. 11 - ROD END PLUGS

2.3.2.1.5 Uranium pellet loading.

It was not necessary to lay out the individual pellets to form fuel columns, since the manufacturer had already supplied column sections cut to length. Each fuel column consisted of six sections. The checks on the fuel columns included :

- Determination of the column length
- Determination of the column weight
- Determination of the water content of the pellets
- Determination of the specific gravity of the pellets
- Visual inspection of the pellets for peeling.

The length and weight of the columns were determined and entered on the rod travel cards. The column numbers given by the pellet manufacturer were noted.

The determination of the water content in the single pellets of various columns showed the excellent value of 3 - 5 ppm, so that no special drying of the columns was required before backfilling.

As a result of the visual inspection of the columns, some of the pellets which showed an inadmissible amount of peeling were replaced. The insertion of the fuel columns into the tubes was carried on manually using a loading bar. The length of the fission gas plenum was measured and entered in the rod travel card. Prior to further treatment, the fuel rods were thoroughly cleaned to prevent any traces of uranium remaining on the surface or in the weld zone. All work handling the fuel was carried out in a separate ventilated room.

2.3.2.1.6 Evacuation and backfilling with helium.

Evacuation and backfilling with helium were done in the vacuum plant room. The pumping and flooding times were defined during a test program. Before the fuel rods were connected to the vacuum plant, an Al_2O_3 disk and a Zircaloy disk were placed in the fission gas plenum and a helical spring was inserted. The upper end plug was pressed into the fuel rod by a ram. This process was complicated by the helical spring protruding from the plenum, and particularly by an Al_2O_3 ring which had to be pushed in between the spring and the end plug. After a holding device for the Al_2O_3 ring had been mounted on the end-plug support, the work proceeded without a hitch.

2.3.2.1.7 Welding the second end plug.

The fuel rods were welded immediately after they left the helium backfilling plant (Fig.B 12) to prevent back diffusion of the helium. For the welding of the upper end plugs the same parameters were used as during the welding of the lower end plugs.

A visual inspection showed that the weld seams were satisfactory. The X-ray tests showed that three rods had small blisters in the weld zone with a diameter of about 0,3 mm. Since our specification only permits blisters with a diameter of up to 0,2 mm, these three fuel rods were re-welded.

To check the reproductibility of the welds after every six welding processes, test welds were carried out, which were X-rayed and examined by metallographic means. All the tests gave satisfactory results.

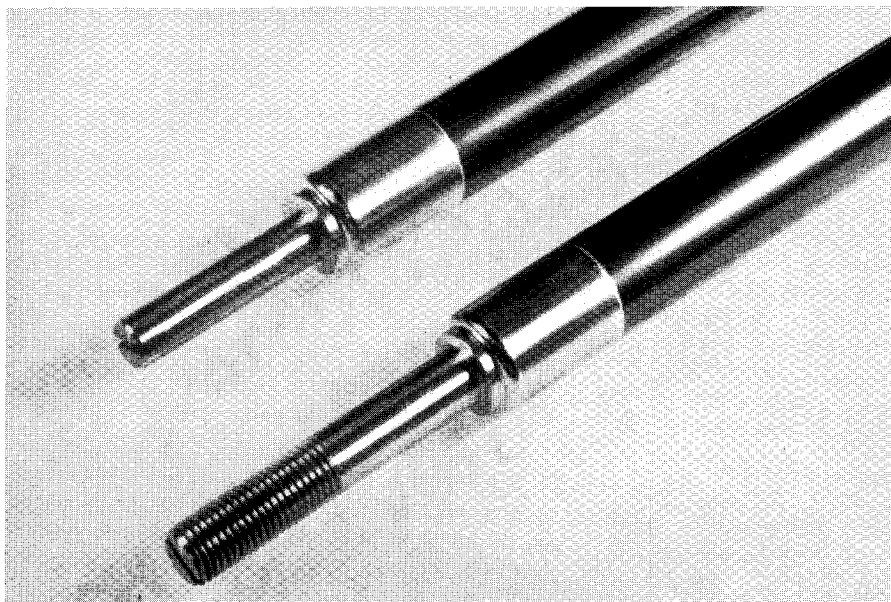


Fig. B. 12 - ROD END PLUGS

2.3.2.1.8. Final tests on the rods.

The fuel rods were finally checked by :

- Helium leakage test,
- Dimension check,
- Visual surface examination,
- Visual weld-seam inspection,
- Straightness test,
- Wiping test,
- Alignment deviation of the end plugs.

The results of the tests were all satisfactory. The test results were entered in the rod travel cards.

2.3.2.2. Tests and work on the twisted tape package after its delivery to the fuel shop.

During the arrival inspection, the length, corner width, flanging radius, angularity, length and width links, the deflection and the fuel rod hole spacing were measured and noted.

The TT package was too long and had to be shortened at both ends. The cutting points were defined during consultations with the manufacturer's representatives.

The specified deflection tolerance of 1,5 mm over the length could not be met. A maximum deflection of 4,8 mm was measured. The hole spacing did not agree with the specified values. The deviation for two channels lying side by side was as much as 0,5 mm (specification 0,05 mm). Since it was to be feared that the end plugs of the fuel rods would not fit into the tie plates, a training assembling was performed. This proved, however, that it was possible to mount the rods without any difficulty. The minimum spaces reached between the fuel rods conformed to the specification for the Kahl elements. During a following test, the Zircaloy channel was pushed over the TT package. It was thereby ascertained that the deflection mentioned above was of no significance for the assembling, due to the great elasticity of the TT package.

The securing links were adapted to fit the recesses in the lower tie plate and the holes for the countersunk bolts punched.

All the other components were also inspected at the arrival. The material certificates, material properties and analysis values were compared with the specified values. The results were entirely satisfactory.

2.3.2.3 The assembling of the bundle.

The bundle was assembled in a vertical position in an assembly device for Kahl bundles (Fig. B 13).

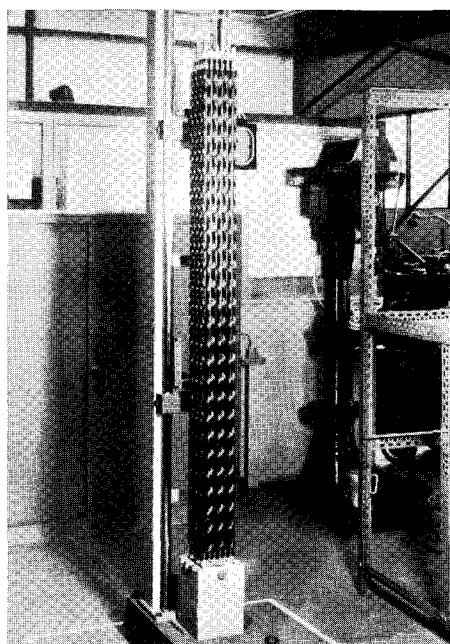


FIG. B. 13 - TWISTED TAPE FUEL BUNDLE FOR IRRADIATION IN THE KAHL REACTOR DURING ASSEMBLAGE IN A.E.G. LABORATORY AT GROSSWELZHEIM

The lower tie plate was inserted in the supporting basement and aligned. Then the TT package was put into place. The securing links of the TT package were bolted to the tie plate and both parts were aligned. The rods, the position of which was laid down in the planning, were inserted into the TT package.

It had already been ascertained during preliminary tests that after the insertion of the rods no scratches or any other damages could be observed on the autoclaved surface. Despite the measured deviations, it was found to be easy to push the rods into the TT package. After all the rods were in place, there was no longer any deflection observed in the TT package. Then the 8 rods were fastened to the lower tie plate by pins. These 8 rods have a thread on the upper end plug to which the upper tie plate is fixed. After placing the helical springs on top of the upper end plugs, the head portion of the bundle (upper tie plate) was put on, bolted down and secured (Fig. B 14).

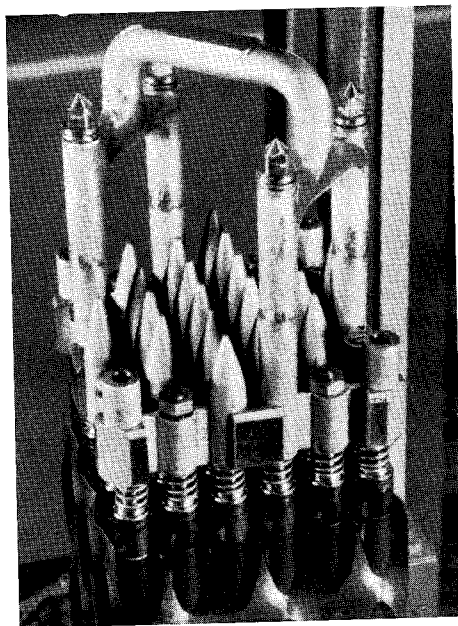


Fig. B. 14 - VIEW OF THE BUNDLE UPPER GRID

After the tests had been carried out on the bundle, the channel was pushed over it and bolted into the head portion.

2.3.2.4 Tests on the bundle.

The spacing between the individual rods was accurately measured in two planes and the values were recorded. The values determined were compared with those of the arrival inspection. It was thus shown that the spacing of the rods deviated by $\pm 0,4$ mm.

The straightness of the bundle was measured by the application of a special ruler and by scanning with a feeler gauge. The TT package had straightened up with the insertion of the rods to such a degree that the deflection lay within the specification limits.

The displacement of the bundle was likewise within the specified limits. After the channel had been pushed over the bundle, the deflection and displacement of the bundle were checked once again. After the assembly had been completed all parts were subjected to a visual inspection for any damage which might have occurred during the assembling. No such damage was ascertained.

3. TASK C - EXPERIMENTAL PROGRAM.

3.1 Subtask C.1 - Corrosion test.

Since the introducing of twisted tapes in a boiling water reactor has been considered, it has also been known that the corrosion problems induced by the tapes had to be solved. As a first step to get an opinion on this particular problem, it was necessary to perform out-of-pile experiments which simulate the reactor conditions.

A 9 rod bundle has been tested on the SNECMA boiling water loop during about 1 000 hours and has then been examined in AEG laboratories.

3.1.1 Test loop and special devices. - by C. CHERON - SNECMA.

3.1.1.1 Short description of the loop.

The SNECMA boiling water test loop has been described in previous reports (15). A flow diagram of it is shown on fig.C1. Let us just remember that all the loop has been built in Stainless Steel and that its hot coolant (up to 300°C) circulation pump enables a non stop loop performance of about 500 hours.

To meet the hydraulic requirements, a second 200 kW preheater has been set upstream the test section giving a total available heating power of 500 kW (fig. C2).

Before the test, a complete cleaning of the loop has been performed using a special mixture, basically nitro-fluorhydric acid. Nevertheless some iron, nickel and chromium aluminate deposits could not be completely removed.

3.1.1.2 Special equipments providing necessary water qualities.

3.1.1.2.1 - Water demineralization.

The normal loop equipment allows to fill up the loop with demineralized water having a resistivity of about $1 \text{ M}\Omega / \text{cm}^2 / \text{cm}$.

To keep the loop water purity at the required high level, a continuously working demineralization equipment was added to the loop. During normal operation it processes 20 grams of water per second. (The total loop capacity is 250 liters). This water is picked up from the main loop at the circulation pump outlet, cooled, demineralized through two kinds of resins, a basic one and an acid one, and sent back to the main loop at the pump inlet (Fig.C3).

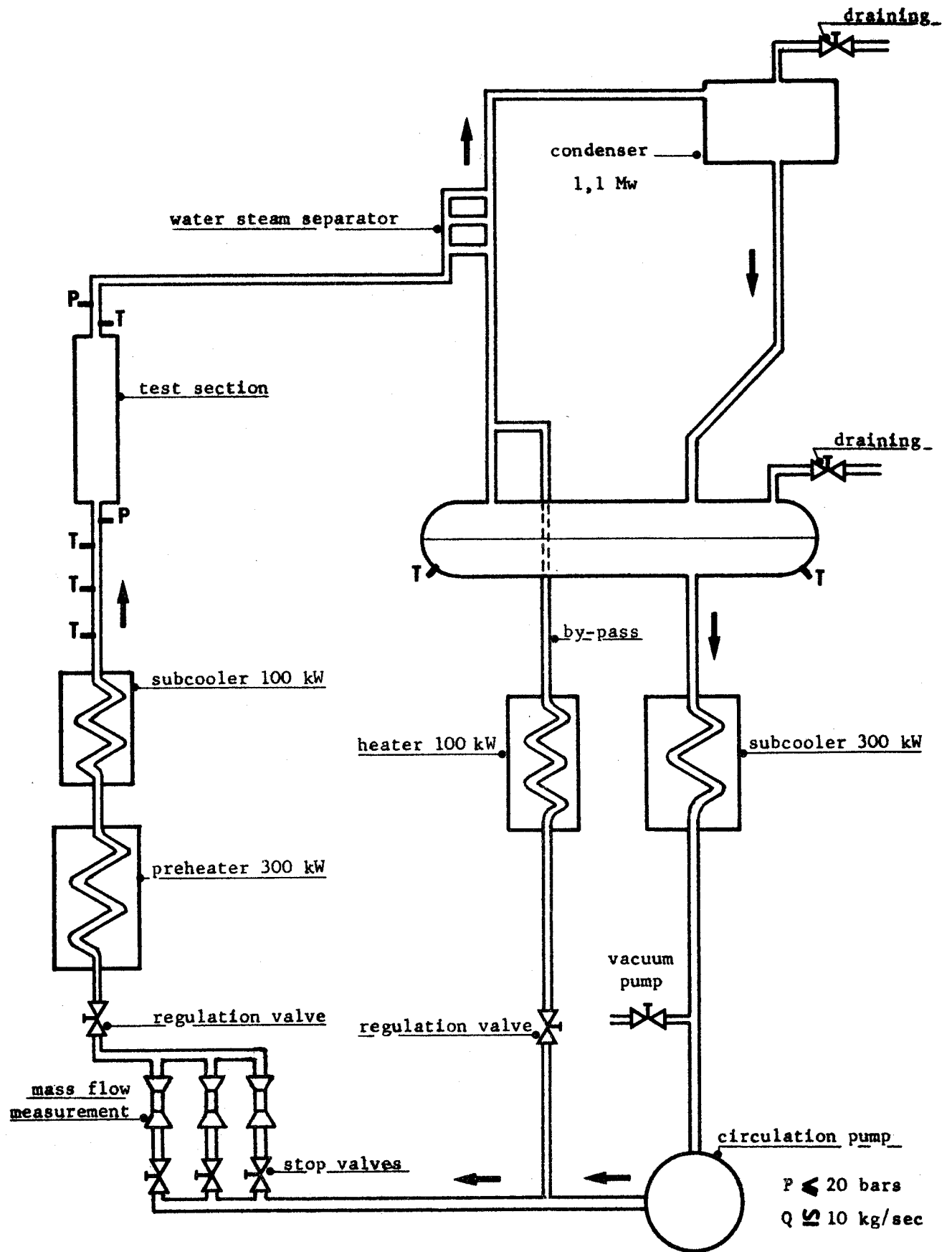


Fig. C1 - BOILING WATER LOOP - 70 bars 285°C

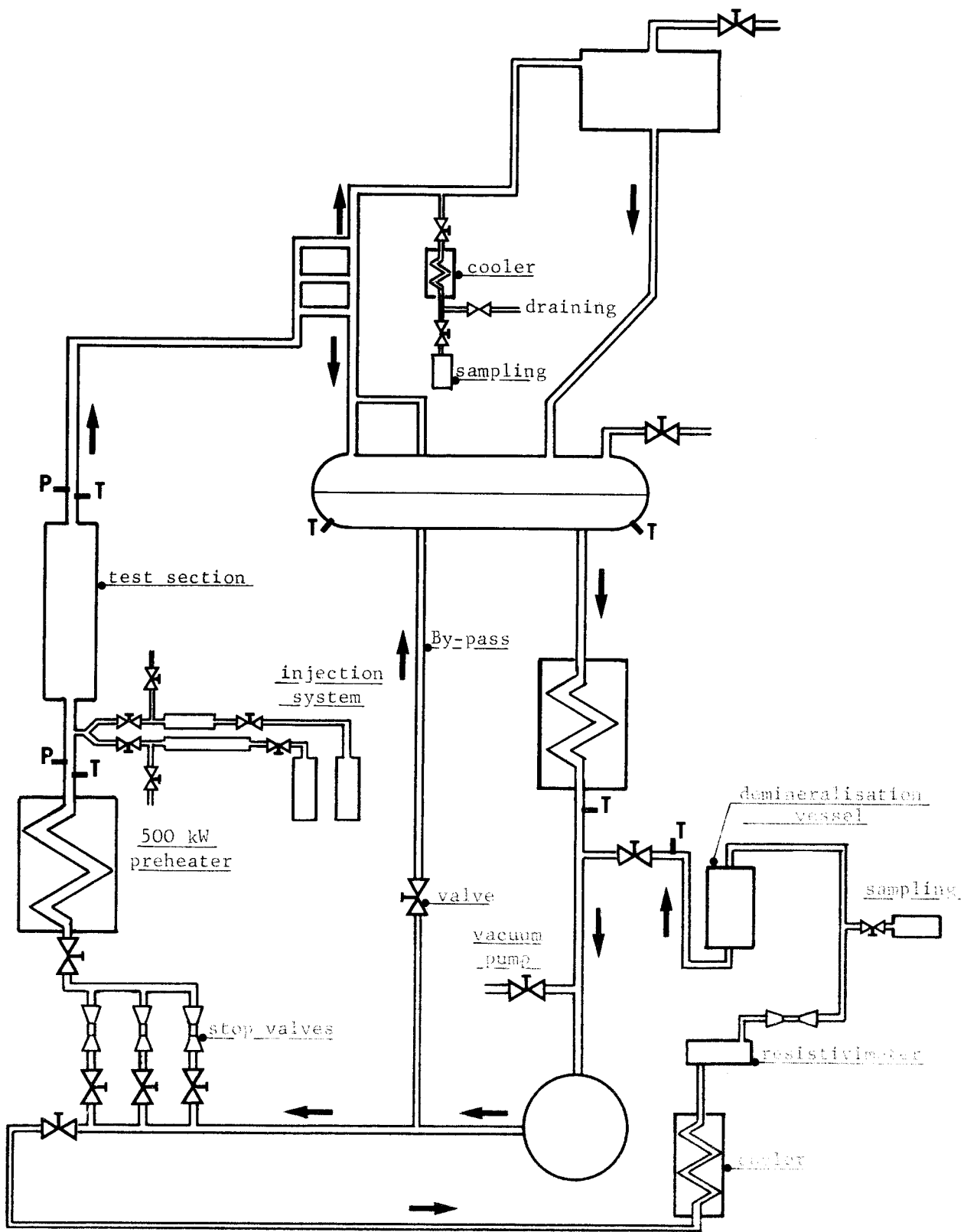


Fig. C2 - BOILING WATER LOOP
SPECIAL DEVICES FOR CORROSION TESTS

This device gave a loop water resistivity higher than $1 \text{ M}\Omega/\text{cm}^2/\text{cm}$ during all the test duration. The water resistivity is measured upstream the demineralization system by means of two apparatus :

- a direct reading PR 9501/00 type PHILIPS conductivimeter
- a CEL II SS 1 Y 23 type "Industrial Instruments" conductivity cell.

3.1.1.2.2 - Oxygen and Hydrogen injection.

The water oxygen and hydrogen contents required to simulate reactor conditions are supplied by means of an injection system. Two vessels (100 cm^3 for oxygen and 200 cm^3 for hydrogen) are first filled up with compressed gas. Then they are connected with the loop upstream the test section.

The pressure inside the vessels and the number of refilling operations give the required amount of injected gas.

Oxygen, Hydrogen and Nitrogen concentrations in water and steam are determined by chromatographic analysis of samples. Water samples are taken upstream the demineralization vessel and steam samples are taken between the water-steam separator and the condensor.

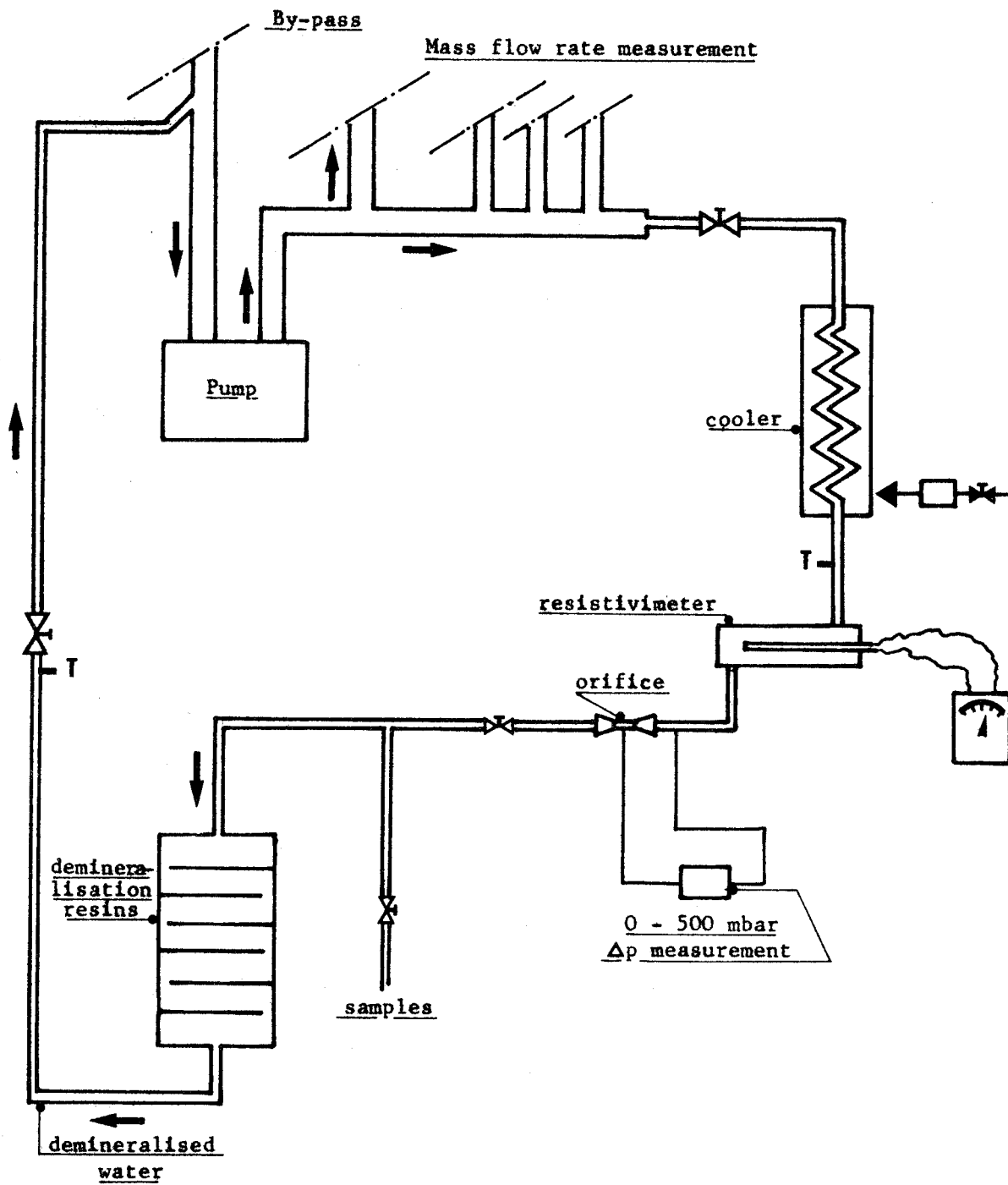
A detailed flow diagram of this sampling system is shown on Fig. C.4 and C.5.

The sampling bottles are first exhausted up to a vacuum of about 10^{-3} cm of Hg, then filled up with water and air locked by glass taps for transportation to the chromatography apparatus. To avoid any air trace amount in the taps and in the connections between the loop and the sampling bottles, it has been found suitable to blow argon through the bottles before connecting them to the vacuum pump.

Oxygen, Hydrogen and Nitrogen dosage is then performed by steam phase chromatography. A detailed description of the measurement apparatus and method is given elsewhere(★). The basic principle is to make the gas mixture absorbed in a molecular sieve at low temperature (-195°C) and then to make them desorbed in an argon flow by heating (at 350°C). As Oxygen, Hydrogen and Nitrogen are desorbed at different times, the chromatograph through which the argon flow is sent detects

(★) R. MORBIOLI and S. FERRE - Dosage par chromatographie en phase gazeuse de l'hydrogène, l'oxygène et l'azote contenus dans l'eau de la boucle à haute pression (SNECMA - Internal Report).

Fig. C3 - DEMINERALISATION EQUIPMENT



SAMPLING EQUIPMENT

Fig. C4 - WATER SAMPLING

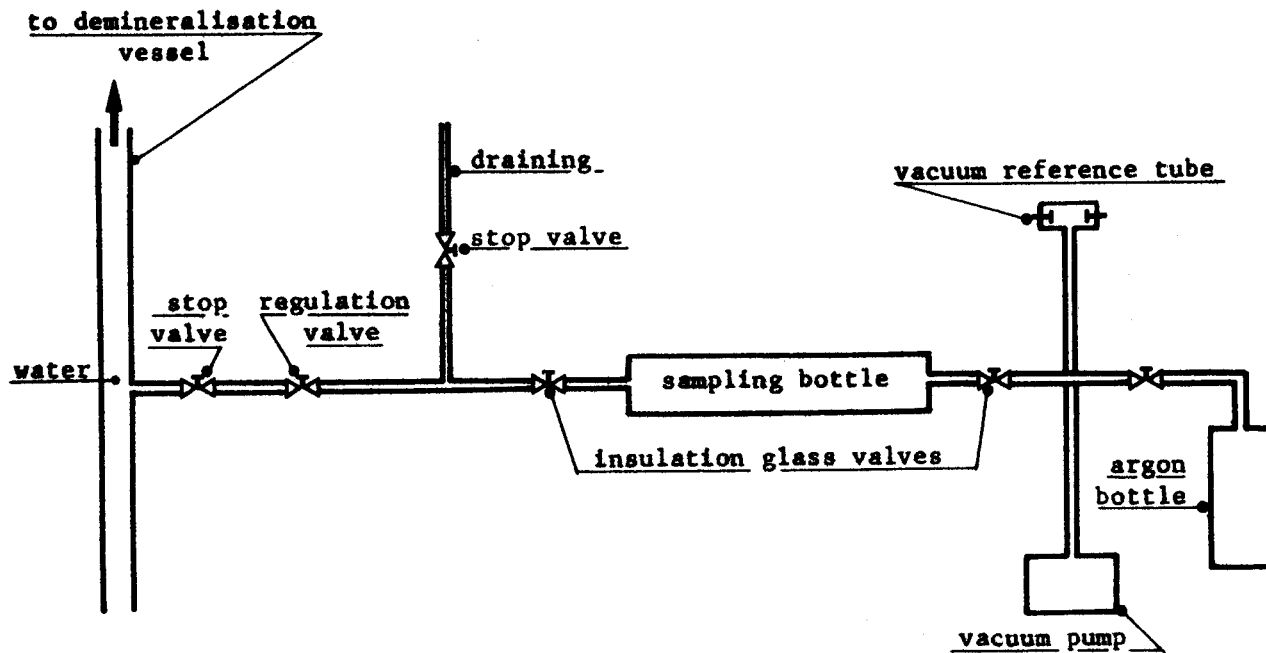
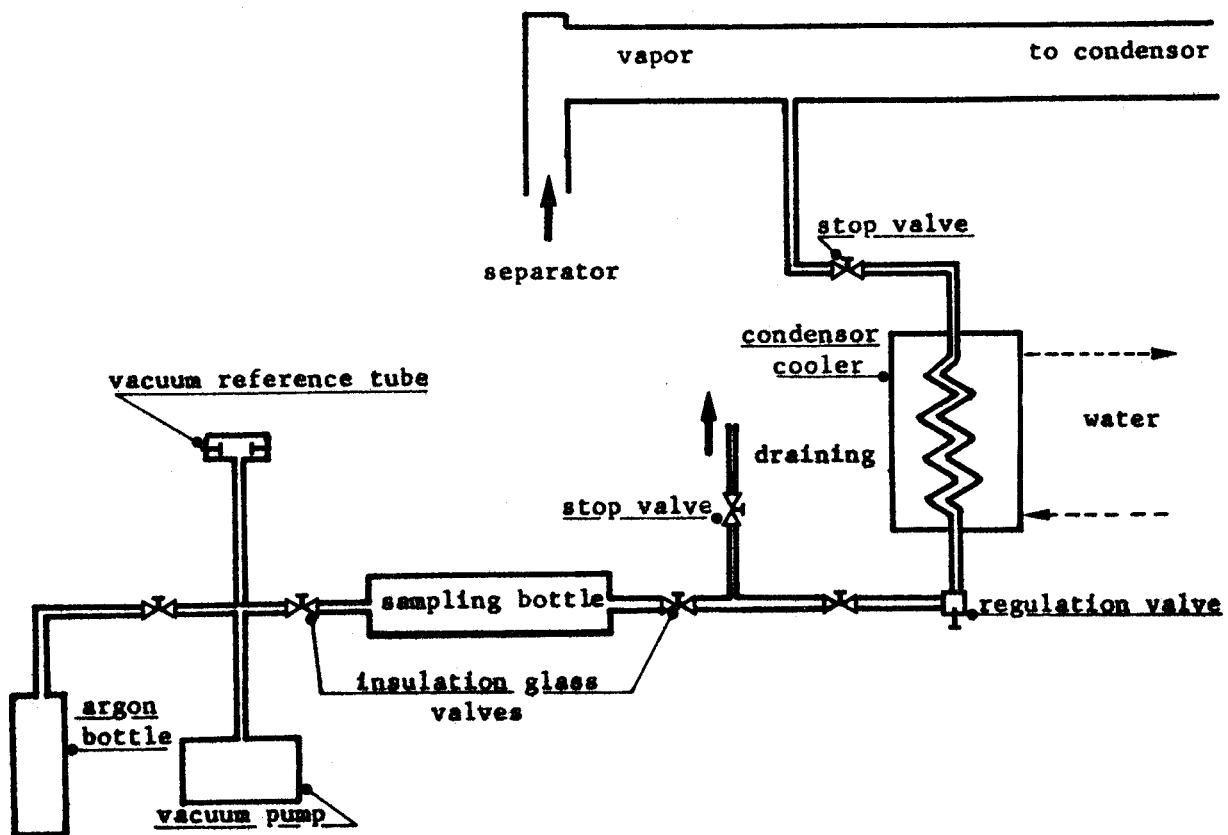


Fig. C5 - STEAM SAMPLING



three sequential peaks which are amplified and recorded. Fig.C.6 shows such a chromatogram. The peaks abscissas are characteristic of the nature of the components. Their height or surfaces depend upon the concentration.

Fig. C.7 shows the operation sequence; Fig. C.8 and C.9 show pictures of the general apparatus and of details.

3.1.2 Test section.

The test section is a 9 rod bundle with twisted tapes. The rods are 10 mm diameter. They were loaded with lead pellets to simulate the uranium dioxide with respect to vibration phenomenons. This mockup and its box (square cross section - 50 mm side length) are put into a pressure tube (102,3 mm I.D. - 114,3 mm O.D.) which is connected to the loop by flanges. The design is shown on Fig. C.10 and C.11. The cruciform type twisted tapes have a reduced half pitch of 3.

The coolant flow area is $1,757 \cdot 10^{-3} \text{ m}^2$.

Fig. C.12 shows parts of the test section before assembling. The rods are made out of Zircaloy 2. The characteristics of this alloy and the control certificates of the rods are given on Tables C.I and C.II.

Zircaloy 2 twisted tapes (0,2 mm thick) were electrically welded together. No special attention has been paid to this process. After an autoclavation test on samples a small alteration could be seen around the welding spots. Welding and grinding have been made using dummy rods (outer diameter equal to $10 \pm 0,05 \text{ mm}$). The pitch (15 mm) was achieved using grids at both ends.

Before the assemblage, the tapes were degreased in acetone and cleaned in nitro-fluorhydric acid. The bundle has been autoclaved before the installation in the loop.

3.1.3 Tests

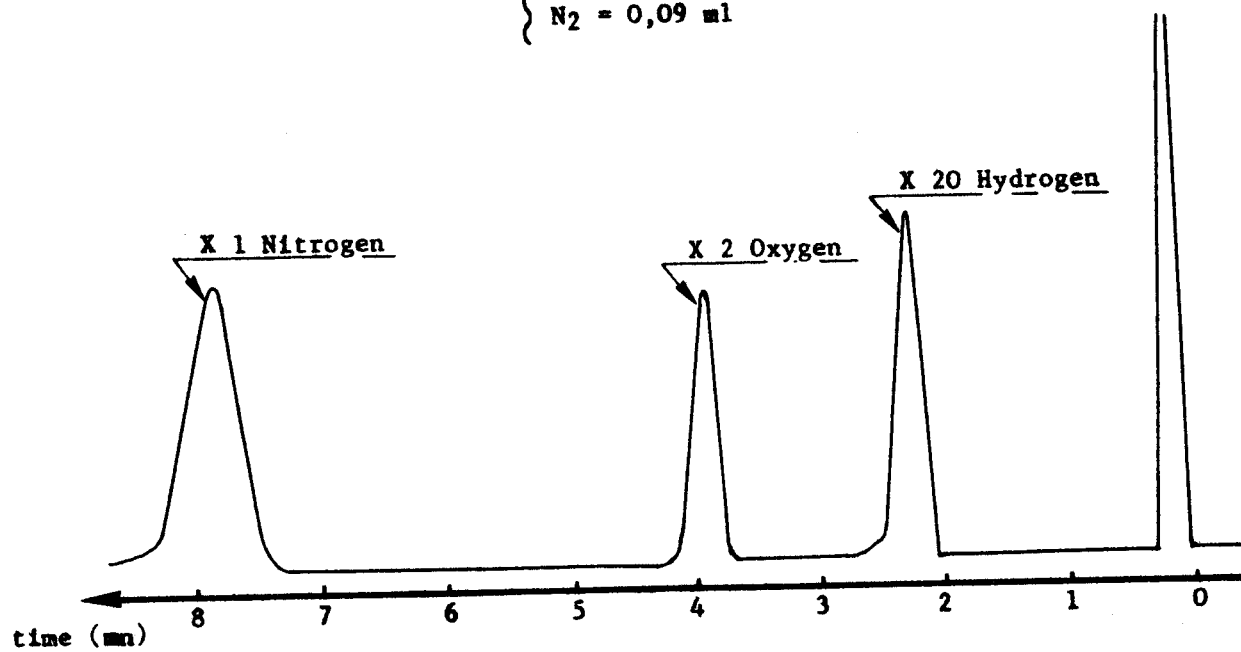
The tests were performed between 1966 April 25 and June 28. During the 1068 hours of operation all flow characteristics were recorded.

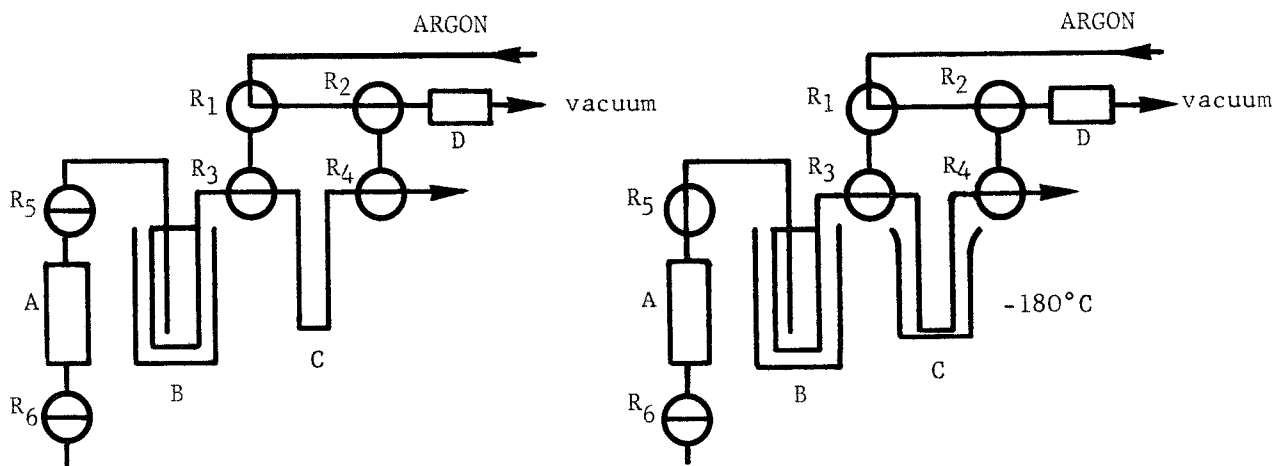
Planned test conditions were as follows

- Mass flow rate	1 500 kg/m ² s
- Steam quality	about 10%
- Coolant temperature	285°C
- Pressure	70 bars
- Chemical water characteristics	2 ppm of Oxygen 0,2 ppm of Hydrogen

Fig. C6 - GAS ANALYSIS RECORDING

gas contents {
H₂ = 0,08 ml
O₂ = 0,08 ml
N₂ = 0,09 ml

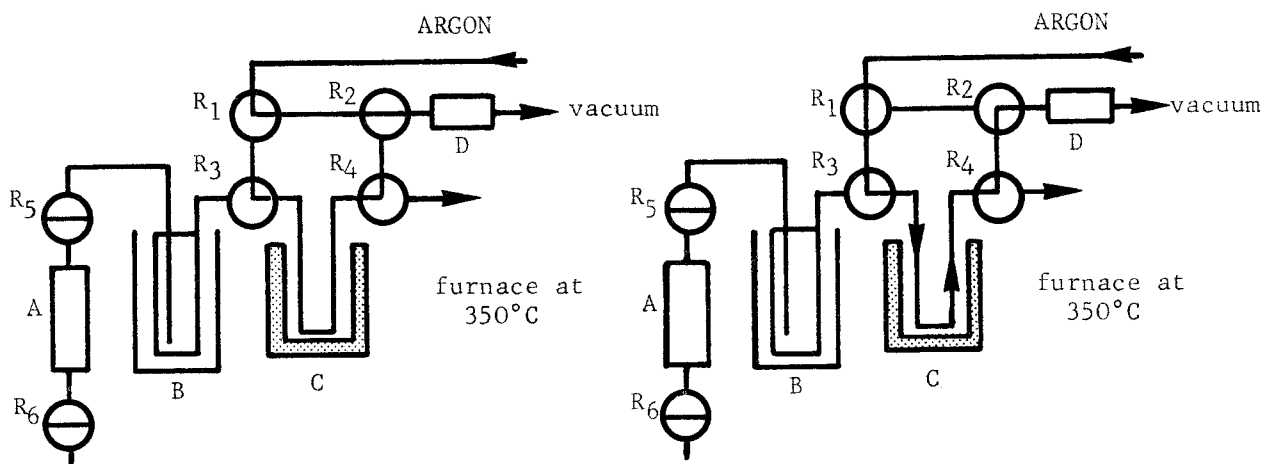




Operation 1 : PUMPING

Operation 2 : ADSORPTION

- A Sampling bottle
- B Cold trap at -80°C
- C Molecular sieve trap
- D Chromatograph
- R₁...R₆ Valves



Operation 3 : DESORPTION

Operation 4 : ANALYSIS

Fig. C7 - CHROMATOGRAPHIC ANALYSIS

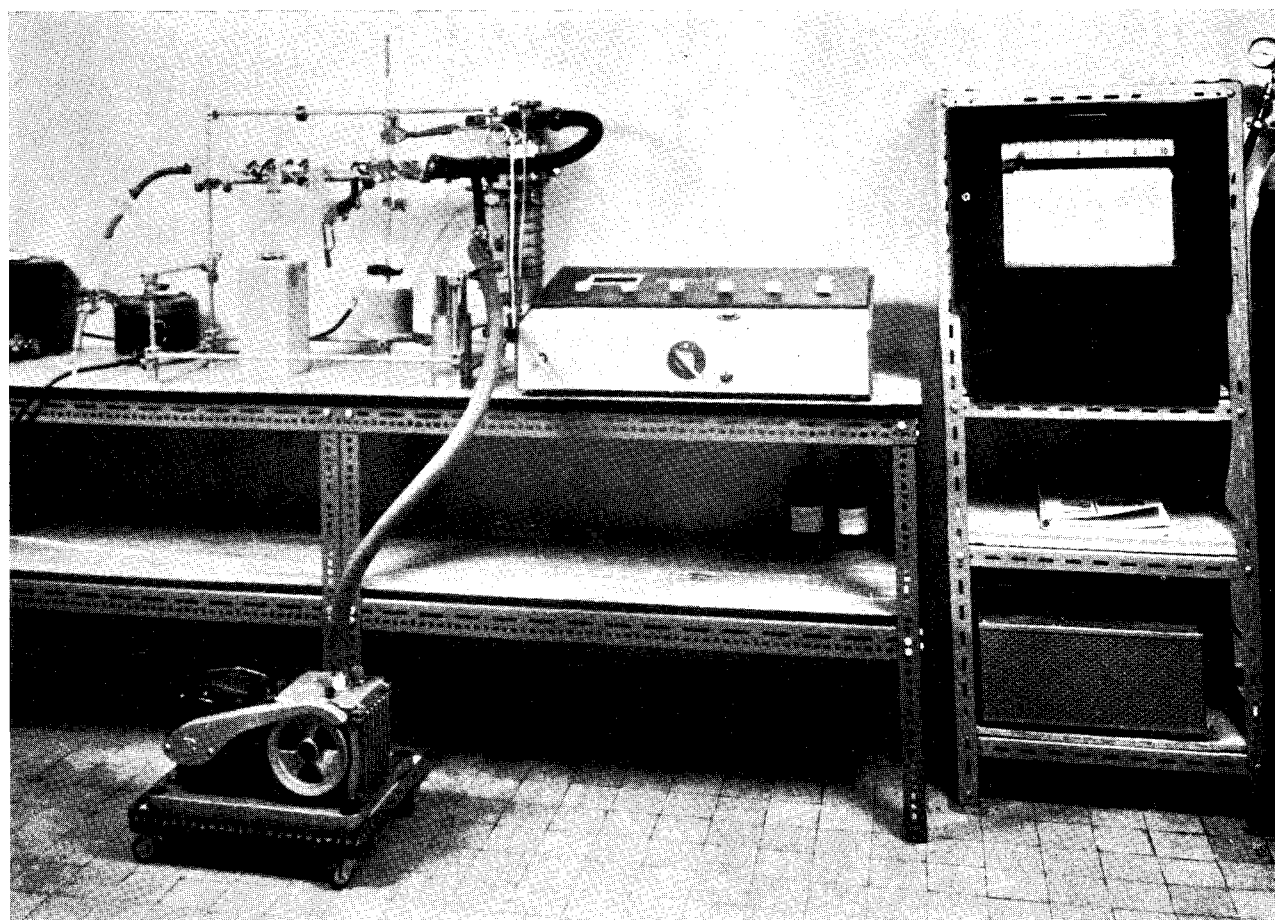


Fig. C 8 - GENERAL VIEW OF THE CHROMATOGRAPHIC ANALYZER

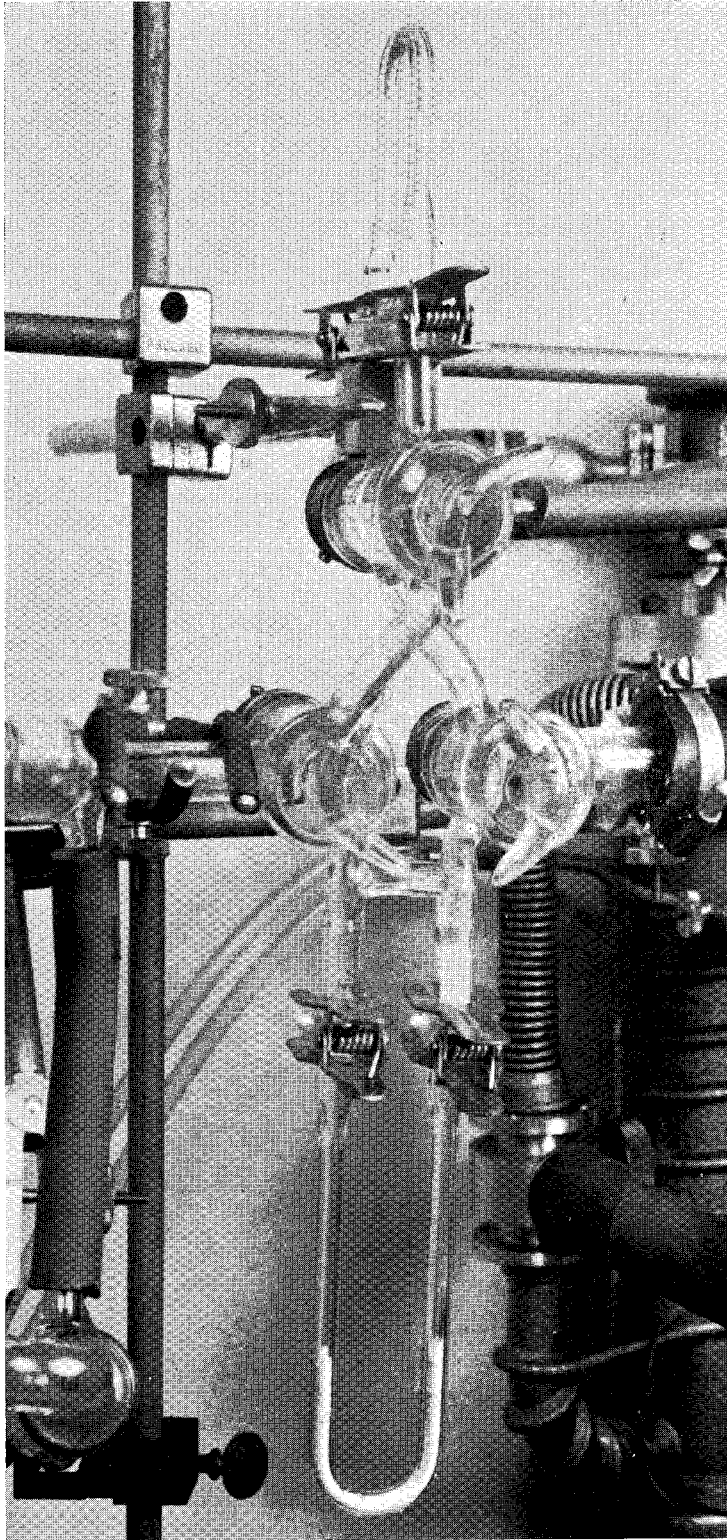
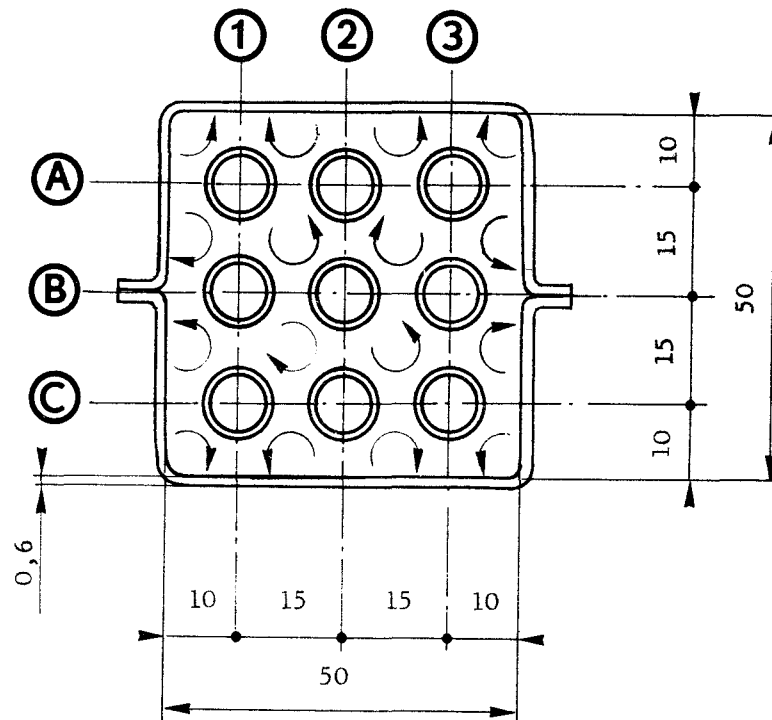


Fig. C. 9 - DETAIL OF THE ADSORPTION-DESORPTION DEVICE

Fig. C.10 - MOCK-UP CROSS SECTION

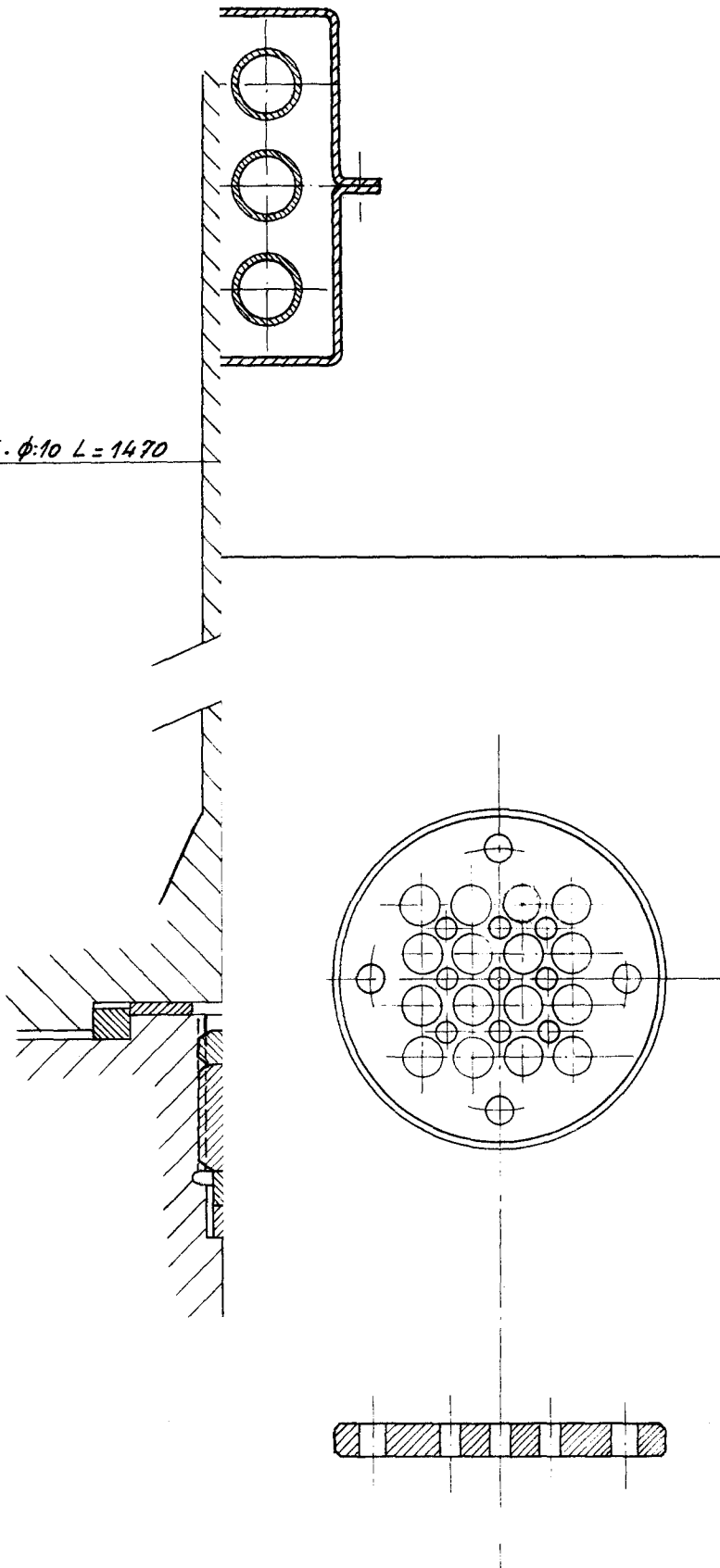


<u>9 tubes</u>	Internal diameter	8,5 mm
	Outer diameter	10 mm
<u>16 tapes</u>	Thickness	0,2 mm
	4 center T.T. - average width	13,2 mm
	8 side T.T. - average width	11,3 mm
	4 corner T.T. - average width	9,2 mm

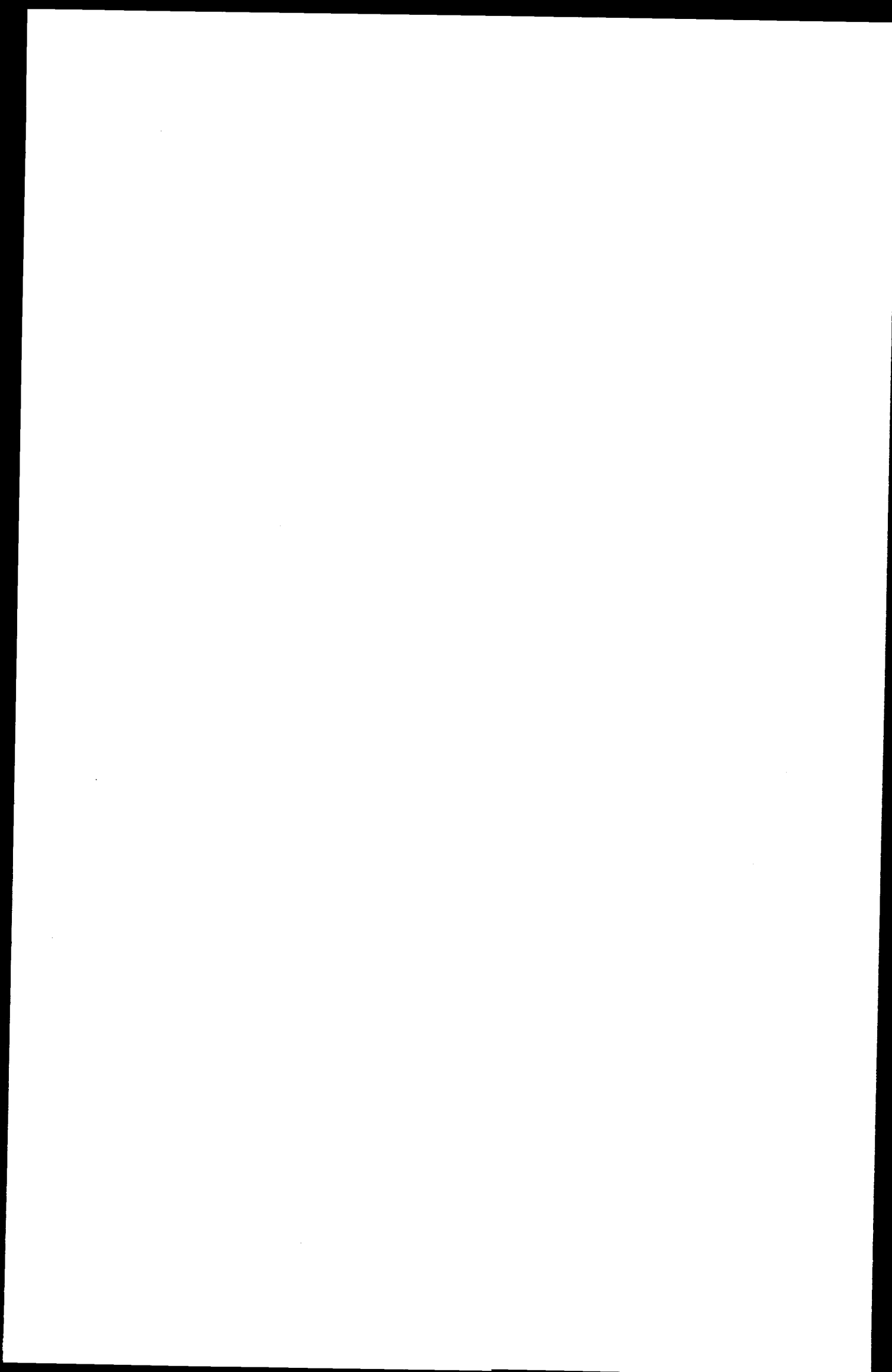
Wetted perimeter : 0,849 m
 Cross section : $1,757 \cdot 10^{-3} \text{ m}^2$
 Hydraulic diameter : $8,278 \cdot 10^{-3} \text{ m}$

CORRO
A-A

9 RODS $\phi: 8,5 \cdot \phi: 10 \quad L = 1470$



UPPER GRID



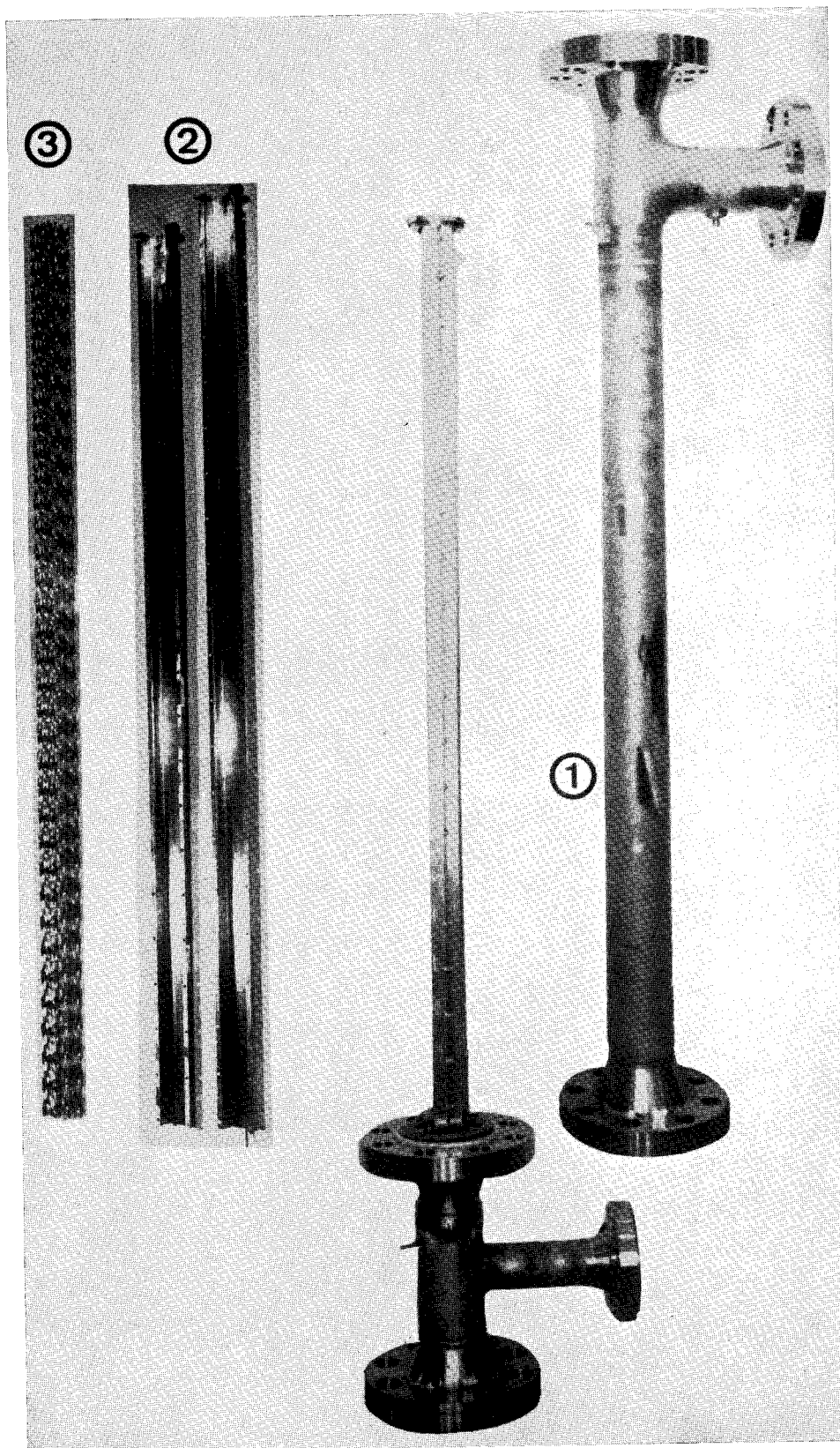


Fig. C. 12 - PARTS OF THE CORROSION TEST SECTION

- 1 Pressure tube
- 2 Channel box
- 3 Twisted tapes package

Values recorded during the tests are listed on Table C.III.

Pressure and temperature measured at the test section, have been kept constant at 70 bars and 285°C. After May 1st, the specific mass flow rate has been kept at 1 550 kg/m²s.

Because of some troubles with the preheater a maximum possible quality of 8,7 % could be reached.

Results obtained from water sampling analysis are given on Table C.IV. Some steam samples have also been processed; however their samplings were not numerous enough to allow a detailed analysis.

The total running period was 1 068 hours.

During the tests, several stops were needed for various reasons. Especially, two stops were necessary to take 3 rods out of the bundle and to replace them by new ones. These rods were used as samples for comparison.

Rods A3 and B3 were taken out after 170 hours.

Rod A1 was taken out after 474 hours.

Small stops have also been needed to meet the required water level in the loop.

After the tests, the test section was dismantled and sent to AEG for detailed analysis, also with the three rods previously put out.

After a short visual examination of the test section, no serious technological defect could be noticed. Especially fretting corrosion problems between the tapes and the rods seem to be non-existent. Weldings look to be safe and no failure have been found on the tapes themselves.

Fig. C.13 shows a picture of the twisted tapes and of the channel walls after 475 hours of operation. Fig. C.14 shows a picture of the twisted tape weldings after the end of the tests.

3.1.4 Examination and results - by A. GERSCHA and H. G. WEIDINGER - AEG.

3.1.4.1 Summary -

A nine rod "twisted tape"-bundle, tested in an out of pile facility under simulated water/steam conditions, was visually and microscopically examined to detect corrosion failures.

As a main result no hints for fretting corrosion could be observed in the contact areas between casing and twisted tapes. Also no hydride enrichment could be detected neither by microscopic nor by chemical examination. Further in-pile tests are recommended.

T A B L E C I



VEREINIGTE DEUTSCHE METALLWERKE A.G.

ZWEIGNIEDERLASSUNG C. HECKMANN

41 DUISBURG

Werksabnahmezeugnis

von Tubes, sans soude, sircaloy-2, reactor grade, recristallisés, recuits, décapés, tol. sur le diam. + 0,05 mm, tol. sur l'épaisseur ± 10 %, tol. sur la longueur -0 +5 mm,

Besteller Société Nationale d'Etude et de Construction de Moteurs d'Aviation SNECMA
150, Bd. Haussmann, Paris / France

Kunden-Nr. 88.908 E 192 dat. 14.1.1966, SP 43.265 Unsere Auftrags-Nr. R 39-030/66

PRÜFBEFUND

Bezeichnung des Materials	Probe-Nr.	Guss-Nr.	Durchmesser oder Dicke Breite des Probestabes		Streckgrenze kg/mm ²		Zerreißeigkei- keit kg/mm ²		Dehnung		Schweißhärte		Bemerkung
			mm	mm	vor-ge- schrie- ben	er- reicht	vor-ge- schrie- ben	er- reicht	Soll Meß- länge	% Ist	b. Vickershärte IV-5 c. Rockwellhärte XXXXXX	Soll Ist	
10 pcs. 10 mm ø ext. x 0,75 mm ép. x 1600 mm 2,3 kgs	1	742	10,00 x		21,8		46,4		30	30		137, 148, 148	
	2		10,05 x		21,0		50,0		"	33		139, 148, 148	
<p>l'épreuve de pression hydraulique à l'intérieur 350 kp/cm² sans fuite</p> <p>diamètre intérieur contrôlé: sans défauts</p> <p>épaisseur: sans défauts</p> <p>Tous les tubes ont subis un épreuve par ultra-sons: sans défauts</p> <p>inspection: sans réclamation</p> <p>dimensions: déviations dans les tolérances admissibles</p>													
Guss-Nr.	Zinn	Eisen	Chrom	Nickel	Zirkonium								
G 742	étain	fer	chrome	nickel	Zirc.								
	1,55	0,11	0,11	0,05	resté								
					impuretés		voir feuille séparée						

Ort und Tag der Prüfung } Duisburg, den 17. März 1966

VEREINIGTE DEUTSCHE METALLWERKE A.G.
ZWEIGNIEDERLASSUNG C. HECKMANN

Abgepr.

Bemerkungen: 0.

Unterschrift: (Petzold)

T A B L E C I I

- 2 -

Les impuretés suivies ne sont pas exécutées:

Aluminium	bore	cadmium	chlore	cobalt	hafnium	plomb	manganè.	silisium	tungstène	cuivre	vanadium	uranium
Aluminium	Bor	Cadmium	Chlor	Kobalt	Hafnium	Blei	Mangan	Silicium	Wolfram	Kupfer	Vanadium	Uran
ppm	ppm	ppm	ppm	ppm	ppm	ppm	ppm	ppm	ppm	ppm	ppm	ppm
75	0,5	0,5	50	20	100	130	50	120	100	50	150	3,5

essai chimique du tube

O	H	N	C
ppm	ppm	ppm	ppm
590	7	15	10
520	8	15	10
370-470	9	15	12
530	7	15	12

Leipzig, 17 mars 1966

VEREINIGTE DEUTSCHE METALLWERKE AG.
Zweigniederlassung C. Heckmann

Abnahme

(Petzold)

T A B L E C I I I

Date	Time (hours)	Massflow kg/s	water resistivity M /cm ² /cm	Steam quality %
25 April	4	2,5	0,53	0
26 "	24	2,9	1,3	0
27 "	21	2,8	0,35	4
28 "	9	3	1	4
29 "	24	3	1	4
30 "	20 h 10	3	1	4
1 May	0			
2 "	15 h 15	2,7	1,25	5
3 "	23	2,7	0,55	5
4 "	24	2,7	3,0	5
5 "	5 h 45	2,7		5
6 "	0			
7 "	0			
8 "	0			
9 "	9 h 30	2,7	0,5	5
10 "	24	2,7	2	6
11 "	24	2,7	1,5	6
12 "	24	2,7	2,5	5
13 "	24	2,7	1,5	5
14 "	24	2,7	2	5
15 "	5 h 45	2,7	2	5
16 "	0			
17 "	0			
18 "	0			
19 "	0			
20 "	16 h 45	2,7	1,4	8,7
21 "	20 h 45	2,7	2	8
22 "	17 h 30	2,7	2	8
23 "	17	2,7	2	8,7
24 "	23 h 15	2,7	2,3	9
25 "	24	2,7	2,3	6,5
26 "	20 h 45	2,7	1,2	4
27 "	24	2,7	2	4
28 "	5 h 30	2,7	2,5	4
29 "	0			
30 "	0			
31 "	0			

Date	Time (hours)	Massflow kg/s	water resistivity M /cm ² /cm	Steam quality %
1 June	0			
2 "	17 h 15	2,7	0,45	8,7
3 "	24	2,7	1,2	8,7
4 "	24	2,7	1,2	8,7
5 "	24	2,7	2	8,7
6 "	23 h 30	2,7	1	8,7
7 "	23 h 45	2,7	2,5	8,7
8 "	24	2,7	3	8,7
9 "	24	2,7	3	8,7
10 "	24	2,7	2	8,7
11 "	24	2,7	2	8,7
12 "	6	2,7	1,5	8,7
13 "	16 h 15	2,7	2	8,7
14 "	24	2,7	0,5	8,7
15 "	24	2,7	2	8,7
16 "	24	2,7	2	8,7
17 "	24	2,7	2	8,7
18 "	24	2,7	2	8,7
19 "	24	2,7	2,5	8,7
20 "	23 h 25	2,7	0,45	8,7
21 "	22 h 30	2,7	2,1	8,7
22 "	24	2,7	1,9	8,7
23 "	24	2,7	2,2	8,7
24 "	24	2,7	2	8,7
25 "	23 h 20	2,7	2	8,7
26 "	24	2,7	2	8,7
27 "	24	2,7	2	8,7
28 "	6	2,7	2	8,7

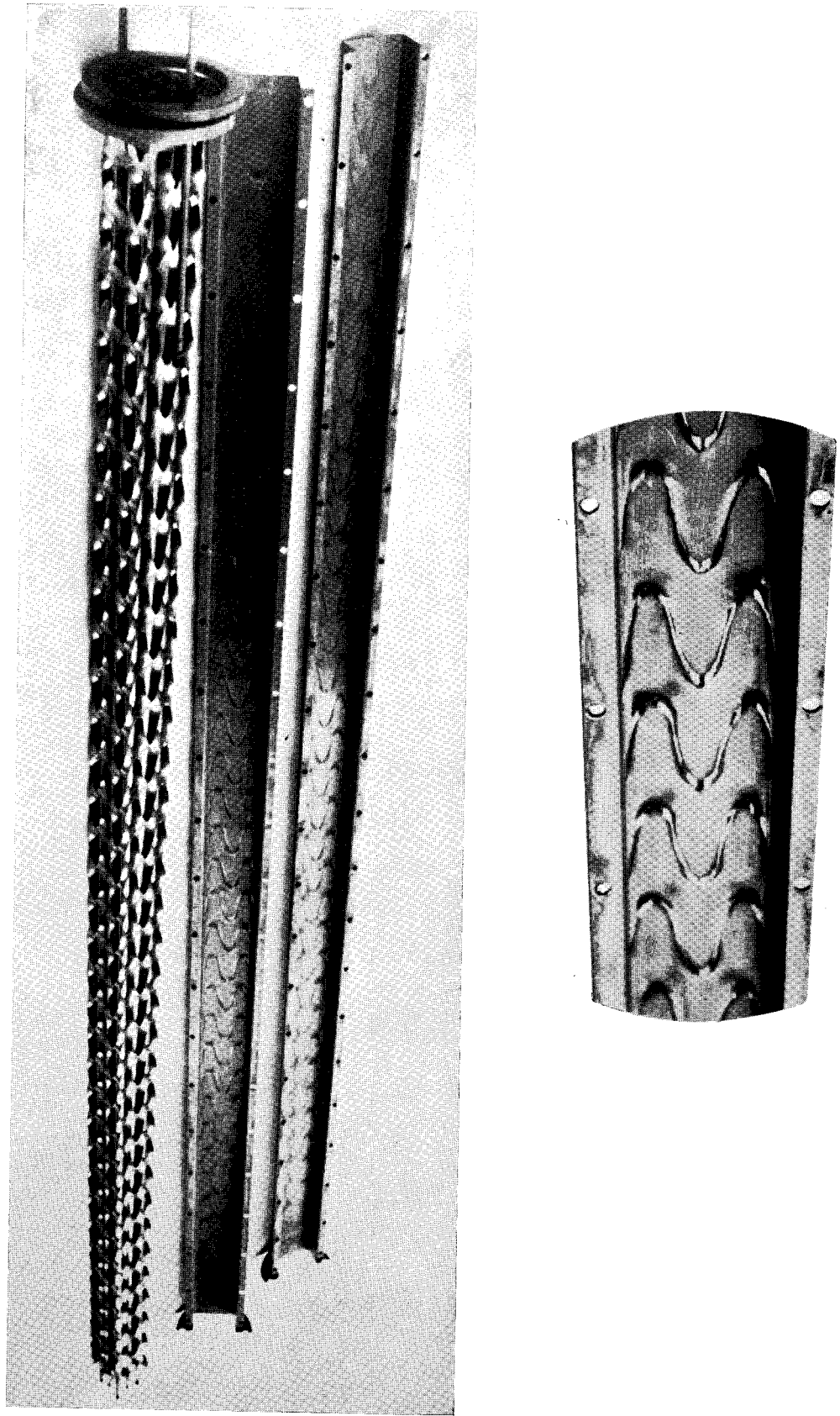


Fig. C. 13 - PARTS OF THE TEST SECTION AFTER 475 HOURS OPERATION

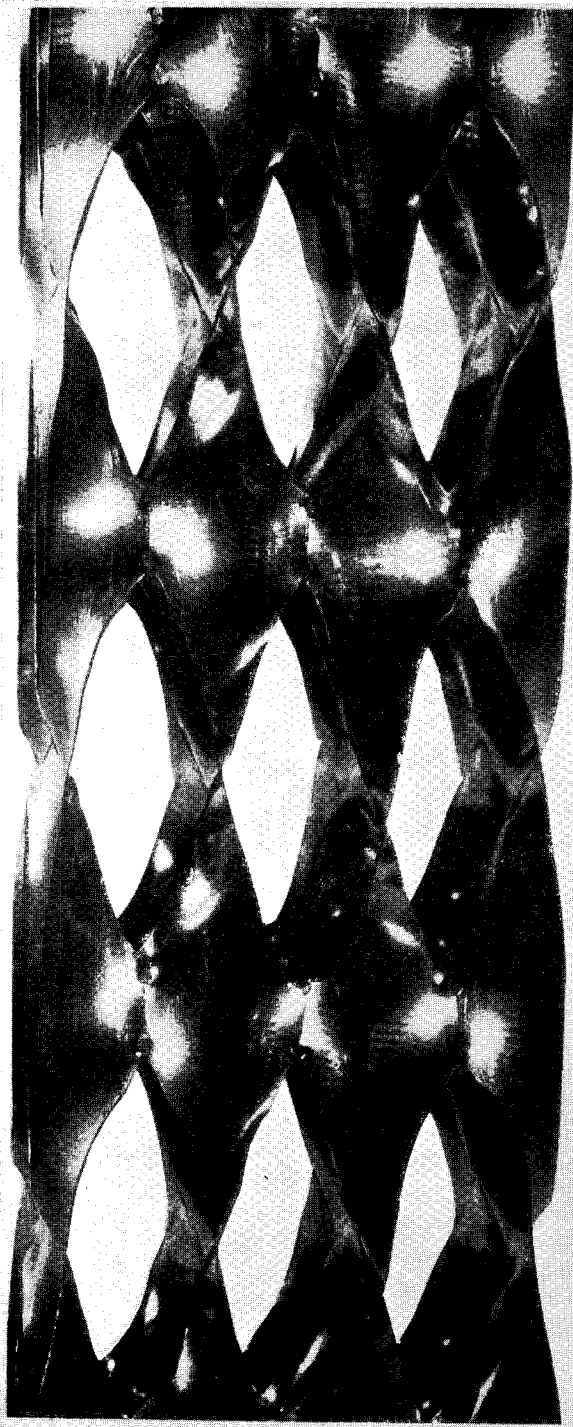


Fig. C. 14 - TWISTED TAPES AFTER CORROSION TESTS

T A B L E C I V

Date	N° sampling	gas content in P.P.M.			
		H ₂	O ₂	N ₂	
A P R I L	26	3	0,29	7,15	29
	27	1	0,36	3,45	10
		3	0,40	4,45	10
		1	0,51	12	15,6
		2	0,53	11	15
		3	0,55	10	15
	29	1	0,066	4,3	8,35
		3	0,145	2,85	7,8
M A I	3	1	0,24	3,6	7
		2	0,235	3,75	7,4
	4	1	0,12	2	2
		2	0,76	3,8	2,5
	12	3	-	3,8	2,5
		3	0,08	2,75	4,1
	24	3	0,084	2	2,4
	25	2	0,62	13	23
	26	2	0,64	30	69
	27	2	0,38	7,4	17,7
J U N E	6		0,175	2,5	6
	7	3	0,05	1,5	4,1
	8	3	0,04	1,15	2
	9	2	0,027	0,71	1,1
	10	3	0,75	19,3	6,5
	15	3	0,034	2,6	4,75
	16	2	0,08	2,2	3,3
	17	3	0,27	2,85	2,5
	20	2	1	14,5	12
	21	0	0,95	-	-
22	2	0,1	3,8	9,5	

3.1.4.2 Introduction.

Corrosion tests in the out of pile test facilities of SNECMA in Saint-Ouen were performed with a 9 rod "twisted tape"-bundle in order to examine fretting corrosion between Zircaloy-2 tubes and twisted tapes. Thermohydraulic reactor conditions were partially simulated, but no heat transfer could be applied.

3.1.4.3 Test section.

The test section was a 3 x 3 rod cluster 1,5 m long (first reactor bundle planned for in-pile tests in the Kahl-Reactor is a 6 x 6 rod cluster 1,5 m long). The tested rods had a diameter of 10 mm and stuck in the holes of a tape system. Each tape is 0,2 mm thick. The tubes as well as the tapes were made of Zircaloy-2. The fixation of the fuel rods within the twisted tapes is done by friction alone, not by any welding or similar procedures. Neither the tubes nor the tapes have been passivated before installation in the corrosion loop.

3.1.4.4 In-pile tests in comparison with the Kahl Reactor-conditions.

	out of pile-test	Kahl Reactor
pressure ata	71	71
temperature °C	286	286
steam content of the water w/o	8,5	10
superficial velocity m/sec	2	0,85
ppm O ₂ in water	0,7 - 30 average 6,2	in steam 20
ppm H ₂ in water	0,01 - 0,95 average 0,31	in steam 2,5

Originally it was planned to measure the gas content of the steam which should be 20 ppm O₂ and 2,5 ppm H₂. Because of technical difficulties it was not possible to analyse the steam. Therefore it was decided to measure the gas content of the water containing 10 w/o steam. According to the gas content of the steam (20 ppm O₂ and 2,5 ppm H₂) the gas content in the water should have been 2 ppm O₂ and 0,2 ppm H₂.

3.1.4.5 Results

The tubes were exposed to the simulated water steam mixture during 200, 400, 638, 838 and 1.038 hours under the test condition reported under 3.1.4.4.

3.1.4.5.1 Macroscopic results

a) Twisted tapes

After an exposure of 1,038 hours the tapes show an uniform brilliant black surface without visible defects.

b) Tubes

The appearance of the oxide layer shows a remarkable influence of the time of testing. The reason may be that the tubes have not been passivated before testing. The tubes tested for 200 hours have a greyish brown colour which becomes darker with increasing testing time.

The contact areas between tubes and twisted tapes are clearly visible as long as the time of exposure is not higher than 400 hours. (Fig. C15 and C16). Possibly the growing of an oxide layer at those areas is much slower than elsewhere. If the time of exposure is long enough (longer than 400 hours), these areas will be oxidized too and are no longer visible.

A local corrosion could not be detected.

3.1.4.5.2 Microscopic results

The metallographic examination was made with the tubes A 3, A 1, A 1', A 3' and C 1 (200, 400, 638 and 1.038 hours testing time). Each tube was sectioned in a distance of 12 cm from the top. The samples A 3 and A 1 have been cut in such a way that the contact area tube/tape could be examined.

The samples A 3 and A 1 (200 and 400 hours testing time) showed no local corrosion on the contact areas tube/tape and showed also no enrichment of hydrides (Fig. C 17). The hydride concentration is the same in all samples. An influence of the exposure time on the hydrogen content of the tubes could not be found (Fig. C 18). The hydrogen content in the Zircaloy-2 tubes has been found to be about 30 ppm according to the metallographic examination. Furthermore, the hydrogen, oxygen and nitrogen contents of the samples A 3 and C 1 (200 and 1.038 hours testing time) have been determined by hot extraction. In both cases 33 ppm hydrogen, 10 ppm nitrogen and about 1.500 ppm oxygen have been determined i.e. practically the same result as by metallographic examination.

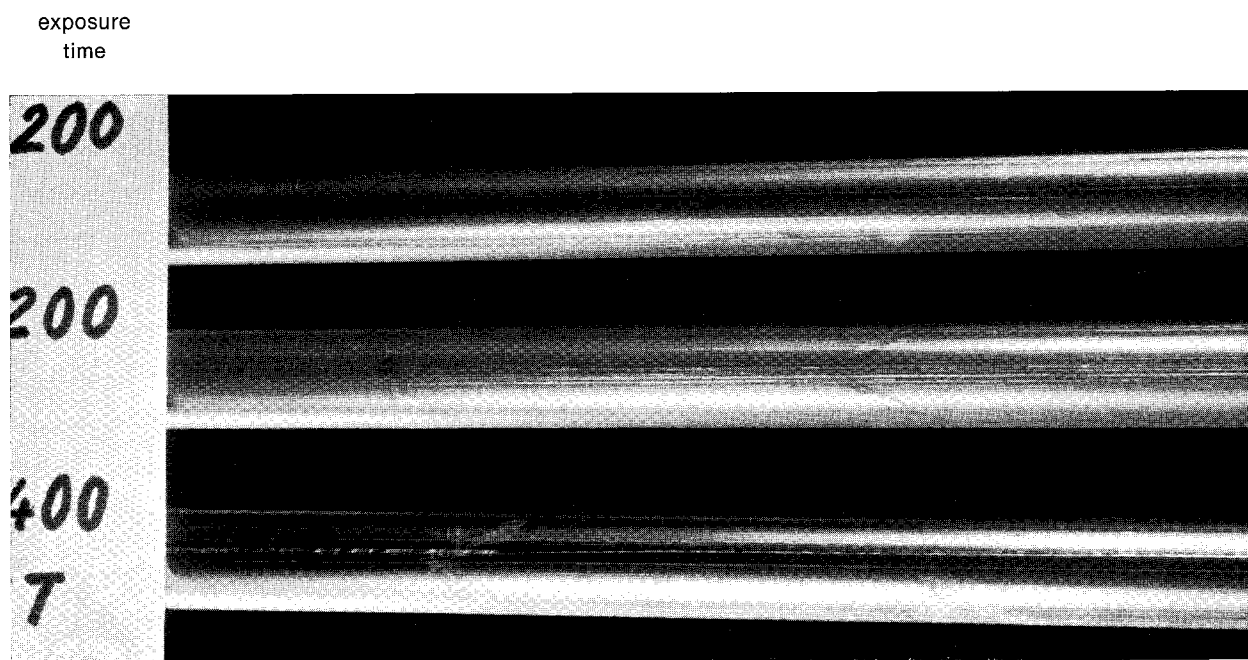


Fig. C. 15 - VIEW OF THE TUBES AFTER VARIOUS RUNNING TIMES

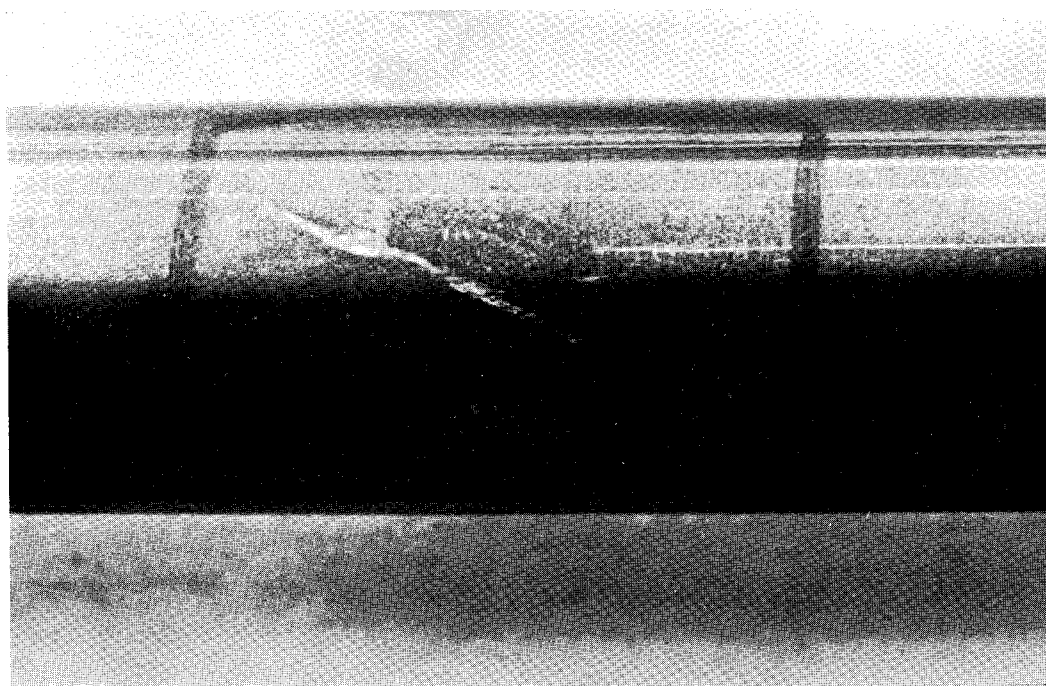
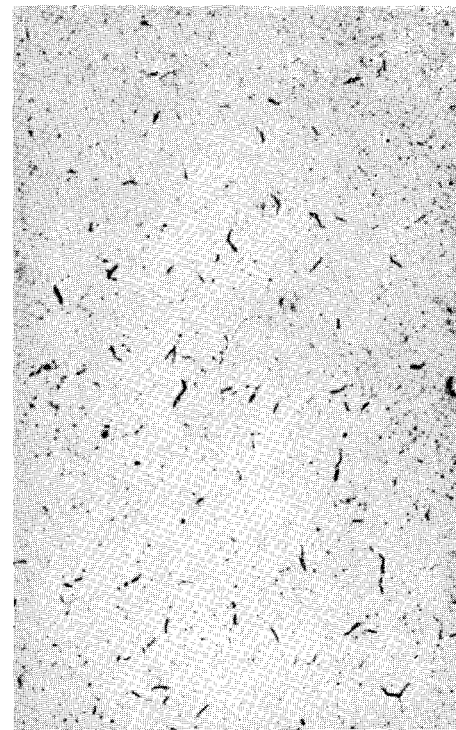
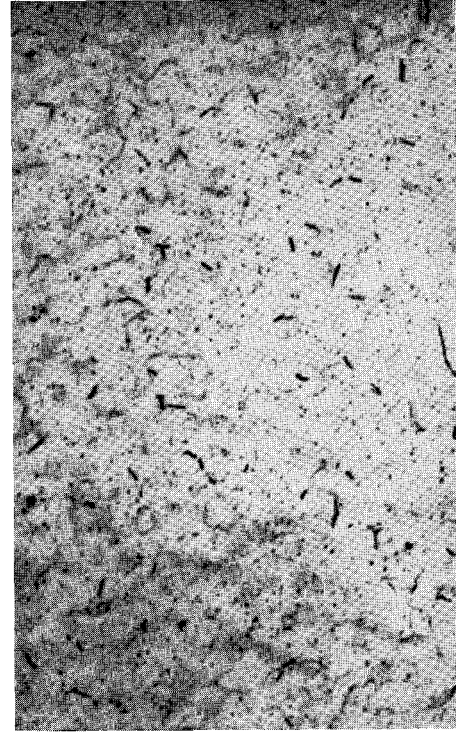
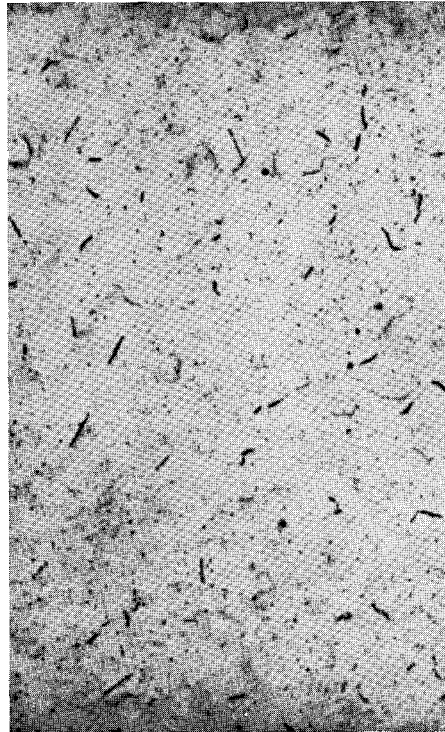


Fig. C. 16 - CONTACT AREA WITH A TWISTED TAPE

Fig. C. 17

specimen A3, Exposure time 200 h

near the contact area tape-tube



specimen A3, Exposure time 200 h

specimen C1, Exposure time 1038 h

Fig. C. 18

3.1.4.6 Remarks

One observation thought of minor significance and not directly connected to fretting corrosion has been made. A white layer of Zirconium-dioxide has been found on the ends of the tubes which have been exposed longer than 400 hours. The layer can only be detected in the region of welding seam. In some cases the whole circumference, in others only small areas are covered (Fig. C 19). We think that one of the welding parameters is the reason for that observation and recommend an examination of the welding process.

3.1.4.7 Conclusion

The examination of these out of pile tested rods showed no signs of fretting corrosion. However it is well known, that fretting corrosion depends very much on vibration conditions. This means, that any difference geometry or stresses between canning and tape may affect these observed results. Therefore it is obviously necessary to check twisted tapes assembly under full reactor conditions which are characteristic for a modern high efficiency boiling water reactor. The Kahl-in-pile-experiment is one step towards this target. Another test in an reactor with higher heat flux and cooling flow rate is strongly recommended.

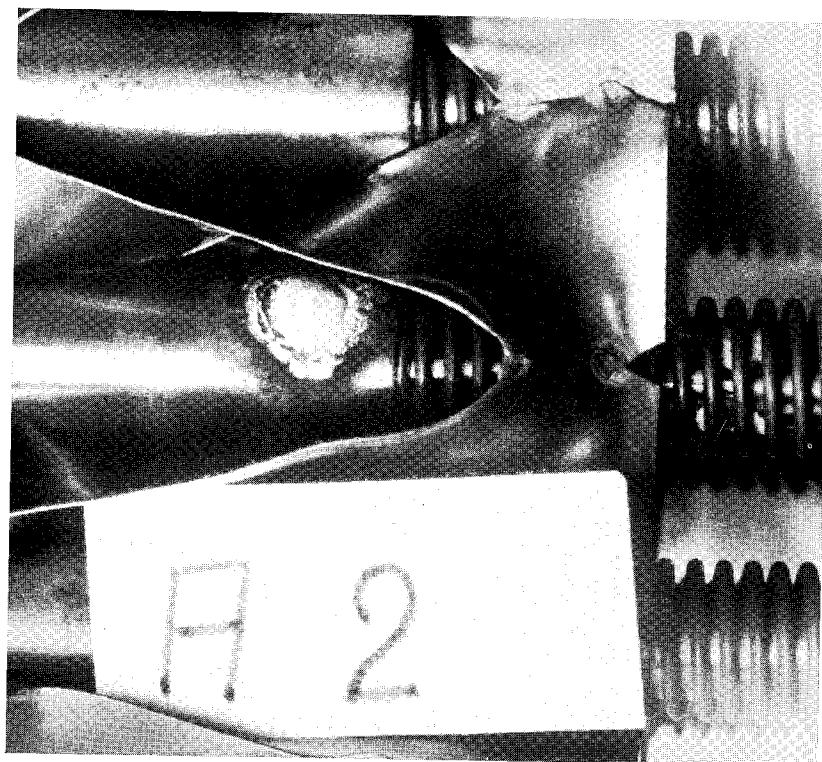


Fig. C. 19 - CORROSION TEST ASSEMBLY - TUBE ENDS

3.2 Subtask C.2 - Definition of further experimental work.

by G. du BOUCHERON - SNECMA.

3.2.0 Purpose of this subtask.

Under this subtask, it was planned to investigate what experimental results were still needed before it becomes possible to start the design of a TTBWR.

The first conclusion was that the goal of the presently reported contract could not be reached without some experiments which were not initially planned. Therefore it was decided to amend the contract technical program on two points :

- a) the corrosion experiment which has been reported above (3.1) and which was initially planned to last 4 weeks has been extended to a duration of 2 months.
- b) CHF measurements on a 4 rod cluster which had already been tested on the SNECMA loop under the EURATOM/SNECMA contract n° 061-64-7 TEE F was decided to be run on the CCR Ispra loop. The choice of this loop was coming from its higher power (1,2 MW instead of 0,8 MW for the SNECMA loop). It was therefore possible to run tests with such experimental conditions that could not be possible elsewhere. Especially it has been possible to perform high inlet subcooling tests. They are reported about below (3.3).

As a second part of this subtask, an experimental program has been defined to be run during the 18 months of a second contract. This program includes critical heat flux measurements, void fraction and pressure drop measurements, stability investigations and post irradiation examination of the Kahl experimental bundle. The program is detailed below.

3.2.1 Critical Heat Flux Measurements.

Critical Heat Flux measurement results from the tests performed at the CCR ISPRA on a 4 rod test-section with twisted tapes gave a confirmation of those which were formerly run on the same test-section at the SNECMA facility. They also gave previously lacking informations in the high inlet subcooling range. However no satisfactory explanation of these results have been given which could be suitable for design. It has therefore been decided to trend further research towards two conditions :

- experiments on non uniformly heated tube test-sections with a CHF detection plain equipment. They should prove how far the CHF in swirling flow can be considered as an inlet phenomenon, a local phenomenon or a global phenomenon.

- experiments on uniformly heated tube test-sections, and later on clusters, with more sophisticated equipment for CHF detection so that it could be possible to localize the burnout and, if necessary, to follow its moving.

The application of this will result in the following tests.

a) Non uniformly heated tube test-section.

The purpose of this test is to reach a better understanding of the CHF in swirling flow.

The test will be run in the following conditions :

- Tube inside diameter about 20 mm
- Tube length about 3 m
- Heat flux shapes uniform
linearly increasing
linearly decreasing
nearly cosine
- Mass flow rate $300 \leq \rho v \leq 2\,500 \text{ kg/m}^2 \text{ s}$
- Inlet quality $-30\% \leq x_{in} \leq +30\%$

CHF detection will be made using outlet thermocouples. These tests will be run by SNECMA on its boiling water loop at Saint-Ouen.

b) Uniformly heated tube test-section.

The purpose of this test is to develop the necessary instrumentation for the localisation of the CHF phenomenon and to use this equipment for providing better understanding of the CHF in swirling flow.

The tests will be run in the following conditions :

- Tube inside diameter about 20 mm
- Tube length - heated part 3 m
non heated part 0 m.50
- Mass flow rate $300 \leq \rho v \leq 2\,500 \text{ kg/m}^2 \text{ s}$
- Inlet quality $-30\% \leq x_{in} \leq +30\%$

These test will be run by EURATOM at the CCR ISPRA on test sections provided by SNECMA. The detection device will be designed in collaboration between CCR ISPRA , AEG and SNECMA.

c) 4 rod cluster test section.

The purpose of this test is to demonstrate the feasibility of high power density operation of TT fuel elements and to gain better understanding of the CHF in TT clusters by localisation of it.

In order to use the results of this test to demonstrate the feasibility of an in-pile experiment in a large BWR, the geometry of this cluster (rod diameter and pitch) will be chosen as close as possible to the Lingen BWR geometry.

The heated length of the test section will be determined according to maximum available heating power on the ISPRA loop.

The cluster will have an unheated length of about 0,5 m.

The test section will be designed by SNECMA in close cooperation with AEG and the CCR ISPRA. It will be supplied by SNECMA. The tests will be run by the CCR ISPRA on their boiling water loop in close cooperation with AEG and SNECMA.

3.2.2 Hydraulics.

As it has been explained above (see § 1.3.1.1) available informations about TTBWR hydraulics do not overlay the total possible range of parameters. Especially, correlations for slip ratio, friction pressure drop coefficient and two-phase pressure drop multiplier are not fully suitable for design.

It has then been decided to perform new tests for measurements of void fraction and pressure drops on a non heated 4-rod cluster with T.T. The experimental conditions will be as following :

- Length of the cluster about 1,50 m
- Mass flow rate $300 \leq \rho v \leq 2500 \text{ kg/m}^2 \text{ s}$
- Inlet quality $0 \leq x_{in} \leq 40\%$
- Pressure about 70 bars

A gamma ray absorption technique will be used to measure the void fraction.

This work will be performed by SNECMA on its boiling water loop at Saint-Ouen.

3.2.3 Stability.

The two-phase flow hydrodynamics on twisted tape fuel assemblies differ substantially from the hydrodynamics in normal straight channels. Both, the higher friction losses along the cooling channel and higher power density of twisted tape fuel should lead to more stringent stability problems. Proposed work includes theoretical and experimental studies of these problems.

A similar study is already being made for normal boiling water channels under EURATOM/AEG contract n° 085-66-1 TEE D (R & D). The test facility used for this work makes it possible to modulate sinusoidally the heating power and the inlet flow velocity and to measure local void fraction along the channel by means of a gamma-ray absorption technique. Transfer functions can be determined by means of an analog computer.

Therefore, using the same measuring techniques as for the stability investigations on normal boiling channels, carried out under the above mentioned contract, the following measurements will be performed on a 4-rod cluster with twisted tapes.

- a) Steady state measurements.

These tests should provide the dynamic constants necessary for the comparison between experiment and theory.

- b) " Power to local void " transfer function measurements.

Should the gamma-ray absorption technique be no longer applicable to measure the local void-fraction, the outlet water flow will be measured instead of the local void fraction.

- c) " Inlet flow to local void " transfer function measurement.

(Same remark as for " 2 ")

- d) Transfer function measurement between power or inlet flow and the differential pressure along the cooling channel.

- e) Theoretical investigations.

The theoretical model tested under the EURATOM/AEG contract 085-66 1 TEE D (R & D) will be taken as a basis for the interpretation of the measurements on the twisted tape test section.

The twisted tape test section will be supplied by SNECMA.

The stability tests will be performed by AEG on the stability test loop at Grosswelzheim. The theoretical investigations and the determination of stability design criteria for TTBWR will be done by AEG in cooperation with SNECMA.

3.2.4 KAHL In-pile test evaluation.

The prototype TT fuel assembly prepared under this contract for irradiation in the VAK-Kahl BWR will be loaded into the reactor.

After irradiation, the bundle will be unloaded and examined by visual techniques. This visual inspection will be done by AEG and SNECMA at the Kahl Plant.

A post-irradiation examination of the prototype fuel assembly will be performed by EURATOM in its hot laboratories of the TRANSURAN-INSTITUT in Karlsruhe. AEG and SNECMA will follow these examinations and give their advice on operatory methods and result interpretation.

3.3 Subtask C.3 - Critical Heat Flux experiments. - by A. ROSUEL - SNECMA.

Under this subtask, Critical Heat Flux experiments, the definition of which has been given above (§ 3.2.1), were conducted on a four rod test section. These tests are a sequel of those carried out on the SNECMA boiling water loop (16). The facility used for these tests was the boiling water loop of the SET at the EURATOM CCR ISPRA, because it could supply a larger power than it is available in the SNECMA loop (1,2 MW instead of 800 kW). It also allows an appreciable subcooling at the heating channel inlet. It is therefore possible to explore a parameter field corresponding to BWR conditions (x_{inlet} varying from 0 to -10%; mass velocity about 1500 kg/m²s).

3.3.1 Description of the test section.

The test section consists mainly of a four rod cluster, having rod outside diameters of 10 mm, a pitch of 15 mm, a square plane surface channel of 35 mm side length and a package of 9 stainless steel twisted tapes of 0,2 mm tick of a reduced pitch $Y = 3$.

At both sides of the heated part of the bundle (1,1 mm length), the twisted tapes are extended by 100 mm. In that area, the stainless steel tubes are replaced by copper tubes which are connected to the power supply.

Since the twisted tapes are not electrically insulated from the heating tubes, a part of the power is dissipated in them. The choice of the tube wall thickness ($e = 2,5$ mm) has yielded the following ratios :

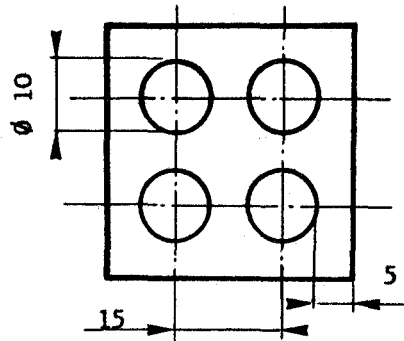
$$\text{- twisted tapes of a thickness of } 0,1 \text{ mm } \frac{W_{tt}}{W_{total}} = 3\%$$

$$\text{- twisted tapes of a thickness of } 0,2 \text{ mm } \frac{W_{tt}}{W_{total}} = 6\%$$

The sparking problems which were noticed during the first tests at ISPRA resulted in the destruction of the tapes at the outlet of the heated channel after a few operational hours. This limited to some extent the number of tests points which could be run with each twisted tape assembly. The brazing of flexible connections between the copper tubes and the tapes made it possible to solve this particular problem.

For the electrical insulation of the channel and the twisted tapes "Durabla" sheets were used.

Test section geometry :



Cross section	892 mm ²
Heating length	1100 mm
Heat exchange area	0,138 m ²
Hydraulic diameter	8,2 mm
Heating perimeter	0,128 m
Wetted perimeter	0,446 m

3.3.2 Detection of the crisis.

The detection is possible by measuring the wall temperature of the heated rods. Two different methods were used :

- a) a thermocouple was located inside the heated tubes at the outlet of the channel.

In this particular case, the two wires of the thermocouple were brazed onto a copper plate which is in turn positioned against the tube walls. The electrical insulation was obtained by using glass-wool tape. The continuous recording of the signals was done by means of four potentiometric recorders.

This method which had already been used during the SNECMA tests has been found to be not absolutely safe - some actual Burn-out could not have been detected and led to the destruction of the test section - and also is not suitable if it is wanted to localize the crisis.

- b) To remedy this, a second detection system was used during the last tests :

Several head-insulated thermocouples are brazed inside the tubes at locations shown in figure C.20. The 3,5 mm inside diameter of the copper connectors brazed at the end of the tubes did not allow the use of more than four thermocouples in each tube.

The signals were recorded on a galvanometer, or transmitted to a detector allowing to cut-off the power above a given temperature threshold.

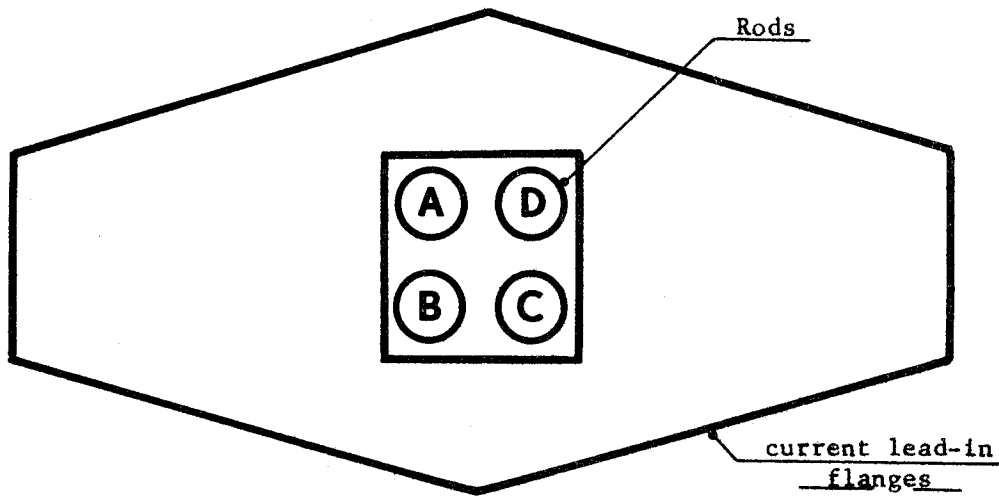
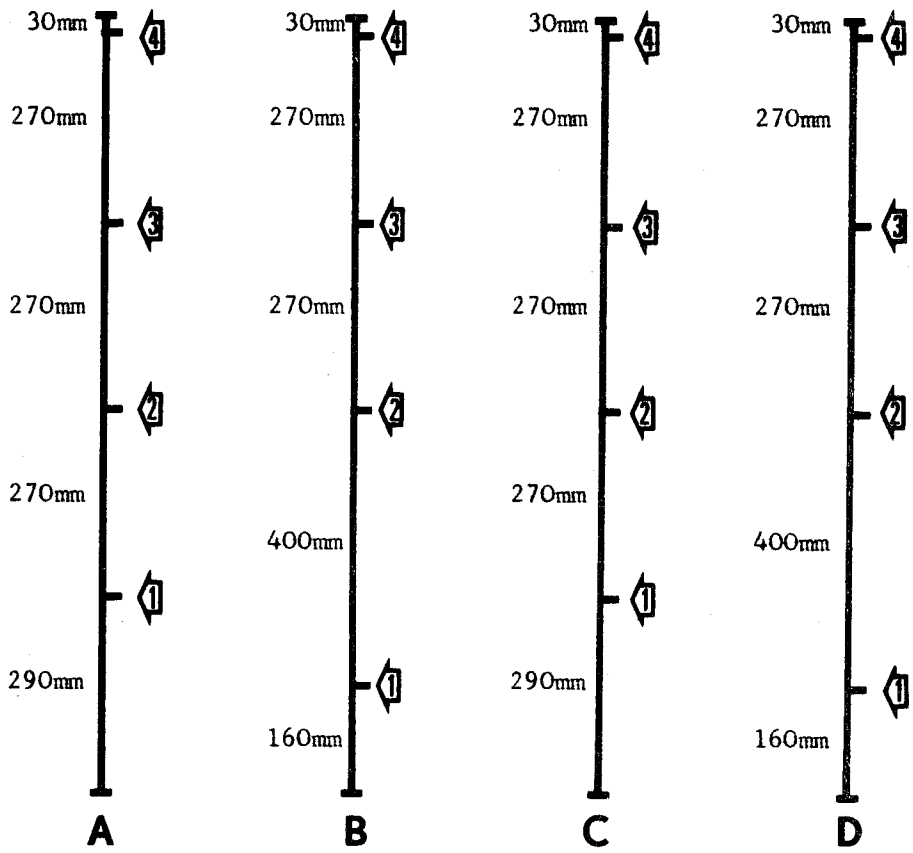
3.3.3 Test results.

Table C.V shows the test results obtained. The inlet conditions vary within the following range :

$$300 \text{ kg/m}^2/\text{s} \leq \rho V \leq 2300 \text{ kg/m}^2/\text{s}$$
$$- 21 \% \leq x_{\text{inlet}} \leq - 2,5 \%$$

Fig. C20

LOCATION OF THE DETECTION THERMOCOUPLES IN THE TEST SECTION



At high mass flow rates, critical heat flux reached values of 5000 kW/m^2 .

Results are shown in Fig. C.21 in which are also mentioned the test points obtained on the SNECMA loop. These results were obtained in the range of positive inlet qualities and for $300 \leq \rho V \leq 600 \text{ kg/m}^2/\text{s}$. In that diagram the critical heat flux is plotted versus inlet quality $\phi_{cr} = f(x_{in})$.

Fig. C.22 shows the same CHF results plotted versus outlet quality.

It has to be pointed out that the results obtained during these tests at ISPRA are in a very good agreement with those from former tests on the SNECMA loop. However there is an appreciable scattering of the results, mainly at $\rho V = 600 \text{ kg/m}^2/\text{s}$.

It has also to be noticed that the CHF values obtained from the tests carried out on the last test section are lower - by about 15% - to the CHF values obtained on the other test sections (Fig. C.23). This is probably coming from the smoother surface of the heated tubes used in the last test section. The effect of the heated tube surface roughness had already been demonstrated during special tests (16).

Table C V summarizes the CHF test results.

3.3.4 Observations on the crisis.

During most of the tests, the crisis was detected as an increase of the temperature of the internal surface of the heated tube, at the outlet of the channel. The thermocouples located at lower levels along the heated tubes did not give any additional informations about the CHF phenomenon. The thermocouples located at levels 1, 2 and 3 (Fig. C.20) either showed no rise of the tube temperature or gave a signal but behind the signal given by the outlet thermocouple.

Fig. C.24 shows such a recording of the wall temperatures along the tubes.

Thermocouple D4, at the channel exit, is connected to the Burnout Detector which cut-off the power.

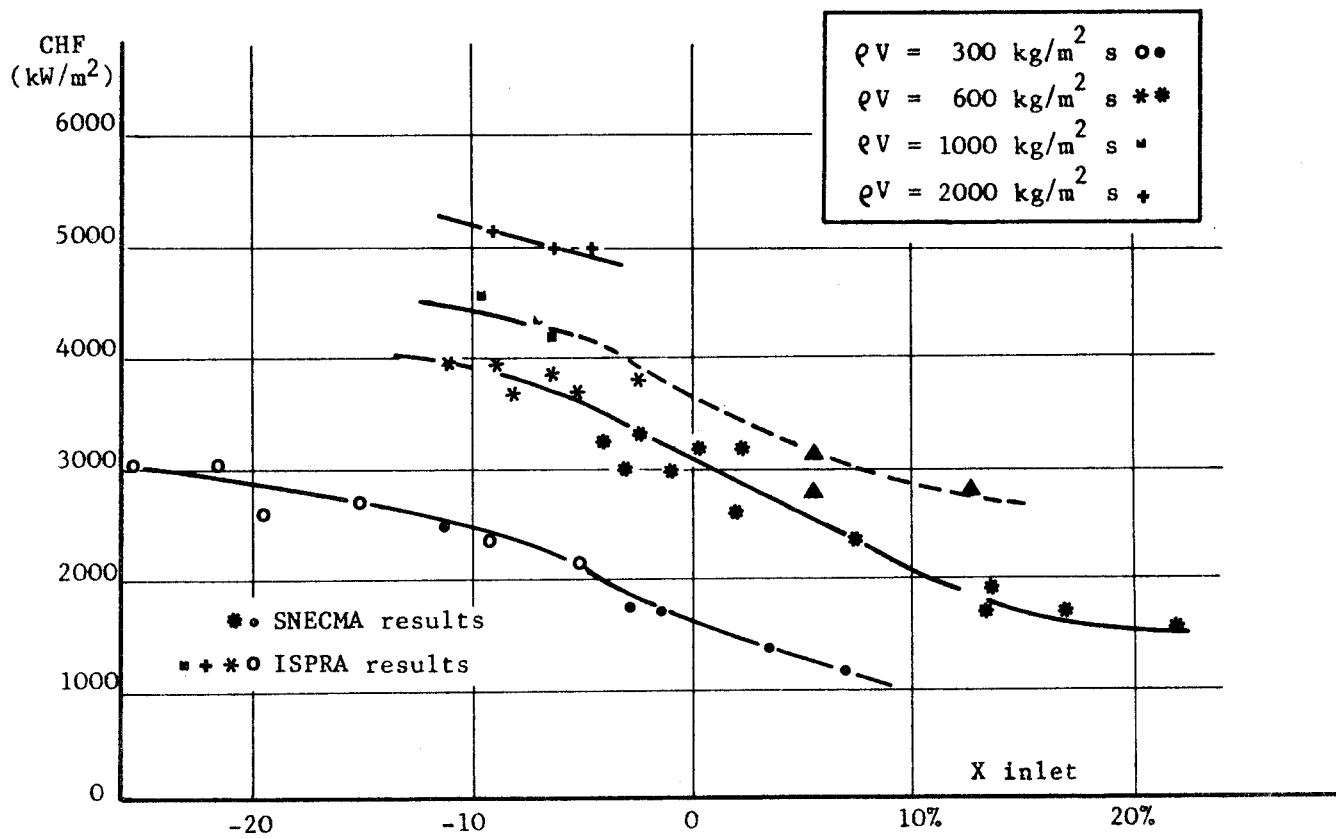


Fig. C21 - CRITICAL HEAT FLUX FOUR ROD TEST SECTION

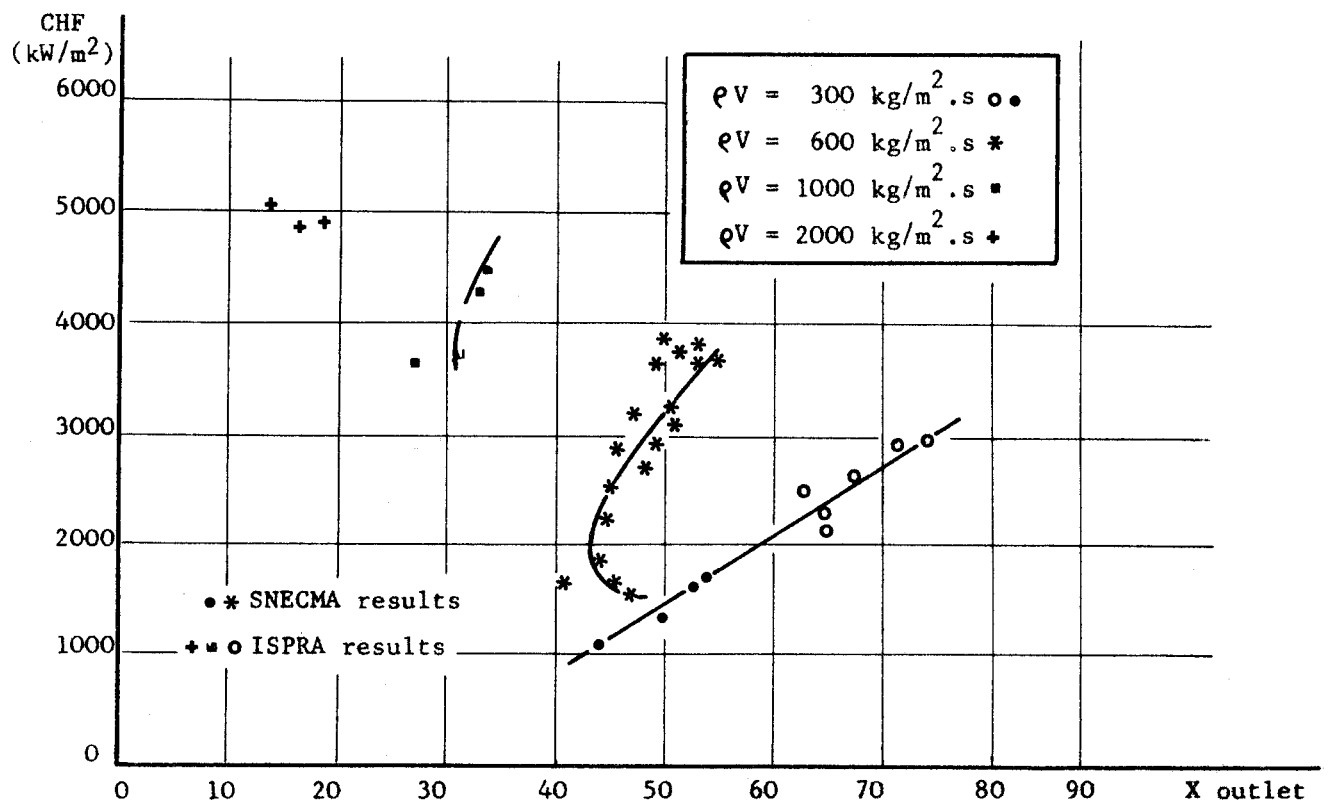


Fig. C22 - CRITICAL HEAT FLUX FOUR ROD TEST SECTION

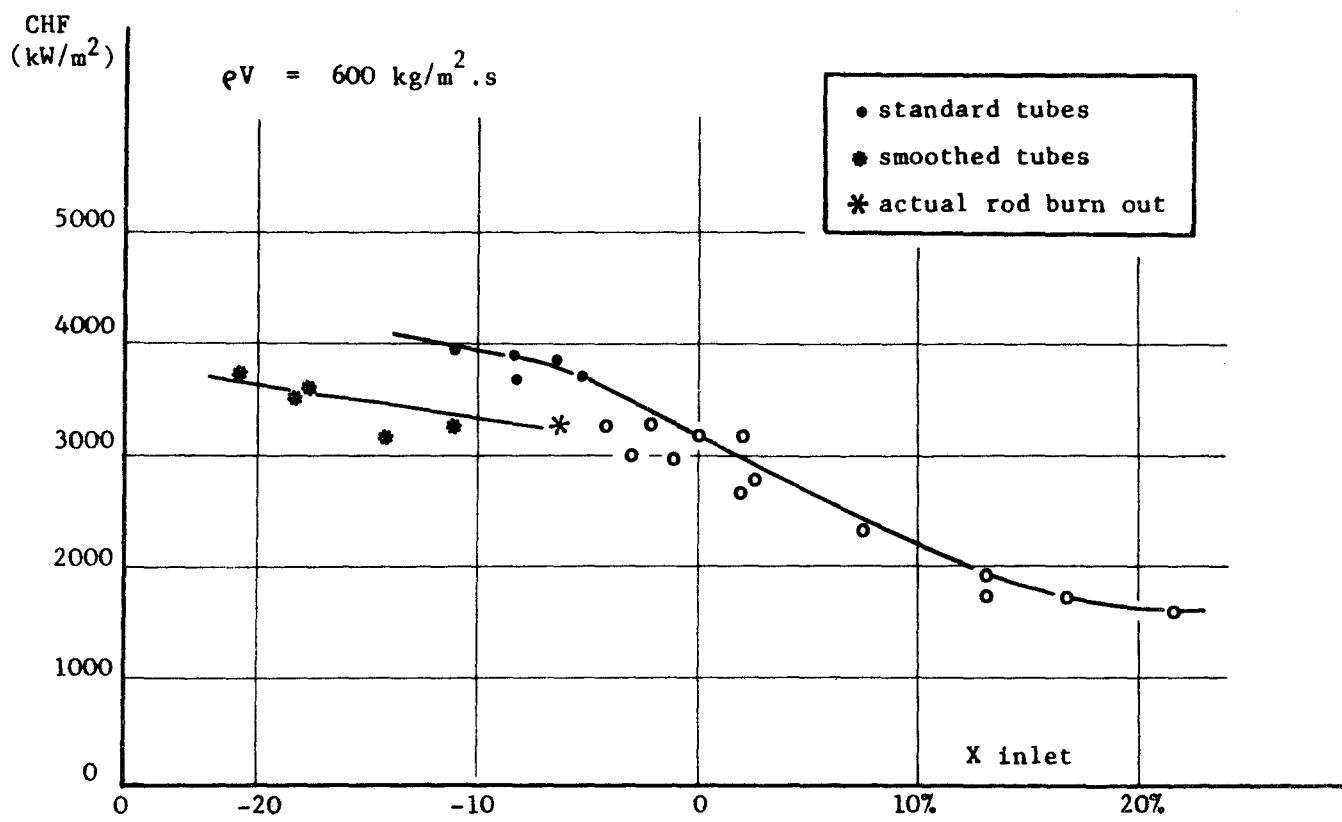


Fig. C23 - CRITICAL HEAT FLUX FOUR ROD TEST SECTION

T A B L E C V

CRITICAL HEAT FLUX EXPERIMENT RESULTS

$P_{abs.}$ Bars	T_{in}	$Q_{kg/s}$	P^V	x % inlet	W_{SE}	CHF kW/m ²	x % outlet	T_p	Detection	Observations
69,5	270	0,298	334	- 5,45	301	2180	65,73			
68,2	256	0,306	343	- 9,45	329	2380	65,73			
68,5	238	0,303	340	-15,3	360	2610	68,14	478		
68,5	224	0,293	323	-19,7	348	2520	63,53			
70,4	209	0,296	332	-25,2	414	3000	74			
68,9	217°1	0,311	349	-21,9	412,5	2995	71,6	478		
69,1	269°8	0,611	685	-5,18	502	3640	52,7	531		
68,5	258°4	0,609	681	-8,67	499	3620	49	531		
68,2	265	1,040	1152	-6,47	575	4160	31	513		
69,7	257	1,000	1112	-9,7	638	4520	33,9	564		
69,5	266°7	2,038	2260	-6,5	684	4950	16,3			
67,9	256°8	2,058	2280	-9,1	700	5100	13,9	600		
69,6	272	2,022	2245	-4,72	686	4980	18,4	600		
67,6	270°5	2,480	2750	-4,62	700	5100	14,27			
69,1	270°5	0,95	1050	-5,18	516	3750	31,73			
68,2	256	1,020	1130	-9,45	526	3820	25,6	530		tube broken at 610 mm from inlet
69,1	278	0,605	670	-2,39	518	3750	55,6	400		
69,1	265°7	0,61	676	-6,65	524	3800	51,7	522		
70,5	258°9	0,604	670	-9,3	540	3920	52,4	522		
70	251°7	0,605	670	-11,45	544	3940	50	541		
71,1	268°2	1,018	1130	- 6,95	589	4260	32,94	550		polished tubes
69,6	250°5	0,605	678	-11,82	442	3200	40	532		
66,2	224	0,596	670	-18,7	472	3420	36,25	532		
69,1	241°7	0,606	680	-14,4	432	3140	37,5	542		
66,2	262	0,598	670	- 6,76	442	3200	44,1	580		
68,9	230	0,616	692	-18	488	3550	38	570		
69,5	221°5	0,615	690	-21	506	3660	37,5	518		tube broken at 625 mm from inlet

1 thermocouple at outlet

4 thermocouples in each rod

Actual B.O. occurred twice, the reasons of which are not fully determined. In both cases the thermocouples did not give any signal. This B.O. resulted in the melting of the tube. The overheated areas can be considered as hot spots (about 2 mm diameter). They were located in the boiling region. The flow characteristics at these points are listed below :

Location of B.O. (from inlet)	610 mm	625 mm
Flow rate	1130 kg/m ² s	690 mm
Local quality	10 %	12,3 %

The hot spots were located at the channel edge, facing the channel box. After dismantling, an examination of the overheated rods showed black spots in the upper half of the test section. The lower part showed no marks of this type.

It is quite uneasy to give an unquestionable explanation of these actual burnouts. However they make us to believe that the crisis can occur at such level of the boiling length which is rather far from the outlet, that is to say at a quality lower than the outlet quality.

3.3.5 Representation of critical heat flux versus inlet quality. (Fig. C.21)

The representation in relation to inlet conditions reveals :

- a decrease of the heat flux in relation to the inlet quality
- the gradient of curves appears to be less in the area of negative inlet qualities
- the heat flux increases with the mass velocity

The latter is the result of the increase of the centrifugal forces caused by the increase of the velocity.

3.3.6 The representation of critical heat flux versus outlet quality (Fig. C.22)

The plotting of CHF versus outlet quality results in dual slope curves. For low values of the outlet quality, no CHF can be found. For higher values of the outlet quality two values of the CHF can be read, one on the positive slope part which corresponds to inlet qualities lower than 10 %, and the other on the slightly negative slope part which corresponds to inlet qualities higher than 10%.

The minimum outlet quality to which a CHF can be related (vertical tangent to the curve) decreases at increasing mass velocities.

The main conclusion that can be made out of this is that the CHF seems not to be determined by the outlet conditions in the same way as in straight flow.

3.3.7 Comparison of CHF, with and without twisted tapes.

Because of the uniform heat flux, a comparison of the admissible heat flux values with and without twisted tapes can be made at constant inlet conditions. Fig. C.25 shows, on the same diagram, (CHF versus inlet quality) the CHF with twisted tapes, with interrupted twisted tapes and without twisted tapes, in the case of a mass velocity equal to $600 \text{ kg/m}^2\text{s}$. The interrupted twisted tapes, contrary to the twisted tapes which cover the whole length of the heated channel, are located along the channel at several levels with the aim to restart the swirling.

In the case of saturation at the inlet ($x_{\text{inlet}} = 0$), the curves indicate an increase of 80% with continuous twisted tapes and of 50% with interrupted twisted tapes.

In order to make a comparison covering the whole range of inlet qualities which has been analysed, the curves relating to the straight flow, based on the CISE correlation, are plotted in Fig. C.25. The data shown on the next table were obtained from this plot.

COMPARISON OF THE CRITICAL HEAT FLUX WITH AND WITHOUT TWISTED TAPES
Four heating rod test section

$\rho^v \text{ kg/m}^2\text{/s.}$	x_{inlet}	- 10%	- 5%	0	5%
600	CHF without T.T.	2200	1980	1750	1550
	CHF with T.T.	3850	3500	2900	2500
	CHF increase	75 %	75 %	66 %	61 %
1000	CHF without T.T.	2600	2350	2000	
	CHF with T.T.	4400	4200	3600	
	CHF increase	70 %	79 %	80 %	
2000	CHF without T.T.	3150	2700		
	CHF with T.T.	5200	4950		
	CHF increase	65 %	83 %		

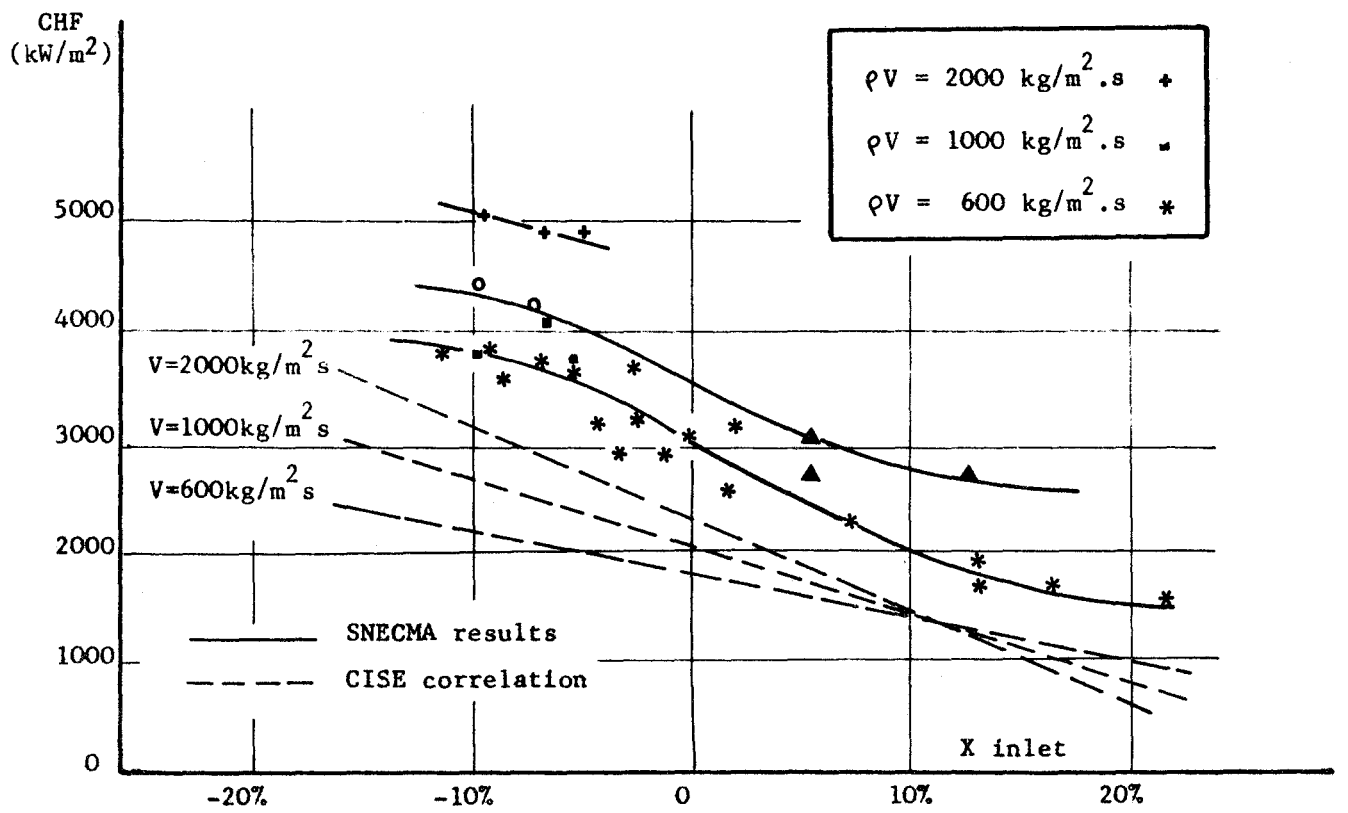


Fig. G25 - CRITICAL HEAT FLUX COMPARISON FOUR ROD TEST SECTION

3.3.8 Conclusion.

The present tests have allowed to prove the effectiveness of the Twisted Tapes increasing the thermal performance of a heated channel having the geometry of a BWR fuel element.

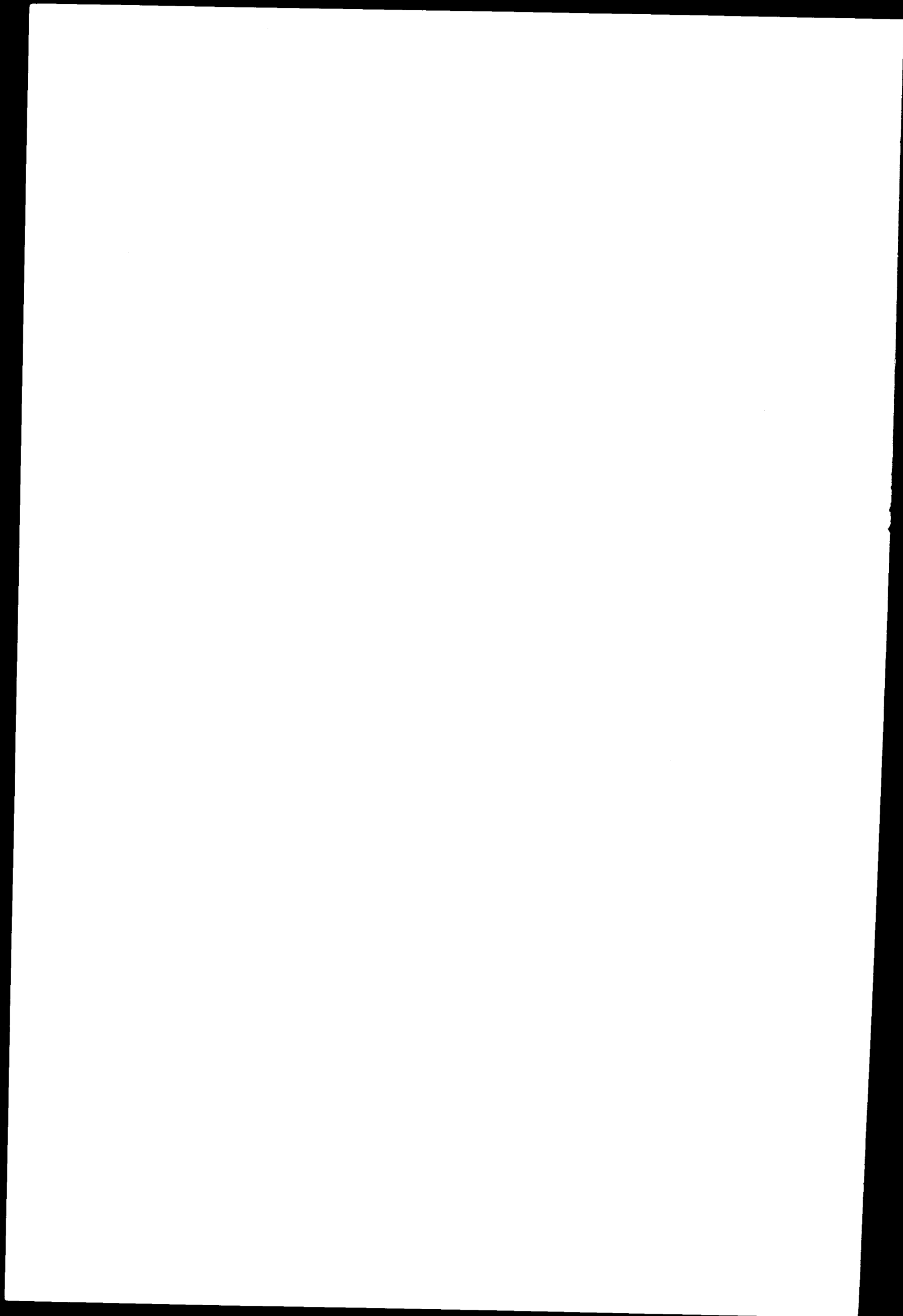
However they have not given a full understanding of the phenomenon. Though a rod surface temperature rise could be detected at the outlet in most of cases, it is not possible to correlate the outlet conditions (heat flux, steam quality and mass velocity) in a satisfactory way. At constant mass velocity two values of the CHF are related to one value of the quality. This can lead to the following conclusion : either the B.O. occurs at the outlet and is determined not only by others, or the B.O. starts upstream in the channel and disturbs the flow so that an overheating of the rod can be detected at the outlet. In both cases the parameters which would clearly define the CHF phenomenon still are to be found.

This cannot be achieved without new experiments. Tests should be run both on clusters and on tubes. This latter geometry is recommended because of its technological simplicity and because it would give basic informations which are qualitatively comparable to those obtained in the more realistic but more difficult to handle cluster geometry.

R E F E R E N C E S

- 1 - Rapport SNECMA-EURATOM N°1 - Volume de vide et pertes de charge dans les écoulements biphasés isothermes et avec ébullition -
par C. MOUSSEZ et G. SOURIOUX.
- 2 - Rapport SNECMA-EURATOM N°2 - Etude des écoulements adiabatiques à deux phases -
par Mmes A. MIHAIL et B. BERNARD.
- 3 - Rapport SNECMA-EURATOM N°3 - Etude des écoulements à deux phases (air-eau) avec vortex -
par Mme B. BERNARD.
- 4 - Rapport SNECMA-EURATOM N°4 - Influence de vrilles centrifugeuses sur le flux de caléfaction du fréon.
par J. VOLTERAS.
- 5 - Rapport SNECMA-EURATOM N°5 - Influence de tourbillon induit dans l'eau bouillante à la pression atmosphérique sur les flux de caléfaction.
par A. ROSUEL et G. SOURIOUX.
- 6 - Rapport SNECMA-EURATOM N°6 - Synthèse des essais thermiques.
par C. MOUSSEZ.
- 7 - Rapport SNECMA-EURATOM N°7 - Etude de la séparation des mélanges eau-vapeur.
par C. FOURE et Mme A. MIHAIL.
- 8 - Rapport SNECMA-EURATOM N°8 - Etude des écoulements à deux phases (air-eau) sur fraction d'assemblage type SENN avec et sans vrilles.
par Mme A. MIHAIL.
- 9 - Rapport SNECMA-EURATOM N°9 - Influence de tourbillons induits \emptyset 10 dans l'eau bouillante à basse pression sur les flux critiques.
par J. VOLTERAS et G. TOURNIER.
- 10 - Rapport SNECMA-EURATOM N°10 - Introduction de vrilles dans un assemblage de type SENN.
par J. MILCENT.
- 11 - Rapport SNECMA-EURATOM N°11 - Mesure de la fraction de vide sur section quatre barreaux par absorption de rayons gamma.
par A. BEGHIN.
- 12 - Rapport SNECMA-EURATOM N°12 - Influence de tourbillons induits quatre barreaux dans l'eau bouillante à basse pression sur les flux critiques.
par J. VOLTERAS et G. TOURNIER.
- 13 - Rapport SNECMA-EURATOM N°13 - Effet d'une crise d'ébullition sur une section d'essais cylindrique circulaire à focalisation de flux.
par C. MOUSSEZ.
- 14 - Rapport SNECMA-EURATOM N°14 - Synthèse des essais portant sur écoulements verticaux adiabatiques à deux phases (air-eau) avec et sans vrilles.
par T. MICHELS.
- 15 - Rapport SNECMA-EURATOM N°15 - Installation d'essais pour l'étude en écoulements giratoires en eau bouillante à 70 bars.
par A. ROSUEL, G. SOURIOUX et J. DOLLE.

- 16 - Rapport SNECMA-EURATOM N°16 - Ecoulements giratoires et flux critiques en eau bouillante à 70 bars.
par A. ROSUEL, G. SOURIOUX et J. DOLLE.
 - 17 - Rapport SNECMA-EURATOM N°17 - Application des vrilles aux réacteurs bouillants.
par J. MILCENT, G. du BOUCHERON et J. MARTINAUD.
 - 18 - Rapport SNECMA-EURATOM N°18 - Ecoulements giratoires dans l'eau bouillante.
par G. du BOUCHERON et J. MARTINAUD.
 - 19 - Rapport SNECMA-EURATOM N°19 - Etude de la déformation du flux axial dans un réacteur à eau bouillante sans barres de contrôle.
par J. MARTINAUD.
 - 20 - Rapport SNECMA-EURATOM N°20 - Ecoulements giratoires dans l'eau bouillante.
par C. MOUSSEZ, A. ROSUEL, G. SOURIOUX et D. EIDELMAN.
 - 21 - Rapport SNECMA-EURATOM N°21 - Etudes hydrodynamiques des écoulements tourbillonnaires diphasés dans un tube.
par A. ROSUEL et G. TOURNIER.
 - 22 - Rapport SNECMA-EURATOM N°22 - Flux critiques en écoulement tourbillonnaire dans un tube.
par A. ROSUEL, G. SOURIOUX, J. DOLLE et Mme J. SANDRIN.
 - 23 - Rapport SNECMA-EURATOM N°23 - Etude des flux critiques en écoulement tourbillonnaire dans un groupe de 4 barreaux.
par A. ROSUEL, G. SOURIOUX, C. CHERON, J. DOLLE et Mme J. SANDRIN.
 - 24 - Rapport SNECMA-EURATOM N°24 - Etude des flux critiques dans une grappe de 9 barreaux équipée de vrilles.
par A. ROSUEL, G. SOURIOUX et J. DOLLE.
 - 25 - Rapport SNECMA-EURATOM N°25 - Etude de la répartition des débits dans une section d'essais à deux canaux.
par A. ROSUEL et A. BEGHIN.
 - 26 - Rapport SNECMA-EURATOM N°26 - Ecoulements giratoires dans l'eau bouillante.
par A. ROSUEL, G. SOURIOUX, J. DOLLE, G. TOURNIER et A. BEGHIN.
 - 27 - EUR 1785.f - Ecoulements giratoires dans l'eau bouillante.
par C. MOUSSEZ, A. ROSUEL, G. SOURIOUX, G. du BOUCHERON et D. EIDELMAN.
 - 28 - EURATOM/AEG-SNECMA - Rapport technique particulier N°1 - Avant-projet de centrale nucléaire de 600 MWe équipée d'assemblages combustibles à vrilles.
par G. du BOUCHERON, D. EIDELMAN et A. ROSUEL.
 - 29 - EURATOM/AEG-SNECMA - 1st Common working report.
 - 30 - EURATOM/AEG-SNECMA - 2nd Common working report (January-March 1966)
 - 31 - EURATOM/AEG-SNECMA - 3rd Common working report (April-June 1966)
 - 32 - EURATOM/AEG-SNECMA - 4th Common working report (July-September 1966)
-



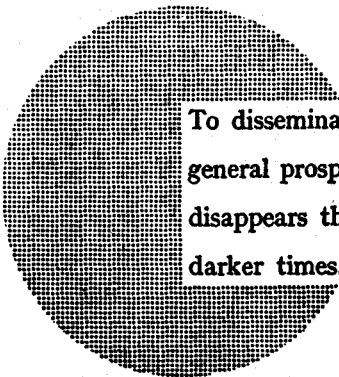
NOTICE TO THE READER

All Euratom reports are announced, as and when they are issued, in the monthly periodical **EURATOM INFORMATION**, edited by the Centre for Information and Documentation (CID). For subscription (1 year : US\$ 15, £ 5.7) or free specimen copies please write to :

Handelsblatt GmbH
"Euratom Information"
Postfach 1102
D-4 Düsseldorf (Germany)

or

Office central de vente des publications
des Communautés européennes
2, Place de Metz
Luxembourg



To disseminate knowledge is to disseminate prosperity — I mean general prosperity and not individual riches — and with prosperity disappears the greater part of the evil which is our heritage from darker times.

Alfred Nobel

SALES OFFICES

All Euratom reports are on sale at the offices listed below, at the prices given on the back of the front cover (when ordering, specify clearly the EUR number and the title of the report, which are shown on the front cover).

OFFICE CENTRAL DE VENTE DES PUBLICATIONS DES COMMUNAUTES EUROPEENNES

2, place de Metz, Luxembourg (Compte chèque postal N° 191-90)

BELGIQUE — BELGIË

MONITEUR BELGE
40-42, rue de Louvain - Bruxelles
BELGISCH STAATSBLAD
Leuvenseweg 40-42 - Brussel

LUXEMBOURG

OFFICE CENTRAL DE VENTE
DES PUBLICATIONS DES
COMMUNAUTES EUROPEENNES
9, rue Goethe - Luxembourg

DEUTSCHLAND

BUNDESANZEIGER
Postfach - Köln 1

NEDERLAND

STAATSDRUKKERIJ
Christoffel Plantijnstraat - Den Haag

FRANCE

SERVICE DE VENTE EN FRANCE
DES PUBLICATIONS DES
COMMUNAUTES EUROPEENNES
26, rue Desaix - Paris 15^e

ITALIA

LIBRERIA DELLO STATO
Piazza G. Verdi, 10 - Roma

UNITED KINGDOM

H. M. STATIONERY OFFICE
P. O. Box 569 - London S.E.1

EURATOM — C.I.D.
51-53, rue Belliard
Bruxelles (Belgique)